Chilly temperatures, polluted air: the health impacts of residential heating emissions

Elena Cottini*, Lorena Popescu**, Luca Salmasi*, Gilberto Turati*

* Department of Economics and Finance, Università Cattolica del Sacro Cuore

** Department of Economics and Management "Marco Fanno", University of Padua

*** Department of Economics and Finance, Università Cattolica del Sacro Cuore, Rome

March 5, 2026

Abstract

Residential biomass heating generates over half of $PM_{2.5}$ emissions in many European countries yet credible causal evidence on its health effects remains limited. Exploiting staggered heating activation across 479 Italian municipalities, we estimate that heating increases $PM_{2.5}$ by 19–27% and NO_2 by 11–20%. These pollution spikes raise hospital admissions for acute myocardial infarction (+17%), STEMI (+18%), and COPD (+23%) during high-pollution winters, with in-hospital mortality from myocardial infarction increasing by 35% in the worst year of exposure. Effects are concentrated in colder regions and among vulnerable populations—older adults and individuals with low education—but extend significantly to patients without prior comorbidities, a finding inconsistent with classic mortality displacement narratives. Our findings point to substantially Underestimated health costs of biomass burning, with implications for renewable energy policy.

Keywords: air pollution, residential biomass heating, hospitalisations, staggered diff-in-diff, environmental inequality.

JEL classification: I18, J13, Q53, Q58.

1 Introduction

Residential heating has become the dominant source of wintertime air pollution across Europe, accounting for 58% of $PM_{2.5}$ emissions-exceeding the combined contributions of transport and industry (European Environment Agency 2023). The EU's Renewable Energy Directive classifies biomass burning as carbon-neutral renewable energy, which has coincided with growing biomass adoption in the residential sector. Despite this shift in the composition of air pollution sources, 96% of the EU's population remains exposed to $PM_{2.5}$ concentrations exceeding WHO guidelines (European Environment Agency 2023). Recently, Zauli-Sajani et al. (2024) further underline that nearly all anthropogenic $PM_{2.5}$ from the residential sector derives from biomass combustion.

Yet research on the health effects of residential heating pollution remains limited. While extensive evidence documents the impacts of traffic and industrial emissions, causal estimates of residential heating pollution are scarce. This gap is particularly consequential given that residential heating now constitutes the largest source of $PM_{2.5}$ in many European countries. Italy provides an ideal setting: residential heating accounts for 62.5% of national $PM_{2.5}$ emissions in 2022 (ISPRA 2014), making it by far the largest single source. Moreover, Italy exhibits substantial geographic variation in heating systems and climate zones, ranging from the mild Mediterranean coast to the cold Alpine regions.

We estimate the causal effect of residential heating activation on air pollution and health outcomes, focusing on urgent hospitalizations and in-hospital mortality for cardiovascular and respiratory diseases with well-established links to $\mathrm{PM}_{2.5}$ exposure: acute myocardial infarction (AMI), stroke, and chronic obstructive pulmonary disease (COPD).[1] We exploit

[1] We analyze AMI both overall and separately by clinical subtype: STEMI (ST-segment Elevation Myocardial Infarction) and NSTEMI (Non-ST-segment Elevation Myocardial Infarction). Stroke estimates distinguish between ischemic and hemorrhagic subtypes.

the universe of administrative hospital discharge records covering all urgent admissions in Italy (2015–2019) across 479 municipalities and 892 hospitals, including detailed clinical outcomes (diagnoses, in-hospital mortality, comorbidities) and sociodemographic characteristics. We link these records with high-resolution pollution data combining satellite measurements (CAMS) and ground monitoring stations (EEA), and weather data from Agri4Cast grids.

Identifying causal effects faces two main challenges. First, $PM_{2.5}$ is endogenous to health outcomes: municipalities with higher heating emissions differ systematically in unobservable characteristics affecting health, making simple comparisons across municipalities invalid. Second, regulatory heating dates poorly capture actual behavior, as households activate heating in response to temperature shocks rather than fixed schedules. We address these issues using a staggered difference-in-differences design (Callaway & Sant'Anna 2021) that exploits temperature-driven variation in heating activation across 479 Italian municipalities. Rather than relying on legal dates, we define treatment using actual heating activation using Google search trends for "Turning on the heating system," which spike when local temperatures fall below comfort thresholds. This approach captures real heating behavior while leveraging quasi-random variation in activation timing across municipalities with different baseline climates. We classify municipalities by biomass heating intensity-measured as appliance-adjusted adoption per municipal area–comparing above-median versus below-median adopters to isolate the health effects of biomass-generated pollution.

We document three main findings. First, heating activation increases $PM_{2.5}$ by 19-27% and NO_2 by 11–20%, driving acute myocardial infarction admissions up 17%, STEMI by 18%, and COPD hospitalizations by 23%. In-hospital mortality from acute myocardial infarction rises 35% in the worst year (2015-16). Second, health impacts exhibit striking patterns of heterogeneity: they concentrate in colder climate zones, they disproportionately affect middle aged (45-64 years) and elderly individuals and those with low educational attainment. Third, and most surprisingly, we find significant effects among individuals *without* pre-existing comorbidities, suggesting that acute pollution exposure triggers health crises even in otherwise healthy individuals—a pattern inconsistent with classic mortality displacement and implying welfare costs larger than prior estimates would suggest.

While the link between biomass combustion and emissions is well-established-individual heating systems release higher NO_2 and CO than district heating (Salva et al. 2023)-causal evidence specifically on residential heating pollution remains scarce, particularly relative to the extensive literature on traffic and industrial sources. The closest evidence comes from coal-fired heating contexts, where winter heating has been shown to increase mortality by 14% (Fan et al. 2020), but whether similar effects hold for biomass-dominated systems in European settings remains an open question.

Short-term exposure to $PM_{2.5}$ and NO_2 raises cardiovascular and respiratory hospitalisations (Giaccherini et al. 2021, Bauernschuster et al. 2017, Schlenker & Walker 2016) and increases mortality risk (Chay & Greenstone 2003, Neidell 2004, Cheung et al. 2020, He et al. 2020), exacerbating risks of respiratory infections, cardiovascular diseases, lung cancer, and premature death (Pope & Dockery 2012). Evidence from coal-fired heating contexts further links heating-related emissions to cardiovascular deaths, particularly among individuals over 60 and children under 5 (Fan et al. 2020, 2023), with adverse effects extending to neonatal health.[2] Existing work identifies vulnerable populations pri-

[2]DeCicca & Malak (2020), Fan et al. (2023), and Palma et al. (2022) associate air pollution with premature births and compromised neonatal health.

marily through age (Deryugina et al. 2019) or broad diagnostic categories, leaving open whether acute pollution exposure harms otherwise healthy individuals. Moreover, prior causal estimates focus on major cities (Bauernschuster et al. 2017, Giaccherini et al. 2021, Margaryan 2021), limiting external validity.

Our paper makes four contributions. First, we introduce a novel identification strategy that exploits the gap between regulated and actual heating activation dates, using Google search trends as a real-time behavioural proxy to identify the temperature threshold at which households actually turn on heating. This approach captures genuine behavioural responses to cold weather while remaining compatible with a staggered difference-in-differences design (Callaway & Sant'Anna 2021). Second, we provide novel causal evidence linking residential heating emissions to both cardiovascular and respiratory health, covering hospitalisations and in-hospital mortality across six acute conditions at national scale — including smaller municipalities and rural areas largely ignored by prior work focused on major cities (Bauernschuster et al. 2017, Giaccherini et al. 2021, Margaryan 2021). Third, and most strikingly, we document significant effects among individuals without pre-existing comorbidities. Unlike Deryugina et al. (2019), who identify vulnerable populations using age-based classifications, we use the Charlson Comorbidity Index, revealing that acute pollution exposure triggers health crises even in otherwise healthy individuals - a finding inconsistent with classic mortality displacement narratives and implying welfare costs larger than prior estimates would suggest. Fourth, we document systematic environmental inequality: health burdens nearly double in colder climatic zones, and fall disproportionately on older adults, middle-aged individuals (45-64), and those with low educational attainment, patterns with direct implications for the targeting of environmental and energy policy.

2 Heating system regulation in Italy

Italy is divided into six climatic zones based on degree-day calculations.[3] Figure A1 illustrates the spatial distribution of climatic zones and Table A2 summarizes major cities by zone.[4] The operation of heating systems is regulated by climate zone framework (Gazzetta Ufficiale della Repubblica Italiana - DPR 412/1993 1993, Gazzetta Ufficiale della Repubblica Italiana - DPR 74/2013 2013), which sets fixed annual activation periods and daily operating hours calibrated to degree-day thresholds. The system assumes heating is unnecessary when outdoor temperatures exceed 18.3°C (65°F). However, three critical nuances emerge: (i) binding schedules apply only to centralised systems, with autonomous heating frequently bypassing regulation[5]; (ii) governments and municipalities may override defaults during unusual temperatures or energy emergencies (e.g., 2022 gas crisis); and (iii) enforcement relies on ex-post inspections rather than real-time monitoring. This divergence between de jure regulations and de facto practices raises concerns for methodological reliance on official heating dates, which may inadequately capture actual heating initiation.

Italian households exhibit substantial heating heterogeneity: 65.7% use autonomous systems, 17.2% rely on single appliances, 17.1% on centralised systems, with 44.5% combining multiple sources (ISTAT 2022).[6] This heterogeneity makes legal heating dates a poor proxy for actual pollution exposure, as private systems allow discretionary use

[3] *Degree days* are calculated by summing, for each day of the year, the positive differences between 20°C (statutory indoor comfort threshold) and the average daily outdoor temperature (T_e), as follows:

$$Deg\_Days = \sum_{e=1}^{n}(20 - T_e) \tag{1}$$

Only days on which $T_e < 20$ are counted. Higher totals indicate colder areas and greater heating demand.

[4] For example, Milan and Turin fall within zone E, Rome in zone D, and Naples in zone C.

[5] Over 70% of homes for sale in Italy have independent heating systems (Idealista, 2024).

[6] Half of households own supplementary appliances. This heterogeneity is further complicated by structural factors (insulation, building size) and socioeconomic disparities, where vulnerable groups depend on heating for health while wealthier households sustain prolonged usage.

bypassing restrictions.

3 Data and sample

We construct a novel municipality-level dataset by merging multiple sources: (i) administrative data on Hospital Discharge Records (HDRs) from the Italian Ministry of Health; (ii) pollution exposure measurements from the Copernicus Atmosphere Monitoring Service (CAMS) and European Environmental Agency (EEA) monitoring stations; (iii) weather controls from Agri4Cast; and (iv) covariates including ISTAT population data, Terna biomass consumption, and Google search indicators. Our analysis focuses on the period 2015-2019 to leverage the first available year of hospitalisation records while avoiding disruptions caused by COVID-19, which abruptly altered both pollution levels and healthcare utilisation patterns. Our sample covers approximately 479 municipalities containing 892 hospitals, representing the complete universe of hospitalisations in Italy[7].

3.1 Hospital Discharge Records (HRD)

The dataset provides information on hospitalisations across both public and publicly funded private hospitals in Italy. The Italian National Health Service (NHS) operates as a tax-funded national insurance scheme, offering comprehensive coverage of a wide range of constitutionally mandated services. It includes socio-demographic details about patients (age, gender, nationality, birthplace, region of residence, education), clinical information (diagnoses, procedures, transfers, discharges), and hospital-specific information (type, specialisation). We focus on urgent unplanned hospitalisations related to respiratory and cardiovascular illnesses to minimize patient self-selection into more efficient hospitals. We

[7]It pertains to municipalities that contain at least one hospital facility.

also exclude patients who have been documented as transferred to a different admission regime (either day hospital or regular admission) or to another type of care activity (acute care, rehabilitation, long-term care) within the same healthcare facility, thereby avoiding duplicate records for the same patient. The main outcome variables are AMI, STEMI, NSTEMI, ischemic stroke, hemorrhagic stroke and COPD. We sum the total number of hospital admissions per month and by municipality of the hospital.

3.2 Pollution and Weather Data

The main dataset that we use to measure $PM_{2.5}$ is CAMS. CAMS provides annual air quality reanalyses for Europe with a significantly high spatial resolution (0.1 degrees, approximately 10km)[8] compared to global reanalyses. CAMS combines eleven European air quality models into a median ensemble, integrating them with EEA monitoring data through data assimilation to produce consistent pollution estimates while also quantifying uncertainty through model variability.[9]

While our primary pollution measures rely on CAMS gridded $PM_{2.5}$ data we supplement these with monitoring station data from the European Environmental Agency (EEA) Airbase database for three key reasons: (i) CAMS lacked complete coverage for secondary pollutants (PM_{10}), Nitrogen Dioxide (NO_2), Sulfure Dioxide (SO_2) and Carbon Monoxide (CO) during our study period; (ii) monitoring stations provide validated ground measurements across European cities, enabling direct comparison with CAMS $PM_{2.5}$ estimates

[8] The decision to employ grid data, over air monitoring stations one, offers numerous advantages. Firstly, it provides full territorial coverage and detailed spatial resolution, ensuring that no area is overlooked and allowing for precise analysis at a granular level. Secondly, grid data ensures uniformity across space and time, facilitating consistency in comparisons and analyses. The continuous monitoring allows for real-time or near-real-time tracking of changes and trends. Additionally, grid data help reduce assumptions about uniform pollutant concentrations, providing a more accurate representation of environmental conditions and allowing for the identification of mesoscale spatial variations in pollution and population exposure, even though very local peaks are better captured by monitoring stations.

[9] CAMS data are highly accurate and reliable(Wu et al. (2020)), making them a valuable resource for monitoring pollution. In addition to in-situ data assimilation, satellite observations and other data sources complement the dataset. The reanalyses are available at hourly intervals and various height levels. For our purposes, we selected data at zero meters above ground level and use the validated reanalysis data.

to assess potential bias; and (iii) multi-pollutant analysis helps isolate $PM_{2.5}$ effects from correlated emissions.

We measure weekly and monthly weather conditions—including mean temperature (°C), mean wind speed at 10 m (m/s), and total precipitation (mm/day)—using Agri4Cast gridded data at 25 km resolution.[10] Pollution and weather variables are collapsed at the weekly and monthly municipality level, depending on the analysis requirements.

3.3 Supplementary data

Data on population were obtained from the ISTAT database (Italian National Institute of Statistics) for all municipalities and years considered. Additionally, the number of residential heating appliances in 2011 by municipality, as recorded in the Census of Population and Housing, was included, representing the only available year of data collection relevant to this study [11]. Data on annual regional biomass consumption (GWh) were retrieved from Terna reports.[12] We obtained the absolute number of weekly Google searches for "Turning on the heating system" by climatic area.

3.4 Data Linkage

We apply geo-spatial matching to link municipalities with pollution and weather data. Each municipality is assigned to its nearest grid point using latitude-longitude coordinates. Hospital discharge records already include municipality codes, enabling direct linkage of hospitalizations to local pollution exposure. For robustness checks on $PM_{2.5}$ and extended

[10] The JRC MARS Meteorological Database (Agri4Cast) contains daily meteorological observations from weather stations, interpolated onto a 25×25 km grid covering the European Union and neighboring countries. Mavromatis & Voulanas (2021) evaluate the suitability of Agri4Cast and E-OBS over ERA-Interim for climate and atmospheric research in Greece.

[11] The ISTAT census is conducted every ten years. However, since 2018, it has transitioned into a permanent, annual survey. Each year, it includes two sample-based surveys: one based on population registry data and the other on an area-based sample of addresses. This new approach involves only a representative sample of approximately 1.4 million households.

[12] Terna is a key player in the energy sector in Italy, providing essential data on energy consumption, production, and infrastructure at both regional and national levels

analysis of other pollutants (PM_{10}, NO_2, SO_2, CO), we use air quality measurements from monitoring stations managed by the European Environment Agency. We assign each municipality to its nearest monitoring station using the same nearest-neighbour approach, but impose a 12.5 km maximum distance threshold between the station and the municipality centroid. This refinement mitigates cases where the geographically closest station lies too far away, thereby reducing the risk of misrepresenting local exposure levels.[13] Overall, these complementary approaches-gridded data (CAMS) for the main analysis and monitoring stations (EEA) for robustness-enhance the comprehensiveness and accuracy of our air quality assessment. The principal reference sample is derived from gridded data, while all supplementary variables are linked using municipality codes.

3.5 Sample

Our main sample covers 2015–2019, structured into biannual intervals comprising data from April to December of the previous year (t) and January to March of the following year ($t+1$). This approach ensures: (i) treatment irreversibility as required in (Callaway & Sant'Anna 2021)[14]; (ii) clean separation of heating and non-heating seasons to identify treatment effects; (iii) comparable pre-treatment trends across groups. We analyze four biennia: 2015–16, 2016–17, 2017–18, and 2018–19.

Table A5 presents a descriptive overview of health outcomes, air pollution, and weather conditions across Italian municipalities in our sample. Hospitalization rates for AMI,

[13] Monitoring stations are often strategically positioned near high-traffic roads to capture peak pollution exposure, which can result in higher recorded levels compared to spatial averages from gridded data. This measurement approach explains the observed 14% divergence between EEA monitoring data and CAMS gridded estimates for $PM_{2.5}$ (see Section 3.5, Table A5)

[14] The irreversibility hypothesis, often termed the "absorbing state" assumption, states that once a unit receives treatment, it remains treated in all subsequent periods. This assumption simplifies staggered DiD designs by allowing potential outcomes to depend solely on the initial treatment timing, rather than the full treatment history. It extends the parallel trends assumption by requiring comparable outcome trends across groups defined by treatment timing, while the no-anticipation condition ensures pre-treatment outcomes are unaffected by future treatment. Although irreversibility enhances tractability, recent work (e.g., (de Chaisemartin & D'Haultfœuille 2020)) explores its relaxation by allowing treatment reversal, but this requires generalisations of the parallel trends assumption and strong "no carryover" assumptions that current outcomes depend only on present treatment status, not past exposure, hence not suitable for our study.

STEMI, NSTEMI, stroke subtypes, and COPD exhibit modest but consistent declines. For instance, ischemic stroke hospitalizations fell from 4.65 cases (SD: 9.32) in 2015–16 to 3.83 (SD: 6.09) in 2018–19, while STEMI admissions decreased by 9.1% over the same period. Mortality rates remained stable for AMI, STEMI, NSTEMI, and hemorrhagic stroke (∼0.30, 0.14, 0.11, and 0.32 events/year, respectively) but declined for ischemic stroke (-16.7%) and COPD (-5.4%).

Air pollution declined over the study period. Mean $PM_{2.5}$ concentrations (CAMS data) fell from 16.40 $\mu g/m^3$ in 2015–16 to 13.35 $\mu g/m^3$ in 2018–19, with days exceeding WHO thresholds (15 $\mu g/m^3$) dropping by nearly 50%. Similar reductions were observed for PM_{10} and particularly for NO_2. Nevertheless, $PM_{2.5}$, PM_{10}, and NO_2 concentrations remained above recommended thresholds reported in Table A6. The observed discrepancies[15] between CAMS and EEA pollution metrics—particularly the 14% higher $PM_{2.5}$ levels in EEA monitoring data—underscore the importance of multiple data sources for exposure assessment. Weather conditions, including wind speed, temperature, and precipitation, remained relatively stable, though minor fluctuations (e.g., higher wind speeds in 2017–18 and greater precipitation in 2016–17) may have contributed to pollution dispersion. Having described our data sources and sample construction, we now turn to our identification strategy.

4 Empirical strategy

We estimate the causal effect of residential heating activation on air pollution and health outcomes using a staggered difference-in-differences design. Our identification strategy rests on two key choices: how we define treatment intensity across municipalities, and

[15] The divergence stems from measurement approaches: EEA monitors target high-exposure urban areas, capturing localized pollution peaks, while CAMS grids provide spatial averages that smooth out extreme values.

how we identify the moment heating is actually switched on. Both choices are motivated by a fundamental gap between regulated and actual heating behavior that we document below. Our ideal specification would classify municipalities by biomass consumption — the dominant source of residential $PM_{2.5}$ — and use official heating activation dates, which vary by climatic zone, as the treatment indicator for the post-period. However, two problems make this approach inadequate. First, over 65% of Italian households operate autonomous heating systems that are legally exempt from activation schedules, meaning official dates poorly capture actual behavior. Second, both households and municipalities respond to temperature shocks rather than fixed calendars, introducing a wedge between regulatory dates and real-world heating activation. We address both problems in turn.

First, we construct a measure of municipal exposure to biomass heating emissions through a three-stage spatial allocation procedure. Initially, we distribute regional biomass consumption obtained from Terna for the period 2015-2019 to municipalities using heating appliance penetration rates obtained from the 2011 ISTAT census. To identify heating systems fueled by biomasses we consider partial[16] residential heating appliances (RHA) and compute the regional share of such appliances as follows:

$$\text{Share\_Biomass\_heat}_{m,2011} = \frac{\text{Biomass\_heat}_{m,2011}}{\sum_{i=1}^{N_r^m} \text{Biomass\_heat}_{m,r,2011}} \tag{2}$$

Where the proportion of partial RHA in the municipality m during 2011 relative to its regional total is given by $\text{Share\_Biomass\_heat}_{m,2011}$. This represents the ratio between the numerator, $\text{Biomass\_heat}_{m,2011}$, which represents the number of partial RHAs in the

[16]The term "partial" residential heating appliances refers to fixed single-point heating systems (including fireplaces, stoves, radiators, or heat pumps) that provide localised heating to specific sections of a dwelling, as opposed to whole-house central heating systems. These appliances are characterised by: spatially limited coverage (heating individual rooms or zones), independent operation from building-wide heating infrastructure, direct combustion (in biomass-based systems) or point-source heat generation. Partial RHAs are particularly relevant for $PM_{2.5}$ exposure studies as they: exhibit higher emission intensities per unit heat output, show greater variation in usage patterns, are more likely to use solid biomass fuels ISTAT (2011).

municipality registered in 2011, and the denominator, $\sum_{i=1}^{N_r^m}$ Biomass_heat$_{m,r,2011}$, which represents the total number of partial RHAs in region r during 2011, with subscripts m, and r indexing municipalities, and regions respectively. Using these appliance shares, we distribute observed regional biomass consumption from Terna to municipalities through spatial disaggregation:

$$\text{Biomass}_{m,t} = \frac{(\text{Biomass}_{r,t} \times \text{Share\_Biomass\_heat}_{m,2011})}{\text{km}^2_{m,t}} \tag{3}$$

This transformation scales annual regional consumption $Biomass_{r,t}$ by each municipality's fixed appliance share, normalised by municipal area (km^2) to account for differences in municipality size. Next, we average these values across the years in our sample as follows:

$$\text{Biomass}_m = \frac{1}{\text{N}^T} \sum_{t=1}^{\text{N}^T} \text{Biomass}_{m,t} \tag{4}$$

Finally, we define as treated (controls) municipalities above (below) the median of such indicator[17].

$$\text{Treatment} = \begin{cases} 1 & \text{if Biomass}_m > 50^{\text{th}}\text{perc Biomass}_m \\ 0 & \text{otherwise} \end{cases} \tag{5}$$

Second, in order to identify the post-treatment period, we rely on behavioural responses to temperature-driven variations in heating demand. We consider that, according to equation 6, households will decide to turn on heating when the outdoor temperatures fall below a certain tipping point (an unknown, exogenous threshold at which heating becomes necessary). In order to identify this tipping point, we adopt a two-step approach. First, we

[17]As a robustness we also use different thresholds to identify treated and controls (above 66^{th} vs below 33^{rd} or above 75^{th} vs below 25^{th} percentile)

estimate the temporal patterns of temperature and heating activation using the following specification:

$$\mathrm{Y}_{r,w} = \gamma_0 + \gamma_r + \gamma_w + \nu_{r,w} \tag{6}$$

where r denotes regions and w indexes week-year observations. The dependent variable $\mathrm{Y}_{r,w}$ captures two distinct measures: (i) regional average temperature, reflecting climatic conditions, and (ii) Google search frequencies for the phrase "Turning on the heating system," serving as a behavioral proxy for household heating activation. The analysis focuses on transitional periods from April (t) to March ($t+1$) across the four biennial spans, with the coefficients of interest γ_w identifying week-year fixed effects that reveal temporal patterns in heating system usage. This approach allows us to disentangle regulatory heating periods from actual behavioral responses to environmental conditions. Specifically, we aim to verify whether a strong correlation exists between temperature drops and increases in Google searches for heating-related queries. If confirmed, Google Trends data will then serve to identify heating systems activation more precisely.

Second, to empirically identify the critical temperature thresholds that trigger heating activation, we estimate:

$$\mathrm{Y}_{r,w} = \delta_0 + \sum_{k=1}^{N_k} \delta_k \,\mathrm{Temp\_bins}_{r,w} + \delta_1 \,\mathrm{Wind\_speed}_{r,w} + \delta_2 \,\mathrm{Precipitations}_{r,w} + \delta_r + \delta_w + \psi_{r,w} \tag{7}$$

where r denotes the region and w the week-year observations. The dependent variable $Y_{r,w}$ captures the Google trend searches for the term "Turning on the heating system", while $Temp\_bins_{r,w}$ represents 0.5-degree temperature bins (from 28 to 0 degrees Celsius). The coefficients of interest are δ_k. We identify the critical temperature threshold for heating activation (T^*) as the first temperature bin at which Google search interest for "Turning on the heating system" becomes statistically significant ($\delta_k \neq 0$). This approach ensures that we exclude post-threshold periods where heating is already widespread, avoiding violations of the common trend assumption in subsequent causal analyses. We define the post-treatment period based on the week when temperature first falls below T^*, but operationalise it at the monthly level to match hospitalization data granularity.

This strategy allows us to capture the causal effect of heating-driven pollution exposure, avoiding the common threats to identification in the literature connected with the presence of compensatory behaviours driven by reactions to pollution alerts, Neidell (2004) for two main reasons: (i) pollution exposure is random, i.e. individuals cannot anticipate the week when the temperature drops below T^*, (ii) the control group of municipalities with under the median biomass consumption is exposed to similar pollution alerts, allowing us to net out their effects with the DD strategy. According to the latter point, one may argue that treated municipalities are likely to be exposed to higher levels of pollution alerts. However, this would bias our estimated coefficients downward, making it a lower bound.

In addition, it must be noted that the week when the outside temperature reaches T^* will be different between municipalities according to their location, year-specific weather conditions and other factors making our design compatible with a staggered DiD (de Chaisemartin & D'Haultfœuille (2020), Callaway & Sant'Anna (2021), and Wooldridge (2021)). In particular, in our analysis, we adopt the regression-adjusted (RA) version of Callaway & Sant'Anna (2021) estimator, which provides several key advantages for our research context. This approach estimates group-time average treatment effects on the treated

(ATT) under three critical identifying assumptions: (1) treatment irreversibility (once a municipality presents biomass heating consumption above the median, it cannot revert to non-treated status), (2) the absence of anticipatory effects (outcomes are unaffected by future treatment adoption), and (3) parallel trends between later-treated groups and never-treated units. The RA estimator is particularly suitable for our setting as it accommodates the observed variation in municipal heating adoption timing while mitigating potential biases from time-varying confounders through covariate adjustment.

We estimate group-time average treatment effects (ATT) as follows:

$$\text{ATT}(g,t) = \mathbb{E}\left[\frac{G_g}{\mathbb{E}[G_g]}\Big(Y_t - Y_{g-1} - \mathbb{E}[Y_t - Y_{g-1} \mid X, G = NT]\Big)\right] \tag{8}$$

Let Y represent both pollution levels - $PM_{2.5}$ (CAMS) and NO_2[18] - and health outcomes - AMI, STEMI, NSTEMI, Ishemic and Hemorrhagic Stroke, and COPD[19] - for municipality g in month-year t. G_g indicates treatment timing (with $G_g = NT$ for never-treated units), and X represents weather controls including wind speed, temperature, and precipitation. We compute weather variables as two-week moving averages, incorporating both the current week's value and its first lag (i.e., the previous week's value). These controls are included to account for potential confounding factors that may influence both pollution levels and health outcomes, such as cardiovascular and pulmonary hospitalisations. Temperature and precipitation can directly affect air quality, while wind speed can influence the dispersion of pollutants. The main model considers municipality fixed effects control for unobserved heterogeneity.

[18] For robustnes pruposes we will use $PM_{2.5}$ (EEA), PM_{10}, SO_2 and CO.

[19] Health outcomes are expressed as rates per 10,000 individuals, calculated by dividing the raw counts by the municipal population.

5 Results

5.1 Identification of treated and controls and of temperature-driven heating systems activations

We first examine variations in pollution levels across the months in which heating systems are activated, distinguishing between the pre-activation and post-activation periods. The pre-activation period encompasses the months from June to September, while the post-activation period covers October to January. By comparing the sub-figures in Figure A3, we observe that $PM_{2.5}$ levels are higher during the heating activation months (Figure A3b). The Po Valley is among the most polluted areas of Italy, with pollution levels exceeding those of other regions even in summer months (Figure A3a). This phenomenon is primarily attributable to its unique morphology, which traps air pollutants, as well as to its high degree of industrialisation, which further exacerbates pollution. During winter, a marked increase in $PM_{2.5}$ levels is also observed in municipalities located in the Apennines, a region characterised by colder average temperatures.

Figure A4 plots estimates of γ_w coefficients from equation 6 for both temperatures and Google search activity related to turning on heating system. The black dashed vertical line marks the first notable temperature drop, coinciding with a sharp increase in Google searches, while the red dashed vertical line indicates the earliest legally permitted activation date (i.e. 15th of October in areas D/E). Across all biennia, search activity rises markedly following the first substantial temperature decline- approximately two weeks before the legal start date. This pattern seems to suggest that Google Trends data provide a reliable proxy for the actual timing of heating activation, capturing behavioral responses more accurately than fixed regulatory dates, which systematically lag behind real-world usage due to their rigid, administrative nature.

In Figure A5, we plot δ_k coefficients estimated from equation 7. Google searches for heating-related terms rise significantly relative to the reference week (week 16[20]) once temperatures fall below 18°C and remain elevated until 12°C, defining a temperature band where the level of uncertainty about the possibility of heating activation is maximum. The critical temperature threshold for heating activation (T^*) is the first temperature bin at which Google search interest for "Turning on the heating system" becomes statistically significant and corresponds to 18°C.

Figure A6 illustrates the distribution of the treatment across Italian municipalities. Notably, when compared with the distribution of $PM_{2.5}$ levels following heating system activation shown in Figure A3b, it is clear that municipalities exhibiting high $PM_{2.5}$ emissions map closely to the treated municipalities.

5.2 Baseline results

5.2.1 Impact of heating system activation on pollutant emissions

Figure 1 shows the effects of treatment on $PM_{2.5}$ levels in treated municipalities relative to controls, across different lengths of exposure to the treatment. The Figure presents monthly lead-lag estimates, calculated as aggregated $ATT(g,t)$ estimates from Equation 8, to show the dynamics between treated (T) and comtrol (C) municipalities n months before and after reaching T^*. Results are shown for $PM_{2.5}$ (from CAMS) over four biennia (2015-2016, 2016-2017, 2017-2018, 2018-2019).

The x-axis reports months relative to heating activation (time 0), including four lead months (pre-activation) and five lag months (post-activation), thereby capturing the tem-

[20]This corresponds to the last week of April.

poral dynamics of the exposure effects. The null lead coefficients indicate no differential pre-trends between treated and control municipalities prior to heating system activation. In contrast, the statistically significant positive lag coefficients indicate a sustained, monotonically increasing divergence in $PM_{2.5}$ concentrations, with treated municipalities consistently exhibiting higher pollution levels than controls following activation.

Figure 1: The monthly effect of Heating system activation on $PM_{2.5}$ (2015-2019)

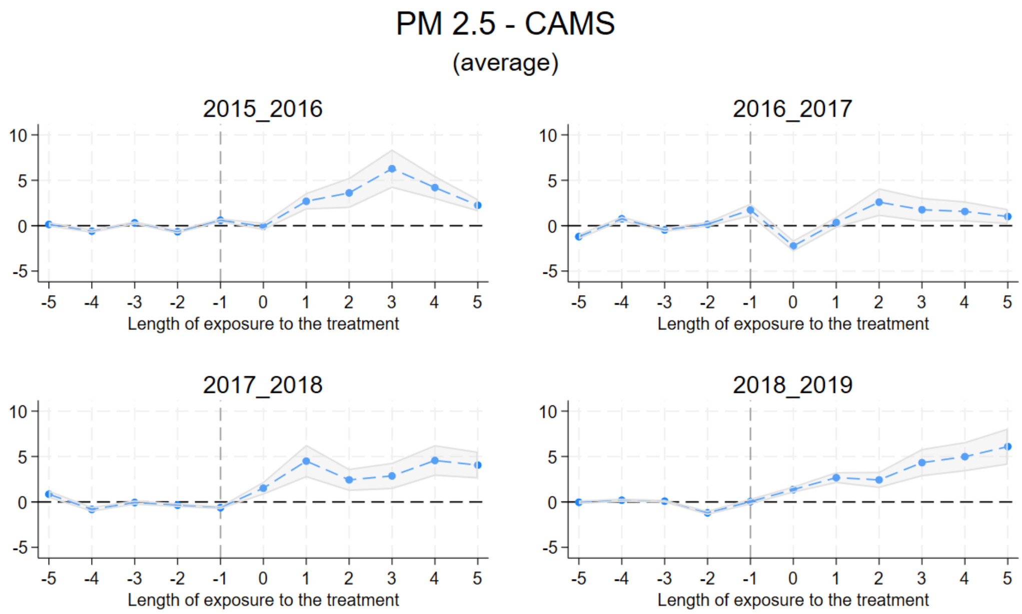

Notes: This figure displays monthly lead-lag estimates of the Average Treatment Effect on the Treated (ATT) for $PM_{2.5}$ levels, comparing treated and control municipalities before and after heating system activation (T^*). The x-axis indicates months relative to activation (time 0), with four pre-activation lead months and five post-activation lag months. Estimates represent aggregated ATT(g,t) values from Equation 8, using $PM_{2.5}$ data from CAMS across four biennia (2015–2016 to 2018–2019). The y-axis shows the ATT magnitude (difference in $PM_{2.5}$ levels between treated and control groups).

The estimated ATTs in Table 1 reveal statistically significant effects of heating system activation on particulate matter concentrations across all biennia analysed. Specifically, for average $PM_{2.5}$ levels (Panel A), the estimates indicate particularly pronounced effects in 2015-16 (3.070 μg/m^3), 2017-18 (3.423 μg/m^3), and 2018-19 (3.416 μg/m^3), corresponding to increases of 18.7%, 26.6%, and 25.5% relative to respective period means. In contrast, the coefficient for 2016-17 (0.831 μg/m^3) suggests a more modest yet still statistically detectable effect (5.3% increase). This attenuated effect may be attributed to milder winter conditions, as illustrated in Figures A4c and A4d, where the 2016/2017 period is characterized by a unique pattern: a sharp, singular drop in temperature occurs precisely when Google Trends searches spike. Notably, in the subsequent weeks, temperatures remain consistently elevated and while Google search volumes decline relative to other years.

Table 1: The effect of Heating system activation on $PM_{2.5}$ (2015-2019)

	2015-2016 (1)	2016-2017 (2)	2017-2018 (3)	2018-2019 (4)
A. Average Effects				
ATT	3.070***	0.831*	3.423***	3.416***
	(0.528)	(0.445)	(0.696)	(0.538)
Mean of Y	16.45	15.64	12.86	13.39
SD of Y	7.181	6.522	6.313	7.598
Observations	5,684	5,679	5,690	5,672
B. Above 75th Percentile				
ATT	0.610***	0.102	0.711***	0.759***
	(0.120)	(0.0979)	(0.147)	(0.131)
Mean of Y	1.578	1.396	0.848	0.898
SD of Y	1.731	1.567	1.409	1.592
Observations	5,684	5,679	5,690	5,672

Notes: The table presents difference-in-differences estimates of the average treatment effect on the treated (ATT) of heating system activation on $PM_{2.5}$ CAMS levels. Panel A shows effects on average $PM_{2.5}$ CAMS levels, while Panel B focuses on the upper quartile of the outcome distribution. Standard errors at municipal level are in parentheses; *** p<0.01, ** p<0.05, * p<0.1.

The average ATT estimates (3.07-3.42μg/m^3) are substantial, exceeding half of the WHO annual mean guideline (5 μg/m^3) in all years. For extreme pollution events (see Panel B: >75th percentile), the ATT coefficients remain statistically significant in three of the four biennia (2015-16, 2017-18 and 2018-19), corresponding to sizable relative increases of 38.7%, 83.8%, and 84.5% respectively. Significant effects for both average and extreme $PM_{2.5}$ in these biennia point to robust effects of heating system activation.

Figure 2 presents monthly lead-lag estimates from Equation 8 for NO_2 across the four biennia (2015-2019). The estimates, also in this case, confirm parallel pre-trends (null leads) and show treatment effects that increase monotonically after activation (significant positive lags), consistent with the heating activation hypothesis.

Figure 2: The monthly effect of Heating system activation on NO_2 (2015-2019)

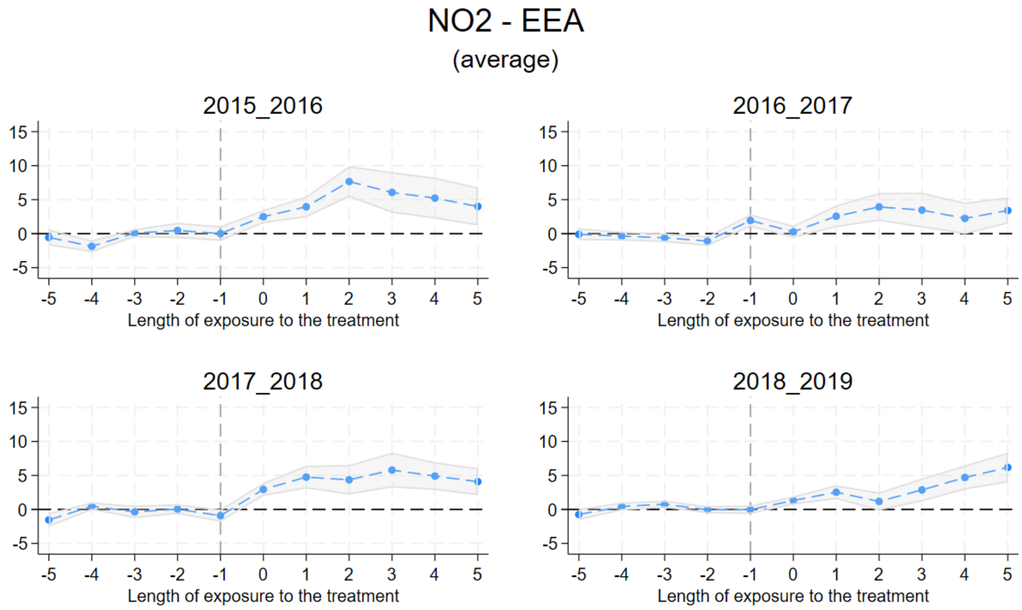

Notes: This figure displays monthly lead-lag estimates of the Average Treatment Effect on the Treated (ATT) for NO_2 levels, comparing treated and control municipalities before and after heating system activation (T^*). The x-axis indicates months relative to activation (time 0), with four pre-activation lead months and five post-activation lag months. Estimates represent aggregated ATT(g,t) values from Equation 8, using NO_2 data from EEA across four biennia (2015–2016 to 2018–2019). The y-axis shows the ATT magnitude (difference in NO_2 levels between treated and control groups).

The analysis shows that heating system activation results in statistically significant increases in NO_2 concentrations across all observed winter periods (2015-2019), as shown in Table 2. The estimated average treatment effects (ATT) range from 2.63 to 4.90 μg/m^3, equivalent to 10.9% to 19.5% increases relative to seasonal means. These results indicate that combustion-based heating is a substantial source of NO_2 pollution. The effects intensify during extreme pollution episodes ($> 75^{\text{th}}$ percentile), with NO_2 levels increasing by 0.54–0.77 μg/m^3—88.2% to 113.6% above the period mean.

Table 2: Impact of Heating system activation on NO_2 EEA (2015-2019)

	2015-2016 (1)	2016-2017 (2)	2017-2018 (3)	2018-2019 (4)
A. Average Effects				
ATT	4.896***	2.628***	4.457***	3.091***
	(1)	(0.804)	(0.873)	(0.619)
Mean of Y	25.13	24.09	23.05	21.49
SD of Y	15.57	15.18	14.62	13.83
Observations	4,456	4,903	5,207	5,276
B. Above 75th Percentile				
ATT	0.769***	0.543***	0.600***	0.556***
	(0.124)	(0.116)	(0.113)	(0.0806)
Mean of Y	0.677	0.616	0.562	0.436
SD of Y	1.476	1.394	1.263	1.118
Observations	4,473	4,978	5,237	5,327

Notes: The table presents difference-in-differences estimates of the average treatment effect on the treated (ATT) of heating system activation on NO_2 EEA levels. Panel A shows effects on average NO_2 EEA levels, while Panel B focuses on the upper quartile of the outcome distribution. Standard errors at municipal level are in parentheses; *** p<0.01, ** p<0.05, * p<0.1.

5.2.2 Impact of heating system activation on health outcomes

We now shift focus on health outcomes, and examine whether the observed changes in air pollution translate into measurable impacts on hospitalisations and in hospital mortality. Figures A7a and A7b present monthly lead-lag estimates (pre and post activation of the heating systems, respectively) of the dynamic $ATT(g,t)$ aggregation from Equation 8 for AMI hospitalisations and in-hospital mortality rates throughout the four winter periods (2015-2019). Lead coefficients are not statistically different from zero, showing the absence of differential trends between treated and controls before the activation of the heating systems. For hospitalisations, all biennia display a clear post-activation increase, with admission rates rising sharply among treated municipalities. This suggests an immediate and substantial health impact associated with the activation of heating systems. In contrast, mortality estimates show no consistent lag pattern, with values fluctuating around zero and suggesting weaker (see 2015-2016) or negligible effects on in-hospital AMI deaths.

Table 3: Average Treatment Effects on the Treated on AMI Outcomes (2015-2019)

	2015-2016 (1)	2016-2017 (2)	2017-2018 (3)	2018-2019 (4)
A. Admission Rate (per 10,000 inhabitants)				
ATT	1.215*	0.865	2.844***	2.675***
	(0.648)	(0.755)	(0.768)	(0.489)
Mean outcome	16.06	16.14	15.96	15.86
SD outcome	21.20	21.34	20.84	20.86
Observations	5,684	5,679	5,690	5,672
B. In-Hospital Mortality Rate (per 10,000 inhabitants)				
ATT	0.385***	-0.022	-0.048	0.113
	(0.147)	(0.149)	(0.249)	(0.110)
Mean outcome	1.097	1.101	1.098	0.985
SD outcome	2.035	2.052	2.035	1.871
Observations	5,684	5,679	5,690	5,672

Notes: The table presents difference-in-differences estimates of average treatment effects on the treated (ATT) on AMI outcomes. Panel A shows effects on hospital admission rates, while Panel B examines in-hospital mortality rates. Standard errors at municipal level are in parentheses; *** p<0.01, ** p<0.05, * p<0.1.

The regression results in Table 3 corroborate the graphical evidence, showing that heating system activation significantly increases AMI hospitalisation rates in three of four winters. In 2015-2016, the ATT of 1.215 per 10,000 inhabitants presents a 7.6% increase over the mean admission rate (16.06). The largest effects occur in 2017-2018 and 2018-2019, with ATTs of 2.844 and 2.675 representing 17.8% and 16.9% increases over their respective means (15.96 and 15.86). These results align with epidemiological evidence linking short-term $PM_{2.5}$ and NO_2 exposure to acute cardiovascular events (Brook et al. (2010)). For in-hospital mortality, only the 2015-2016 shows a significant ATT (0.385, an 35.1% increase wrt to its 1.097 mean value), while other years show no effects, suggesting that effective acute care may offset mortality risks despite higher admissions.

Estimates for STEMI outcomes (see Figure A8) confirm the absence of pre-trends. In contrast, lags estimates reveal distinct temporal patterns for hospital admissions and in-hospital mortality. For hospital admissions (see Figure A8a), significant increases are observed in 2017-2019. Conversely, in-hospital mortality (see Figure A8b) shows a significant elevation only in 2015-2016 that persists throughout all the 5 monthly lags, with no statistically significant effects in subsequent periods.

Table 4: Average Treatment Effects on the Treated on STEMI Outcomes (2015-2019)

	2015-2016 (1)	2016-2017 (2)	2017-2018 (3)	2018-2019 (4)
A. Admission Rate (per 10,000 inhabitants)				
ATT	0.591	0.100	1.051***	1.180***
	(0.441)	(0.402)	(0.359)	(0.290)
Mean of Y	6.749	6.575	6.352	6.184
SD of Y	10.14	9.993	9.399	9.260
Observations	5,684	5,679	5,690	5,672
B. In-Hospital Mortality Rate (per 10,000 inhabitants)				
ATT	0.287**	-0.0130	0.0448	0.0492
	(0.116)	(0.106)	(0.106)	(0.0810)
Mean of Y	0.563	0.565	0.550	0.513
SD of Y	1.277	1.281	1.248	1.194
Observations	5,684	5,679	5,690	5,672

Notes: The table presents difference-in-differences estimates of average treatment effects on the treated (ATT) on STEMI outcomes. Panel A shows effects on hospital admission rates, while Panel B examines in-hospital mortality rates. Standard errors at municipal level are in parentheses; *** p<0.01, ** p<0.05, * p<0.1.

The estimates in Table 4 show statistically significant increases in STEMI admission rates during the 2017-2018 (ATT = 1.051) and 2018-2019 (ATT = 1.180) winters. These effects correspond to substantial relative increases of 16.6% and 19.1% above their respective mean admission rates of 6.352 and 6.184 per 10,000 inhabitants. For in-hospital mortality, a significant effect appears only in 2015-2016 (ATT = 0.287), representing a 51.0% increase from the baseline mortality rate of 0.563 per 10,000 inhabitants. Overall, these results indicate a significant effect on STEMI morbidity, with notably stronger effects on admission rates in recent years, whereas mortality effects appear more sporadic.

For NSTEMI outcomes, lags in Figure A9 reveal significant increases in admission rates during 2017-2018 and 2018-2019 following heating activation, while in-hospital mortality rates show a significant rise only in 2018-2019. Null leads support parallel pre-trends.

Table 5: Average Treatment Effects on the Treated on NSTEMI Outcomes (2015-2019)

	2015-2016 (1)	2016-2017 (2)	2017-2018 (3)	2018-2019 (4)
A. Admission Rate (per 10,000 inhabitants)				
ATT	0.326	0.665	1.746***	1.355***
	(0.457)	(0.582)	(0.560)	(0.385)
Mean of Y	8.537	8.860	8.898	8.913
SD of Y	12.21	12.43	12.05	12.19
Observations	5,684	5,679	5,690	5,672
B. In-Hospital Mortality Rate (per 10,000 inhabitants)				
ATT	0.0835	0.0613	0.0105	0.161***
	(0.0909)	(0.0739)	(0.0889)	(0.0577)
Mean of Y	0.334	0.370	0.373	0.325
SD of Y	0.918	1.048	1.003	0.897
Observations	5,684	5,679	5,690	5,672

Notes: The Table presents difference-in-differences estimates of average treatment effects on the treated (ATT) on NSTEMI outcomes. Panel A shows effects on hospital admission rates, while Panel B examines in-hospital mortality rates. Standard errors at municipal level are in parentheses; *** p<0.01, ** p<0.05, * p<0.1.

This is corroborated by the DID results in Table 5, which show statistically significant increases in NSTEMI admission rates during 2017–2018 (ATT = 1.746) and 2018–2019 (ATT = 1.355), corresponding to relative increases of 19.6% and 15.2% above mean rates of 8.898 and 8.913 per 10,000 inhabitants, respectively. For in-hospital mortality, only the 2018-2019 period shows statistical significance (ATT=0.161), representing a 49.5% increase from the mean mortality rate (0.325 per 10,000).

We next examine stroke subtypes. The analysis reveals distinct patterns between ischemic and hemorrhagic strokes. As shown in Figures A10 and A11, all lead estimates are statistically insignificant, confirming the presence of parallel pre-treatment trends. Similarly, the lag estimates seem to indicate no significant effects during the five months following heating system activation.

For ischemic stroke, we identify no statistically significant impact of heating system activation on either admission or mortality rates across all study periods, as reported in Table 6. In contrast, hemorrhagic stroke outcomes show some, significant effects (see Table 7):

Table 6: Average Treatment Effects on the Treated on Ischemic Stroke Outcomes (2015-2019)

	2015-2016	2016-2017	2017-2018	2018-2019
	(1)	(2)	(3)	(4)
A. Admission Rate (per 10,000 inhabitants)				
ATT	0.532	2.850	0.961	-0.661
	(0.857)	(2.101)	(1.475)	(0.521)
Mean of Y	15.72	15.35	14.96	14.20
SD of Y	21.02	20.72	19.65	18.62
Observations	5,684	5,679	5,690	5,672
B. In-Hospital Mortality Rate (per 10,000 inhabitants)				
ATT	0.164	0.234	0.0515	0.182
	(0.262)	(0.201)	(0.233)	(0.144)
Mean of Y	1.553	1.501	1.504	1.324
SD of Y	2.782	2.723	2.711	2.386
Observations	5,684	5,679	5,690	5,672

Notes: The table presents difference-in-differences estimates of average treatment effects on the treated (ATT) on Ischemic Stroke outcomes. Panel A shows effects on hospital admission rates, while Panel B examines in-hospital mortality rates. Standard errors at municipal level are in parentheses; *** $p<0.01$, ** $p<0.05$, * $p<0.1$.

admission rates rose by 26.2% (ATT=1.310) in 2016–2017 relative to the mean rate of 5.004 per 10,000 inhabitants, while mortality rates increased significantly in 2015–2016 (ATT=0.446, +37.0% vs. mean 1.207/10,000) and 2017–2018 (ATT=0.528, +41.7% vs. mean 1.265/10,000). These results suggest that heating-related pollution may disproportionately affect hemorrhagic stroke outcomes compared to ischemic events, particularly for acute mortality.

Lastly, Figure A12 for COPD reveals no evidence of pre-existing differential trends across its leads and a consistent upward trend in hospitalizations lags for treated municipalities with respect to controls, while showing no discernible pattern for in-hospital mortality.

Table 8 shows statistically significant increases in admission rates for all biennia: 2015-2016 (ATT = 2.136, +23.8% versus mean 8.972 per 10,000 inhabitants), 2016-2017 (ATT = 1.279, +14.5% versus 8.802), 2017-2018 (ATT=2.284, +27.4% versus 8.323), and 2018-2019 (ATT=1.828, +22.5% versus 8.137). In contrast, in-hospital mortality shows no significant effects in any year. These results indicate that while heating system activation

Table 7: Average Treatment Effects on the Treated on Hemorrhagic Stroke Outcomes (2015-2019)

	2015-2016	2016-2017	2017-2018	2018-2019
	(1)	(2)	(3)	(4)
A. Admission Rate (per 10,000 inhabitants)				
ATT	0.511	1.310*	0.991	0.0552
	(0.555)	(0.783)	(0.646)	(0.427)
Mean of Y	4.921	5.004	5.158	5.031
SD of Y	7.683	7.859	7.948	7.884
Observations	5,684	5,679	5,690	5,672
B. In-Hospital Mortality Rate (per 10,000 inhabitants)				
ATT	0.446***	-0.0100	0.528*	0.124
	(0.173)	(0.164)	(0.280)	(0.128)
Mean of Y	1.207	1.232	1.265	1.233
SD of Y	2.318	2.352	2.418	2.454
Observations	5,684	5,679	5,690	5,672

Notes: The table presents difference-in-differences estimates of average treatment effects on the treated (ATT) on Hemorrhagic Stroke outcomes. Panel A shows effects on hospital admission rates, while Panel B examines in-hospital mortality rates. Standard errors at municipal level are in parentheses; *** p<0.01, ** p<0.05, * p<0.1.

substantially exacerbates COPD morbidity (with relative increases of 14.5-27.4% above baseline admission rates), it does not appear to significantly impact short-term mortality outcomes. The persistent hospitalization effects observed across years, despite fluctuations in pollution and meteorological conditions, underscore the heightened vulnerability of COPD patients to heating-related air pollution.

Table 8: Average Treatment Effects on the Treated on COPD Outcomes (2015-2019)

	2015-2016	2016-2017	2017-2018	2018-2019
	(1)	(2)	(3)	(4)
A. Admission Rate (per 10,000 inhabitants)				
ATT	2.136**	1.279*	2.284**	1.828***
	(0.916)	(0.668)	(1.016)	(0.664)
Mean of Y	8.972	8.802	8.323	8.137
SD of Y	13.07	13.34	12.12	11.47
Observations	5,684	5,679	5,690	5,672
B. In-Hospital Mortality Rate (per 10,000 inhabitants)				
ATT	-0.00365	0.0559	0.0459	-0.0565
	(0.0822)	(0.113)	(0.137)	(0.0923)
Mean of Y	0.427	0.454	0.439	0.387
SD of Y	1.094	1.293	1.220	1.075
Observations	5,684	5,679	5,690	5,672

Notes: The table presents difference-in-differences estimates of average treatment effects on the treated (ATT) on COPD outcomes. Panel A shows effects on hospital admission rates, while Panel B examines in-hospital mortality rates. Standard errors at municipal level are in parentheses; *** p<0.01, ** p<0.05, * p<0.1.

5.3 Robustness

To ensure the reliability of our findings, we conduct several robustness checks. First, we introduce interaction terms between the treatment indicator and contemporaneous weather conditions (wind speed, precipitation, and temperature). Second, we assess the impact of heating system activation on alternative pollution measures, namely $PM_{2.5}$, PM_{10}, SO_2 and CO from EEA ground-level monitoring stations. Third, to assess sensitivity to exposure intensity definitions, we vary the classification of treated and control municipalities using alternative thresholds: (i) above the 66^{th} versus below the 33^{rd} percentile and (ii) above the 75^{th} versus below the 25^{th} percentile in municipal biomass consumption. Fourth, we apply the robust inference and sensitivity analysis of Rambachan & Roth (2023) to assess the validity of the parallel trends assumption and quantify potential bias from violations. Fifth, we conduct falsification tests using health outcomes unrelated to pollution. We further extend our main analysis by (i) weighting estimates by municipal population to account for heterogeneous exposure across densely versus sparsely populated areas, (ii) controlling for spillover effects from neighboring municipalities (within 30 km) to ensure pollution impacts are not confounded by cross-boundary diffusion, and (iii) implementing the augmented inverse probability weighting (AIPW) version of the Callaway & Sant'Anna (2021) estimator for improved efficiency and double robustness. Finally, we test for selective migration by examining whether individuals systematically relocate away from (or avoid moving into) high-pollution municipalities, which could bias our health effect estimates. Collectively, these robustness checks substantially reinforce the credibility of our causal inferences.

5.3.1 Alternative weather specifications

Table A3 and A4 present the ATT estimates from the augmented specification that interacts the treatment indicator with contemporaneous weather conditions. This specification allows the effect of meteorology to vary across groups, ensuring a causal comparison between units with similar weather-response dynamics. The point estimates are highly consistent with our baseline findings in both magnitude and statistical significance, providing strong evidence that this potential source of heterogeneity does not confound the identified effects.

5.3.2 Impact of heating system activation on other pollutant emissions

Figure A13 displays the dynamic aggregation of ATTs estimated from Equation 8 for EEA $PM_{2.5}$ across four biennia (2015-2019). Results are confirmed: null pre-treatment trends and monotonically rising $PM_{2.5}$ divergence post-activation. However, the effect magnitudes exceed previous estimates. The discrepancy is attributable to non-random station placement, as EEA monitors are strategically located in high-pollution urban areas. The point estimates in Table A7 demonstrate ATTs consistent with those reported in the previous Table 1, though larger in magnitude confirming the results in Figure A13. Figure A14 displays dynamic aggregation of ATTs estimated from Equation 8 for PM_{10} across the four biennia (2015-2019). Null lead coefficients confirm parallel pre-treatment trends, while significant positive lags indicate monotonically increasing PM_{10} divergence post-activation, with treated municipalities exhibiting systematically higher pollution than controls, as before. The ATTs point estimates in Table A8, also in this case, confirm an increase in the level of PM_{10}.

Figures A15 andA16 extend our analysis to additional pollutants. While parallel pre-trends hold for SO_2 and CO, the post-activation effects differ markedly: most lag coefficients are statistically insignificant or weak (notably SO_2 in 2018-19 and CO in 2015-16 and 2017-18).

The analysis further examines the impacts of heating system activation on the additional pollutants (SO_2 Table A9 and CO Table A10), which exhibit distinct patterns compared to the primary combustion-related pollutants ($PM_{2.5}$, PM_{10}, and NO_2). Although SO_2 shows modest but significant increases (0.45-0.63 μg/m^3; 15.9-22.76% increase relative to the respective average value) in most years, consistent with fossil fuel combustion, effects on CO are more sporadic, with significant spikes only in certain periods, likely reflecting incomplete combustion episodes. Most importantly, we observe these variations in mean pollutant concentrations rather than extreme (peak) exposure levels where we register an increase of 71% for SO_2 in 2018-19 and another for CO by 77.5% in 2017-2018. These findings suggest that while PM and NO_2 remain the dominant health threats from heating systems, ancillary pollutants like SO_2 and CO may contribute to acute exposures, particularly in areas reliant on sulfur-rich fuels or inefficient combustion (Zhang & Smith (2007), WHO (2014)).

5.3.3 Alternative treatment thresholds

Table A11 demonstrates robust evidence that residential heating activation significantly increases air pollution concentrations ($PM_{2.5}$, PM_{10}, NO_2) and regulatory exceedance days across multiple treatment thresholds (66^{th} vs. 33^{rd} and 75^{th} vs. 25^{th} percentiles), with most estimates statistically significant.[21] Effects are consistently positive and statistically significant, with larger magnitudes under stricter thresholds, supporting a dose-

[21] One exception is $PM_{2.5}$(CAMS) "Days Over Threshold" in 2016–17, where ATT estimates (0.102, 0.148, 0.304) are positive but not statistically significant, reflecting a milder winter in those years.

response relationship. These findings confirm that heating systems disproportionately harm highly exposed areas.

The results remain robust across alternative threshold definitions for residential heating activation, with consistent findings also observed in the estimated health effects, as shown in TableA12. For AMI, STEMI, and COPD hospitalisations, the treatment effects not only maintain statistical significance across all threshold specifications but also exhibit a dose-response pattern, with point estimates generally increasing in magnitude under stricter exposure cutoffs. This monotonic relationship is particularly evident in the case of AMI (rising from 1.22 at median to 2.76 at 75-25) and COPD hospitalisations (increasing from 2.14 to 4.03). Similarly, the in-hospital mortality effects are confirmed. The few exceptions (notably ischemic and hemorrhagic strokes' null effects at median but significant estimates at higher thresholds) suggest a critical exposure-intensity threshold for cardiovascular impacts. The consistent treatment effects across threshold specifications demonstrate robustness to exposure classification with particularly pronounced health impacts observed in the most highly exposed areas.

5.3.4 Diagnostics for parallel trends violations

We also evaluate potential violations of the parallel trends assumption using the "honest" approach developed by Rambachan & Roth (2023). This method quantifies how much the post-treatment trend can deviate from the pre-treatment pattern before our results become invalid. Specifically, we consider the break point parameter M (ranging from 0.25 to 2), where M=2 represents a 200% deviation from the pre-treatment trend that would nullify our findings.

The results in Table A13 demonstrate remarkable resilience: $PM_{2.5}$ and PM_{10} effects remain statistically significant up to M=1.25 at Lag 4 (4 months after heating activation), while NO_2 effects persist up to M=1. Notably, considering the number of days with pollution levels above the 75^{th} percentile, the estimates are consistent with similar deviations without falling below. These effects would only be invalidated by implausibly large violations (M>1.75), providing strong evidence that residential heating activation causally increases pollution levels. The results of Table A14 demonstrate varying resilience to parallel trends violations across health outcomes when measured by the M parameter (range: 0.25-2). COPD effects at Lag 5 persist up to M=1.5, indicating robust causal evidence, as this exceeds typical pre-treatment fluctuations (M<1). Acute cardiovascular outcomes remain significant up to M=1.0-1.25, still above plausible violation thresholds. The required M values to nullify effects (M>1.5 for COPD, M>1.0-1.25 for AMI/STEMI) exceed observed pre-period deviations, supporting causal interpretation.

5.3.5 Placebo: effects of heating activation on unrelated-pollution health outcomes

We next evaluate whether heating system activation influences health outcomes unrelated to pollution exposure, including fractures, infections, traumatism, poisoning, elective admissions, and nervous system and mental health disorders[22]. Figure A17 and the DiD estimates in Table A15 show no statistically significant effects of heating system activation throughout the 2015-2019 period. Most ATT estimates are small and statistically insignificant, with only a few isolated exceptions (e.g., a marginally significant effect on traumatism hospitalizations in 2015-16 and 2018-19, and a weakly significant effect on mental health mortality in 2018-19). The absence of systematic effects across these unrelated outcomes supports the validity of our identification strategy and strengthens the causal interpretation of our main results.

[22]See Table A16 for ICD9-CM classification of placebo outcomes.

5.3.6 Alternative weighted estimates

The extended analyses confirm robust heating system effects on emissions across three critical dimensions (see Table A17). Population-weighted estimates show systematically larger effects than baseline results, consistent with disproportionate urban exposure, while spatial adjustments yield smaller estimates (e.g., $PM_{2.5}$ CAMS decreasing from 3.96 to 2.41 μg/m^3) due to cross-boundary pollution diffusion. The doubly robust AIPW estimates confirm our core findings, with particularly strengthened $PM_{2.5}$ effects during the 2017-18 winter period. These patterns remain consistent when examining threshold-exceedance days (Table A6), suggesting that our baseline estimates represent conservative lower bounds, with true causal effects likely lying between the spillover-adjusted and population-weighted values.

The health outcomes analyses in Table A18 show consistent treatment effects across methods, though with greater outcome-specific variation than pollution results. Population-weighting reveals stronger effects for respiratory and cardiovascular emergencies, highlighting disproportionate impacts in dense, heating-system areas. Spatial adjustments yield larger hospitalisation estimates (e.g., AMI: 3.08 vs 1.74 for 2017-18), likely reflecting cross-boundary patient mobility. AIPW estimates confirm causal effects for key outcomes (AMI, STEMI, NSTEMI, COPD), while showing nuanced mortality patterns (e.g. insignificant hemorrhagic stroke mortality). COPD effects are generally positive across specifications, underscoring respiratory vulnerability. [23]. These results, also in this case, confirm that our baseline estimates are conservative, with true impacts likely between population-weighted and spillover-adjusted values.

[23] The typical magnitude of statistically significant estimates ranges from 1.42 to 2.53 hospitalisations. Some estimates, such as the AIPW result for 2016–17 (0.478, s.e. 0.702), are smaller and not statistically significant, reflecting imprecision in certain estimator–year combinations.

5.3.7 Mobility

Table A19 reports the estimated coefficients for $PM_{2.5}$, NO_2, SO_2 and CO exposure are statistically insignificant in most specifications, with two exceptions. First, NO_2 exposure is associated with a significant increase in emigration (coefficients ranging from 5.87 to 7.54). Second, SO_2 exposure shows a weakly negative effect on emigration in specification (11) (-6.38) while net inflow remains statistically indistinguishable from zero. This suggests that elevated SO_2 levels do not induce protective migration behaviour. Critically, $PM_{2.5}$, the primary pollutant of interest in our main analysis, has no significant effect on mobility across all specifications.[24] The absence of systematic migration responses to pollution supports the exogeneity of exposure variation in our setting and suggests that mobility-related confounding is unlikely to drive our main results.

5.4 Heterogeneity

The estimates presented in previous sections may conceal substantial heterogeneity. We explore two dimensions. First we check whether the effects of heating activation on $PM2.5$, $PM10$, and $NO2$ vary by climatic zones. Second, we investigate differential effects on main health outcomes by socioeconomic and demographic characteristics (including gender, age, level of education, comorbidity status [25]).

[24] Income and weather controls (precipitation, wind speed) show no consistent patterns, except for precipitation's robust negative association with emigration (-5.61), likely reflecting broader seasonal migration trends.

[25] We define comorbidity as the presence of at least one of the following conditions: congestive heart failure, peripheral vascular disease, cerebrovascular disease, dementia, chronic pulmonary disease, connective tissue/rheumatic disease, peptic ulcer disease, mild liver disease, diabetes with or without complications, paraplegia and hemiplegia, renal disease, cancer, moderate or severe liver disease, metastatic carcinoma, and AIDS/HIV.

5.4.1 Climatic areas

Figures A18a and A18b, show that colder climatic zones (D/E), exhibit consistently higher concentrations of $PM_{2.5}$ [26], PM_{10}, and NO_2, with the largest absolute differences observed for NO_2. The persistent pollution gradient across years indicates that climate-driven heating demands, are a key driver of emissions, with colder regions facing markedly worse winter air quality. The analysis of extreme pollution events (above the 75^{th} percentile) reveals a pronounced climatic gradient in the effects of heating system activation: ATT estimates are significantly larger in colder D/E zones (figure A18d) than in milder B/C zones (figure A18c) across all pollutants ($PM_{2.5}$, PM_{10}, and NO_2). Effects are particularly pronounced for $PM_{2.5}$, where heating-related impacts on extreme pollution events nearly double those observed in B/C zones. These findings extend our baseline results on average pollution levels, highlighting a disproportionate burden on colder regions during peak episodes — driven not only by higher baseline emissions but also by a marked amplification in the frequency and intensity of extreme air quality events.

5.4.2 Socioeconomic and demographic factors

Turning to health outcomes, heterogeneity analyses reveal consistent patterns across conditions. AMI admissions (Figure A19) are most affected among the elderly (65+), low-educated individuals (nearly double the effect vs. high-educated), residents of D/E climatic zones, and those without pre-existing comorbidities. STEMI admissions (Figure A20) show pronounced effects in 2017-18 and 2018-19 for comorbidity-free patients and D/E area residents, with in-hospital mortality elevated among low-educated individuals in 2015-2016 and 2016-2017. NSTEMI admissions (Figure A21) increase among the elderly

[26] Using both CAMS and EEA measurements

(65+), adults (45-64), low-educated groups, comorbidity-free patients, and D/E zone residents in 2017-19. Ischemic stroke shows no significant effects (Figure A22), consistent with our main estimates. For hemorrhagic stroke (figure A23), admissions rise weakly among the elderly and low-educated in 2015-18, while in-hospital mortality spikes among the elderly and D/E zone residents in 2015-16 (the most polluted winter in our sample). Finally, COPD admissions (Figure A24) are elevated among the elderly (2015-16, 2017-18), comorbidity-free patients (2017-18), and D/E zone residents (2016-19), with an unexpected effect in B/C zones (2017-18). Across all conditions, socioeconomic and geographic disparities are most pronounced among the elderly, low-educated individuals, those without comorbidities, and residents of colder climatic zones.

6 Conclusions

This paper examines the causal effects of residential heating activation on air pollution and health outcomes using a novel identification strategy that employs a staggered difference-in-differences estimator (Callaway & Sant'Anna (2021)). Treatment is defined by municipal biomass consumption and heating appliance prevalence, with the post-period triggered by the first weekly temperature drop below a certain threshold identified through Google search trends for heating activation — thereby accounting for systematic deviations from legal activation dates.

This study makes four key contributions. First, we provide new causal evidence linking heating-generated $PM_{2.5}$ and NO_2 to both cardiovascular and respiratory outcomes, covering hospitalizations and in-hospital mortality across six acute conditions. Second, we introduce a novel identification strategy that exploits the gap between regulated and actual heating activation dates, using real-time behavioral data to identify the temperature threshold at which households actually turn on heating. Third, we define vulnerable individuals using the Charlson Comorbidity Index and document significant health effects among those *without* pre-existing comorbidities — a finding inconsistent with classic mortality displacement narratives. Fourth, we document systematic environmental inequality: health burdens concentrate in colder climatic zones and among low-educated individuals. Our main analysis reveals that residential heating activation significantly increases most pollutants considered, in particular $PM_{2.5}$ and NO_2 concentrations by 19-27% and 11-20% respectively. This translates into substantial health impacts: AMI, STEMI, NSTEMI, and COPD admission rates increase by 8-18%, 17-19%, 15-20%, and 15-27% respectively. In-hospital mortality rises significantly for cardiovascular conditions in specific years (+35% for AMI, +51% for STEMI, +50% for NSTEMI), with sporadic effects on hemorrhagic stroke mortality during high-pollution winters (2015-16 and 2017-18), while we find no significant effects for ischemic stroke

Our results remain robust to a series of checks. First, alternative pollution measures confirm our main findings: $PM_{2.5}$ (EEA) and PM_{10} show increases consistent with the CAMS-based results, while SO_2 and CO effects are primarily observed at mean levels, with more limited and period-specific evidence in the upper tail. Second, alternative treatment thresholds confirm that effects on pollution concentrations and health outcomes remain statistically significant, with larger effects when comparing municipalities above the 66th and 75th percentiles of biomass consumption against those below the 33rd and 25th percentiles — consistent with a clear dose-response pattern. Third, sensitivity analyses confirm robustness to a wide range of plausible deviations from the parallel trends assumption, with estimated effects remaining statistically significant unless subjected to implausibly large post-treatment trend violations. Fourth, population-weighted and AIPW estimators confirm our main estimates. Fifth, placebo analyses show null effects of heating system activation on health outcomes unrelated to pollution, and mobility analyses rule out substantial selection bias.

Heterogeneity analyses reveal striking patterns. Colder regions (D/E zones) experience pollution increases nearly double those in milder zones, with particularly pronounced effects during extreme pollution events. Health impacts concentrate among adults (45-64), the elderly (65+), and low-educated individuals — but also, notably, among individuals without pre-existing comorbidities, suggesting that acute pollution exposure can trigger health crises even in otherwise healthy individuals, implying welfare costs larger than prior estimates would suggest.

The substantial health costs we document — concentrated in colder regions and among low-educated individuals and those without pre-existing comorbidities — suggest that the welfare costs of residential biomass heating are systematically underestimated. These results contribute to the ongoing debate on the EU Renewable Energy Directive: incentivizing biomass burning as carbon-neutral renewable energy has come at an unaccounted health cost. Our evidence points to considerable potential health gains from policies accelerating the replacement of obsolete biomass heating systems with cleaner alternatives, particularly in high-biomass municipalities where health burdens are most severe.

7 Appendix

Table A1: Degree-Days Range for Different Climatic Zones

Zone	Degree-Days Range
A	Municipalities with degree-days < 600
B	Municipalities with $600 <$ degree-days < 900
C	Municipalities with $901 <$ degree-days < 1400
D	Municipalities with $1401 <$ degree-days < 2100
E	Municipalities with $2101 <$ degree-days < 3000
F	Municipalities with degree-days > 3000

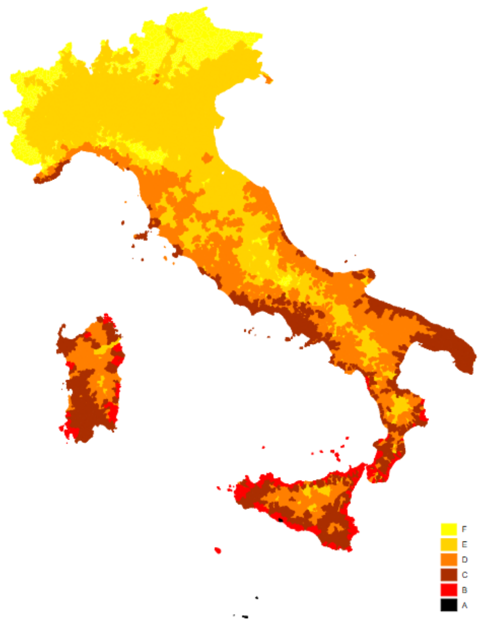

Figure A1: Italian Climatic Zones

Notes: The Figure illustrates Italian municipalities categorized by their classified climatic zone. Municipalities highlighted in yellow correspond to the coldest climatic zone with the highest degree days, climatic zone F. As the colour intensity increases, the zones transition in ascending order of temperature and descending degree days: zone E, D, C, B, and finally the warmest zone, characterized by a few municipalities and depicted in black, identified as climatic zone A.
Source: own elaboration.

Table A2: Main Municipalities for Different Climatic Zones

Zone	Municipalities
A	Lampedusa, Porto Empedocle, and Linosa
B	Agrigento, Catania, Crotone, Messina, Palermo, Reggio Calabria, Siracusa, and Trapani
C	Bari, Benevento, Brindisi, Cagliari, Caserta, Catanzaro, Cosenza, Imperia, Latina, Lecce, Napoli, Oristano, Ragusa, Salerno, Sassari, and Taranto
D	Ascoli Piceno, Avellino, Caltanissetta, Chieti, Firenze, Foggia, Forlì, Genova, Grosseto, Isernia, La Spezia, Livorno, Lucca, Macerata, Massa Carrara, Matera, Nuoro, Pesaro, Pescara, Pisa, Pistoia, Prato, Roma, Savona, Siena, Teramo, Terni, Vibo Valentia, Viterbo
E	Alessandria, Aosta, Arezzo, Asti, Bergamo, Biella, Bologna, Bolzano, Brescia, Campobasso, Como, Cremona, Enna, Ferrara, Frosinone, Gorizia, L'Aquila, Lecco, Lodi, Milano, Modena, Novara, Padova, Parma, Pavia, Perugia, Piacenza, Pordenone, Potenza, Ravenna, Reggio Emilia, Rieti, Rimini, Rovigo, Sondrio, Torino, Treviso, Trieste, Udine, Varese, Venezia, Verbania, Vercelli, Verona, Vicenza
F	Belluno, Cuneo, and Trento

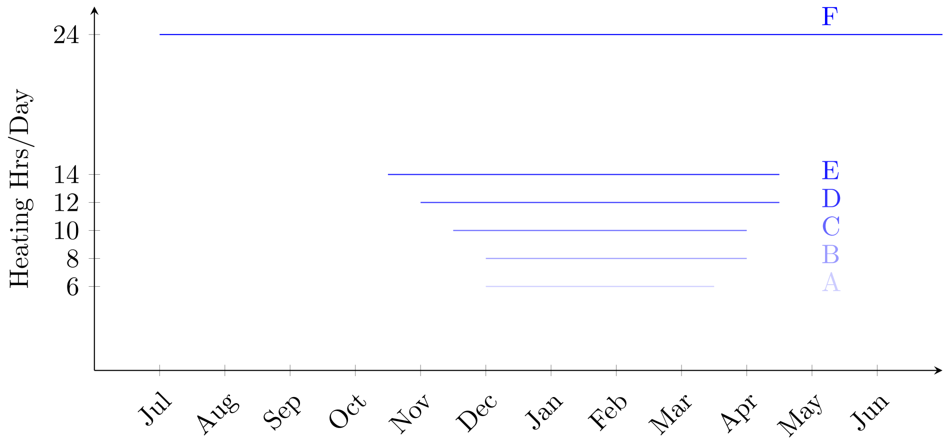

Figure A2: Italian Heating Restrictions

Notes: The x-axis represents the months of the year, and the y-axis denotes hours in a day. Horizontal lines indicate heating restriction zones in Italy, with highlighted lines indicating the permitted heating months and how many hrs/day: Zone A (Dec 1 - Mar 15, 6hrs/day), Zone B (Dec 1 - Mar 31, 8hrs/day), Zone C (Nov 15 - Mar 31, 10hrs/day), Zone D (Nov 1 - Apr 15, max 12hrs/day), Zone E (Oct 15 - Apr 15, up to 14hrs/day). Zone F has no restrictions.

Figure A3: Spatial distribution of $PM_{2.5}$ before (left) and after (right) heating system activation in Italy.

(a) Average CAMS $PM_{2.5}$ levels from 2015 to 2019 during the pre-heating activation months (June, July, August, and September), focusing on the weeks spanning from the 22^{nd} to the 40^{th} week.

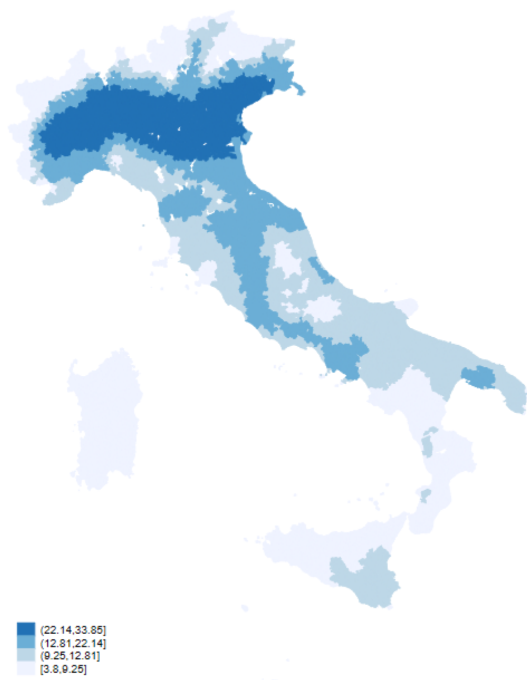

(b) Average CAMS $PM_{2.5}$ levels from 2015 to 2019 during the post-heating activation months (October, November, December, and January), specifically examining the weeks from the 41^{st} to the 52^{nd} week and the 1^{st} to the 5^{th} week.

Figure A7: ATT on AMI hospitalisations and in hospital mortality across (2015-2019)

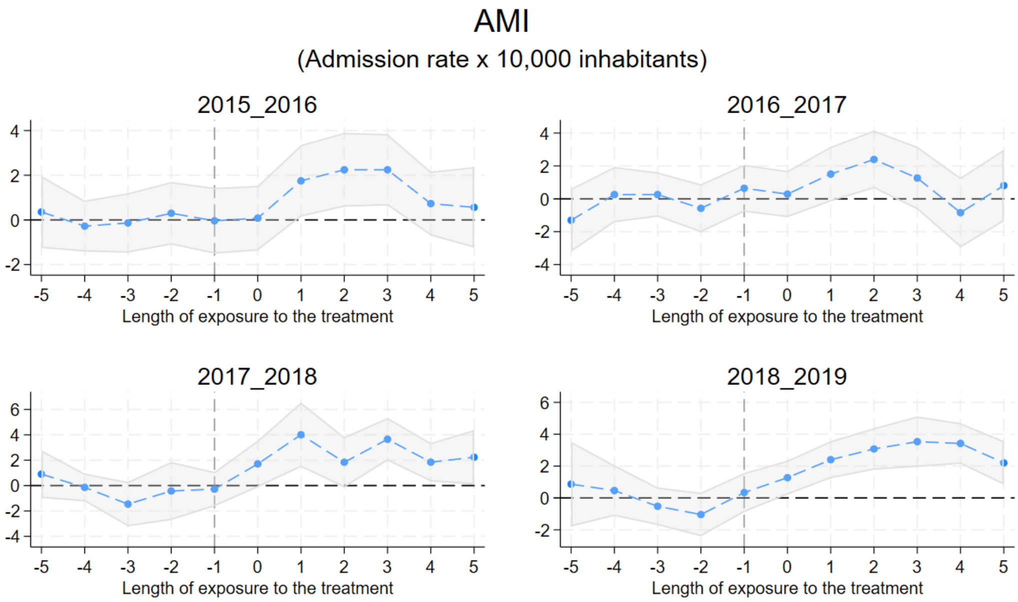

(a) ATT on AMI hospitalisations across (2015-19)

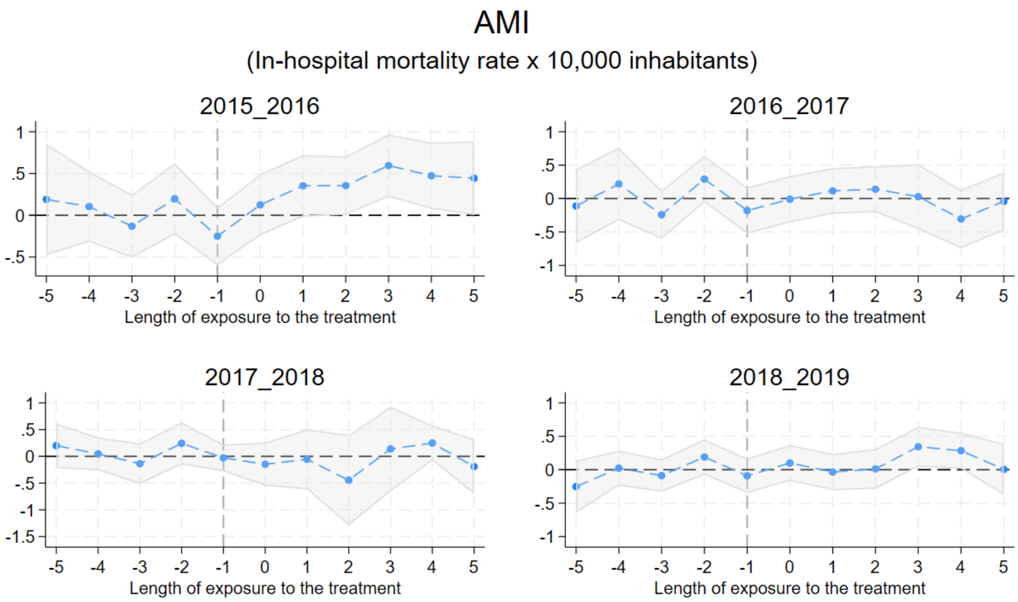

(b) ATT on AMI in-hospital mortality across (2015-19)

Figure A4: Turning on heating: actual week vs regulation

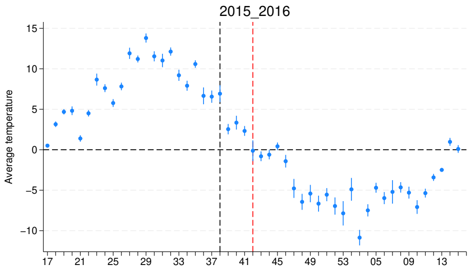

(a) Temperature 2015-2016

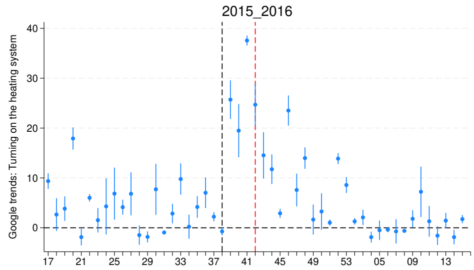

(b) Google 2015-2016

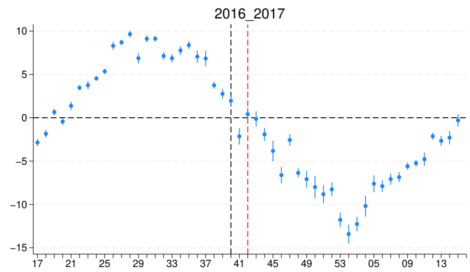

(c) Temperature 2016-2017

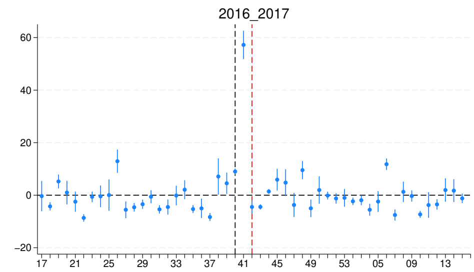

(d) Google 2016-2017

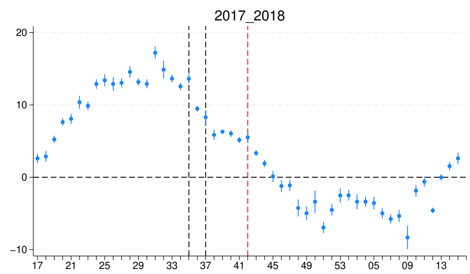

(e) Temperature 2017-2018

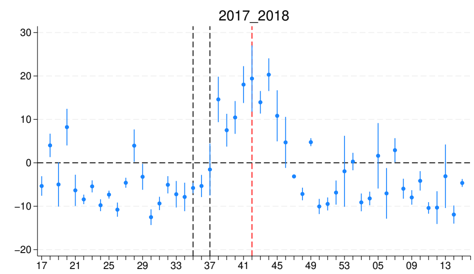

(f) Google 2017-2018

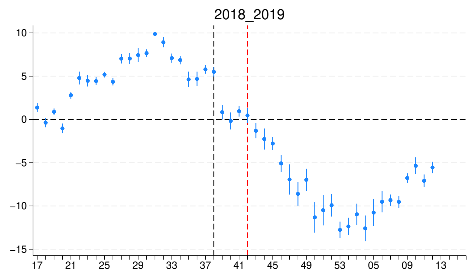

(g) Temperature 2018-2019

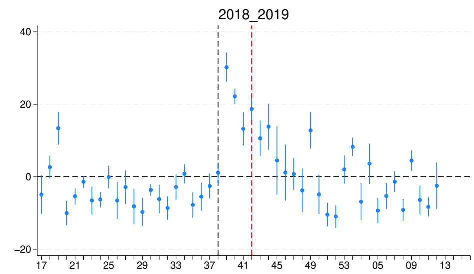

(h) Google 2018-2019

Notes: This Figure illustrates the trend of deviations from average temperature (left column) and the absolute number of Google searches for "Turning on the heating system" (right column) over four biennial periods: 2015-2016, 2016-2017, 2017-2018 and 2018-2019. The x-axis in all sub-figures represents weekly intervals, covering April-December of the first year and January-March of the second year. The black dashed vertical line marks the first temperature drop and the corresponding rise in Google searches. For 2017-18 (A4e) we highlight two remarkable drops in temperatures and the corresponding activity on Google (A4f). The red dashed vertical line represents the first week in which it is theoretically allowed to switch on the heating system (i.e. 15th of October in areas D/E).

Figure A5: Temperatures and Google searches

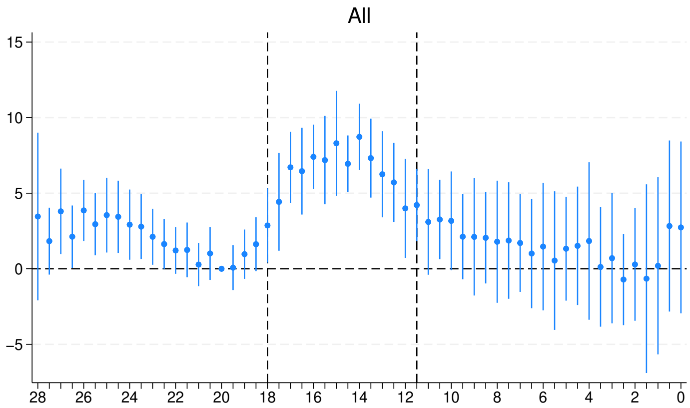

Notes: This Figure illustrates the relationship between the absolute number of Google searches for "Turning on the heating system" (y-axis) and the decrease in temperature (x-axis). The dashed vertical lines highlight the increase in Google searches as temperatures range between 18-12°C. The data cover all the considered biennial periods: 2015-2016, 2016-2017, 2017-2018, and 2018-2019.

Figure A6: Treatment distribution map across Italian municipalities

Figure A8: ATT on STEMI hospitalisations and in hospital mortality across (2015-2019)

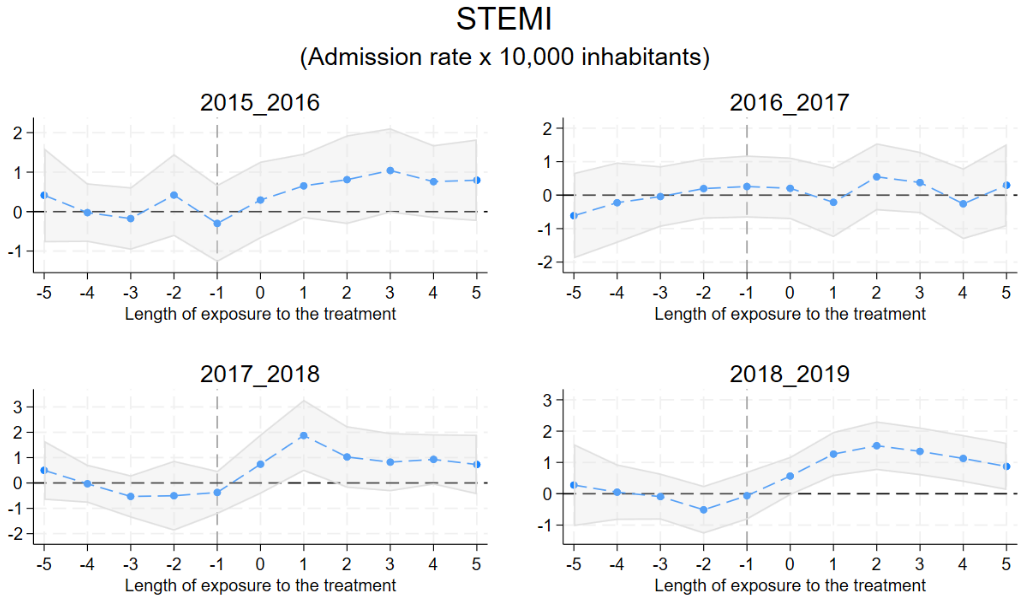

(a) ATT on STEMI hospitalisations across (2015-19)

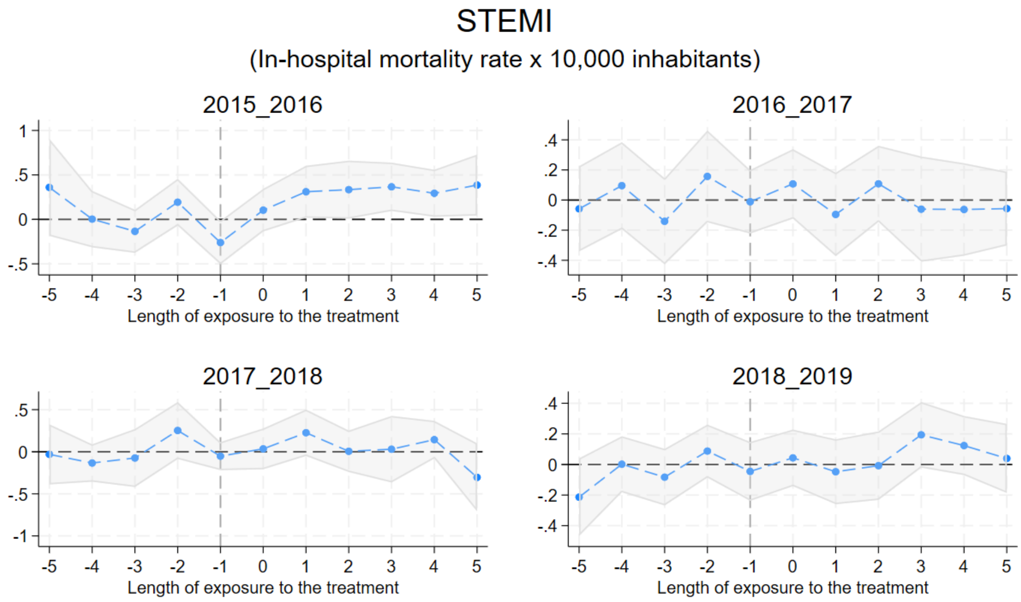

(b) ATT on STEMI in hospital mortality across (2015-19)

Figure A9: ATT on NSTEMI hospitalisations and in hospital mortality across (2015-2019)

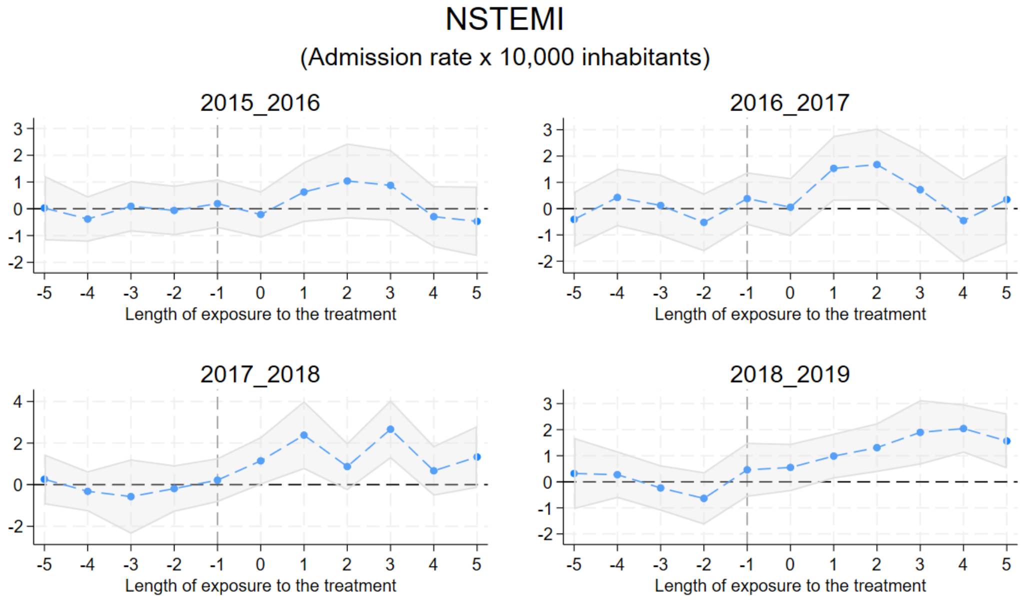

(a) ATT on NSTEMI hospitalisations across (2015-19)

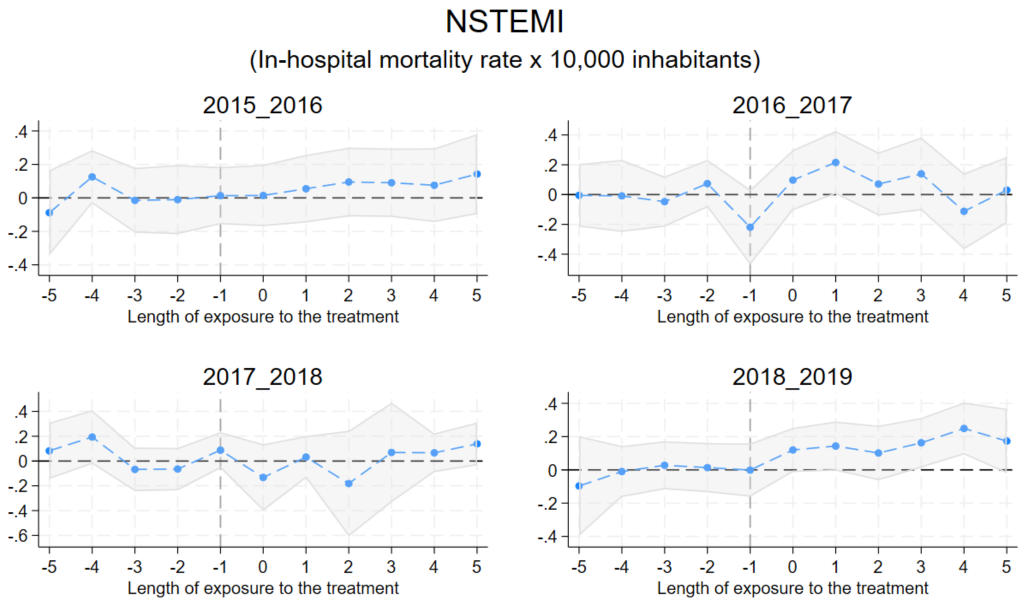

(b) ATT on NSTEMI in-hospital mortality across (2015-19)

Figure A10: ATT on Ischemic Stroke hospitalisations (LHS) and in hospital mortality (RHS) across (2015-2019)

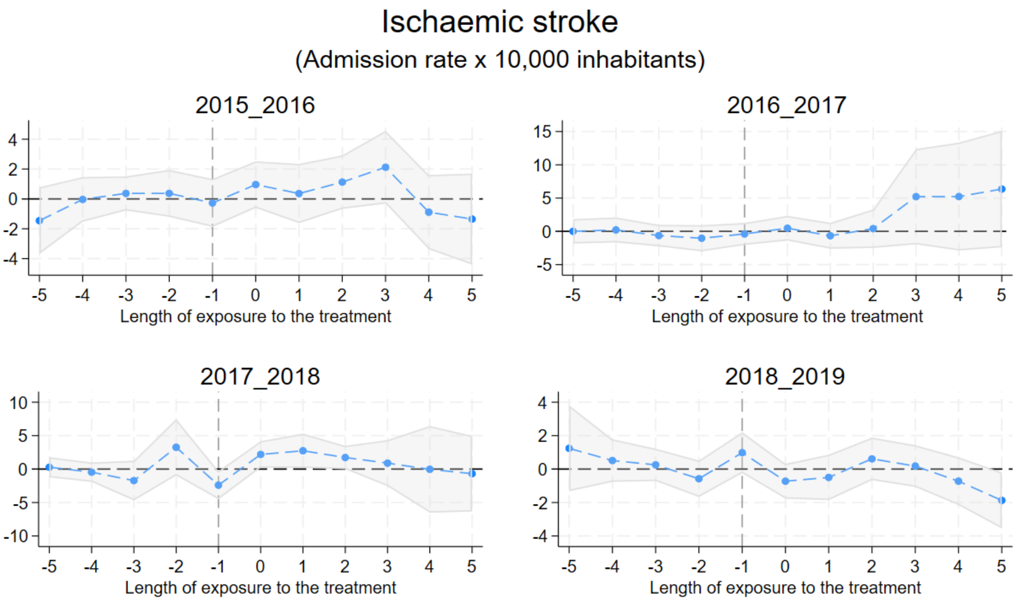

(a) ATT on Ischemic Stroke hospitalisations across (2015-19)

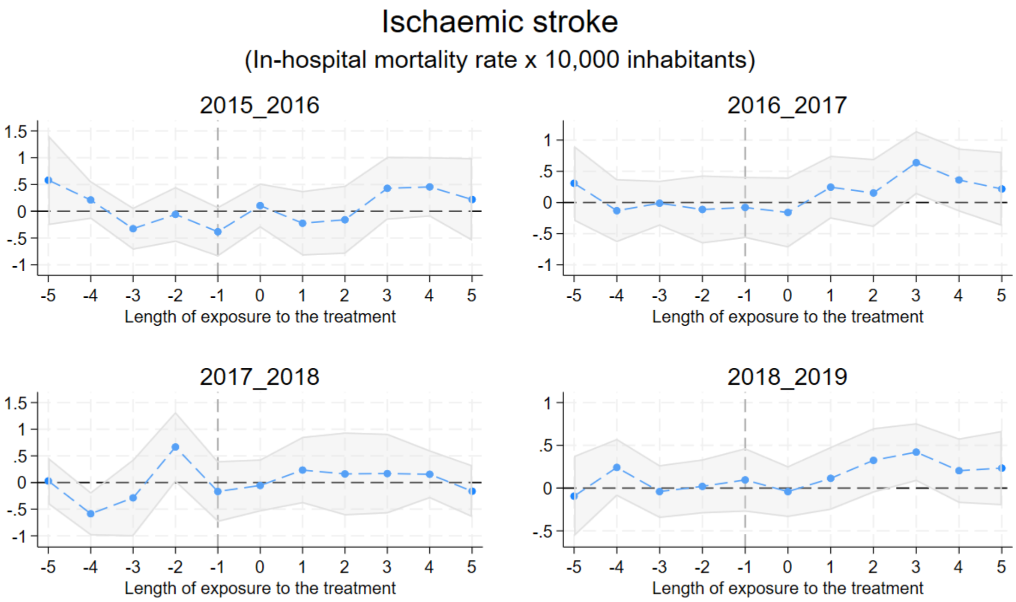

(b) ATT on Ischemic Stroke in hospital mortality across (2015-19)

Figure A11: ATT on Hemorrhagic Stroke hospitalisations (LHS) and in hospital mortality (RHS) across (2015-2019)

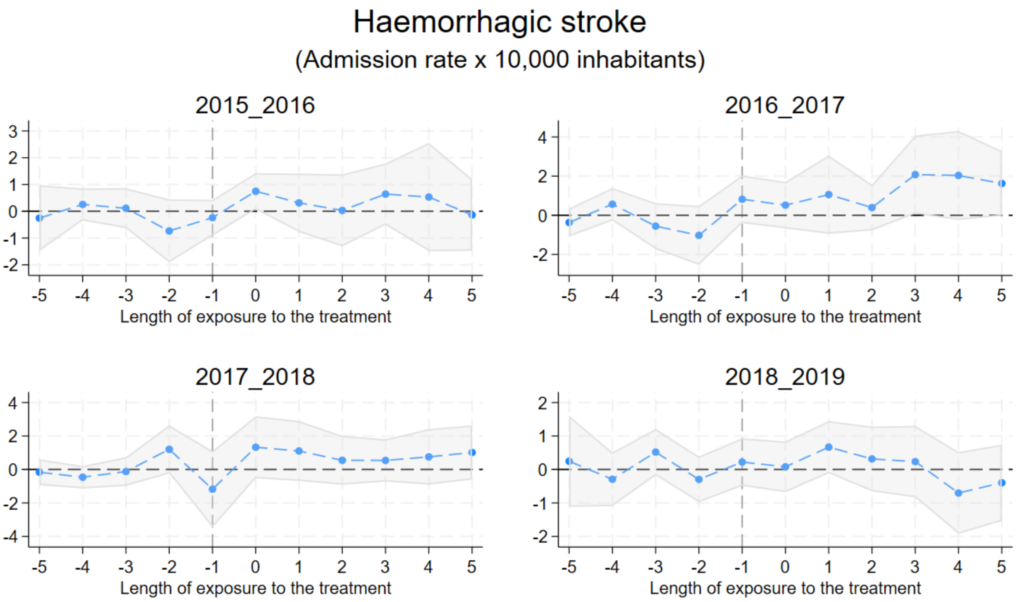

(a) ATT on Hemorrhagic Stroke hospitalisations across (2015-19)

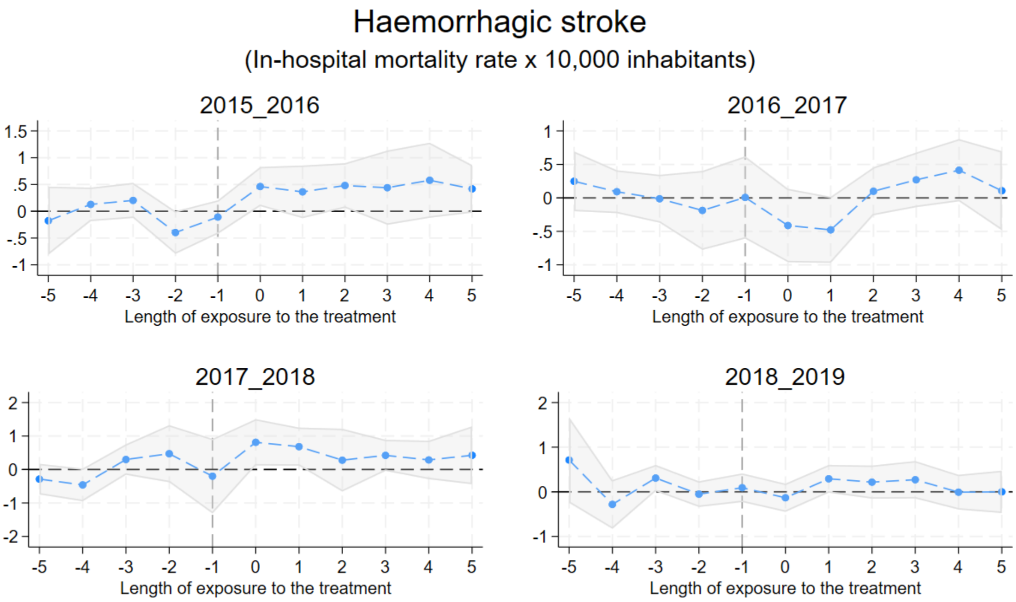

(b) ATT on Hemorrhagic Stroke in hospital mortality across (2015-19)

Figure A12: ATT on COPD hospitalisations and in hospital mortality across (2015-2019)

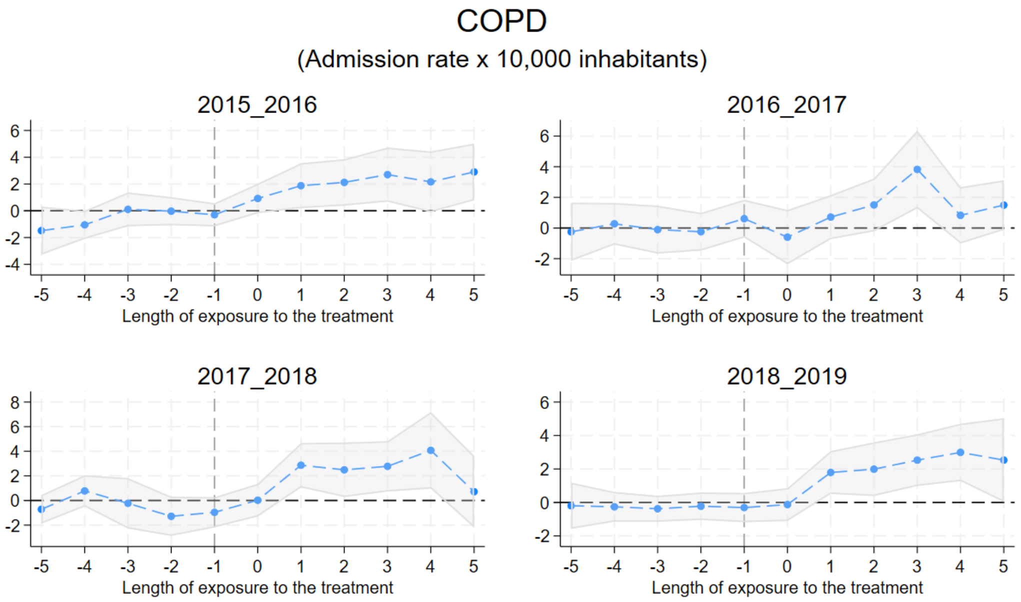

(a) ATT on COPD hospitalisations across (2015-19)

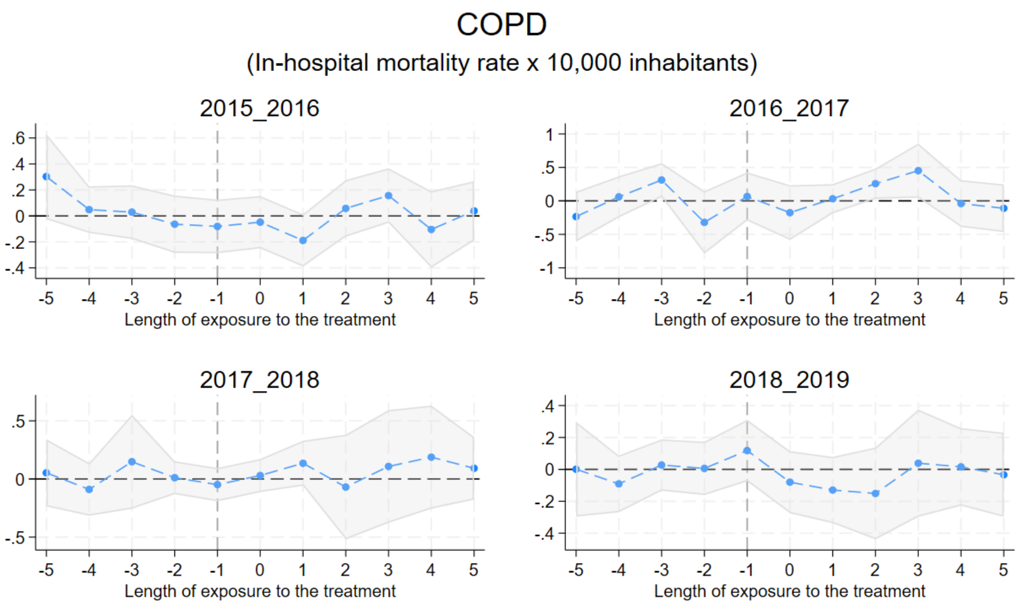

(b) ATT on COPD in-hospital mortality across (2015-19)

Table A3: Impact of Heating system activation on $PM_{2.5}$ CAMS, $PM_{2.5}$ EEA, PM_{10} EEA and NO_2 EEA with weather-season interaction (2015-2019)

	2015-2016	2016-2017	2017-2018	2018-2019
	(1)	(2)	(3)	(4)
A. Average Effects				
		$PM_{2.5}$ CAMS		
ATT	3.491***	1.265***	3.824***	3.486***
	(0.506)	(0.49)	(0.636)	(0.568)
		$PM_{2.5}$ EEA		
ATT	6.818***	4.893***	7.818***	5.47***
	(1.114)	(1.178)	(1.135)	(0.761)
		PM_{10} EEA		
ATT	6.803***	4.226***	8.604***	5.577***
	(1.204)	(1.056)	(1.368)	(0.793)
		NO_2 EEA		
ATT	5.128***	2.53***	4.772***	3.441***
	(1.137)	(0.939)	(1.04)	(0.703)
B. Above 75th percentile				
		$PM_{2.5}$ CAMS		
ATT	0.769***	0.216**	0.83***	0.767***
	(0.118)	(0.103)	(0.13)	(0.138)
		$PM_{2.5}$ EEA		
ATT	0.951***	0.645***	1.12***	0.898***
	(0.152)	(0.172)	(0.169)	(0.127)
		PM_{10} EEA		
ATT	0.686***	0.449***	0.784***	0.541***
	(0.11)	(0.109)	(0.117)	(0.0887)
		NO_2 EEA		
ATT	0.723***	0.497***	0.584***	0.579***
	(0.137)	(0.139)	(0.158)	(0.0767)

Notes: The table presents difference-in-differences estimates of the average treatment effect on the treated (ATT) of heating system activation on $PM_{2.5}$ CAMS, $PM_{2.5}$ EEA, PM_{10} EEA and NO_2 EEA levels. The empirical specification interacts the treatment and the post-period indicator with contemporaneous weather conditions (wind speed, precipitation, and temperature) to control for the differential effect of meteorology on pollution during the heating season. Panel A shows effects on average pollutant levels, while Panel B focuses on the upper quartile of the outcome distribution. Standard errors at municipal level are in parentheses; Significance levels: *** p<0.01, ** p<0.05, * p<0.1.

Table A4: Impact of Heating system activation on Hospitalisations vs. In-hospital mortality rates with weather-season interaction (2015-2019)

	2015-2016 (1)	2016-2017 (2)	2017-2018 (3)	2018-2019 (4)
A. Hospitalisations				
		AMI		
ATT	1.089*	1.209	3.157***	2.339***
	(0.648)	(0.825)	(1.028)	(0.57)
		STEMI		
ATT	0.638*	0.131	0.879**	0.91***
	(0.387)	(0.378)	(0.381)	(0.328)
		NSTEMI		
ATT	0.124	1.049	1.933***	1.317***
	(0.456)	(0.744)	(0.74)	(0.415)
		Ischemic Stroke		
ATT	1.483	3.415	1.929	-0.773
	(0.938)	(2.73)	(1.252)	(0.639)
		Hemorrhagic Stroke		
ATT	0.123	1.31	0.67	0.195
	(0.323)	(1.057)	(0.477)	(0.329)
		COPD		
ATT	1.848*	0.994	2.122**	1.312*
	(1.016)	(0.728)	(0.99)	(0.733)
B. In-hospital mortality				
		AMI		
ATT	0.461***	0.0463	0.104	0.0813
	(0.172)	(0.147)	(0.259)	(0.115)
		STEMI		
ATT	0.328***	0.0233	0.031	0.0353
	(0.11)	(0.0997)	(0.12)	(0.0878)
		NSTEMI		
ATT	0.074	0.085	0.142	0.144**
	(0.102)	(0.0929)	(0.119)	(0.0598)
		Ischemic Stroke		
ATT	0.336	0.28	0.257	0.144
	(0.264)	(0.216)	(0.34)	(0.159)
		Hemorrhagic Stroke		
ATT	0.405**	-0.0542	0.519**	-0.0493
	(0.185)	(0.185)	(0.256)	(0.178)
		COPD		
ATT	0.0102	0.113	0.0566	-0.107
	(0.0868)	(0.105)	(0.132)	(0.093)

Notes: The table presents difference-in-differences estimates of the average treatment effect on the treated (ATT) of heating system activation on hospitalisations (Pnael A), and on in-hospital mortality (Panel B) for AMI, STEMI, NSTEMI, Ischemic Stroke, Hemorrhagic Stroke and COPD. The empirical specification interacts the treatment and post-period indicator with contemporaneous weather conditions (wind speed, precipitation, and temperature) to control for the differential effect of meteorology on pollution during the heating season. Standard errors at municipal level are in parentheses; Significance levels: *** p<0.01, ** p<0.05, * p<0.1.

Figure A13: $PM_{2.5}$ EEA main estimates for 2015-16, 2016-17, 2017-18, 2018-19.

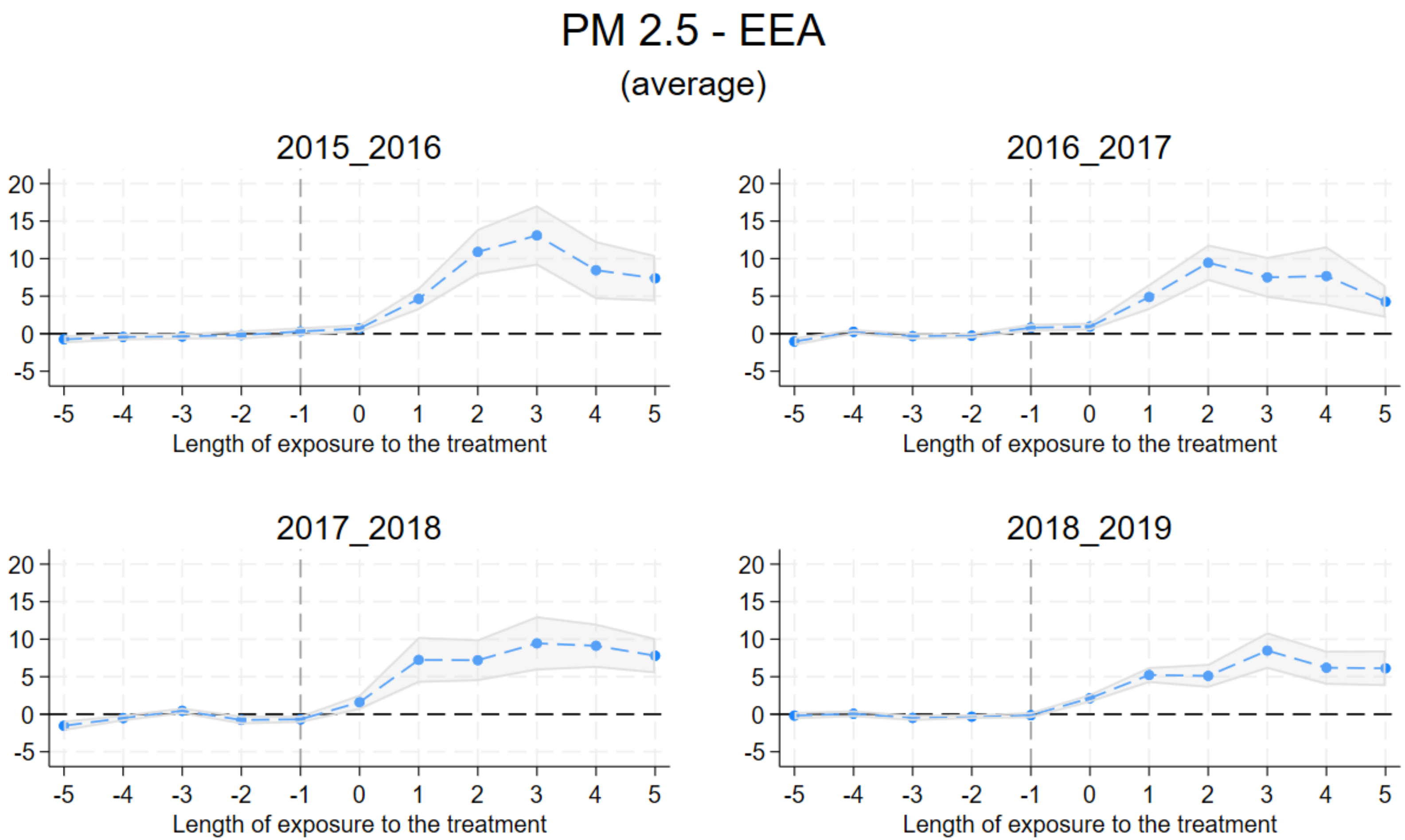

Figure A14: PM_{10} EEA main estimates for 2015-16, 2016-17, 2017-18, 2018-19.

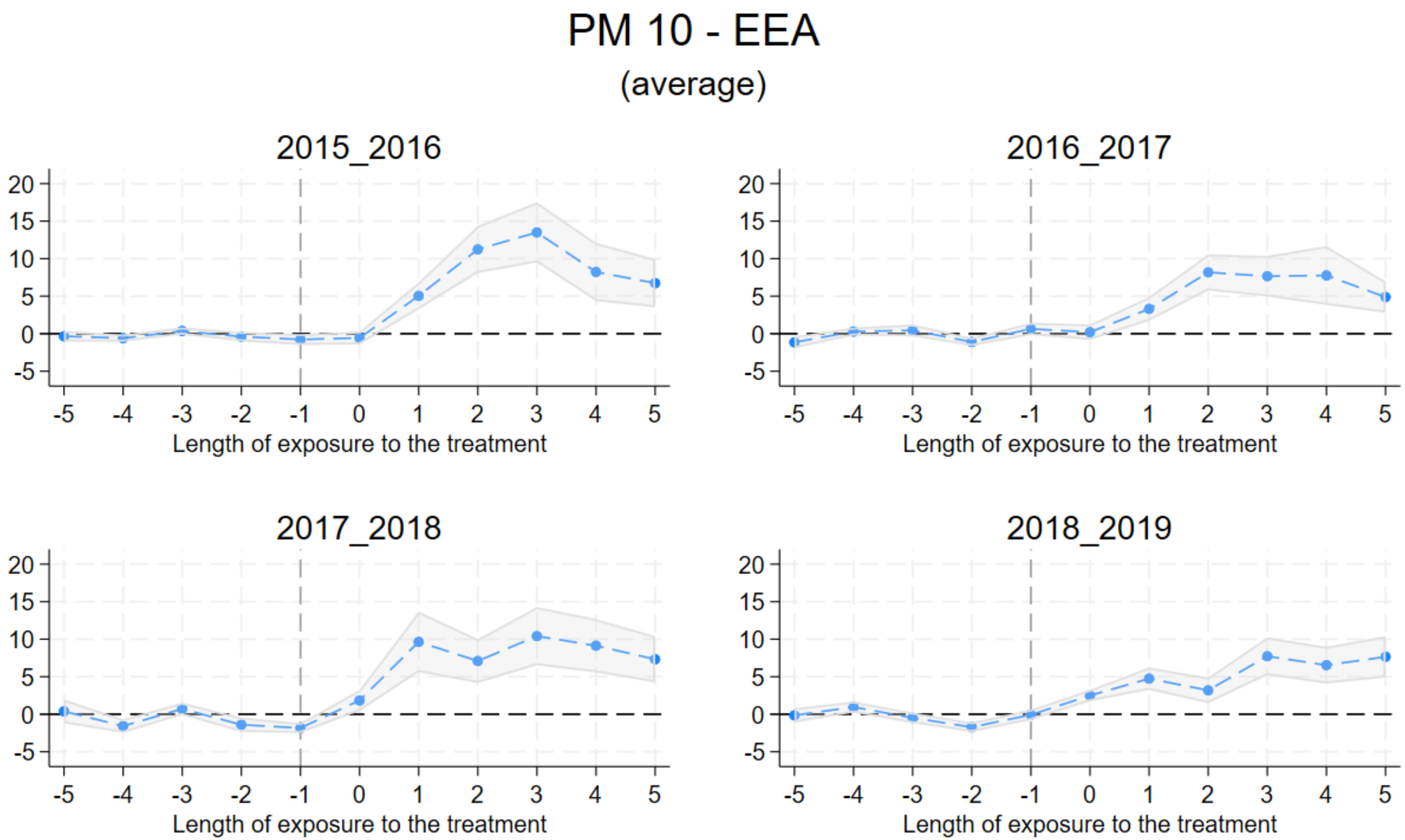

Figure A15: SO_2 EEA main estimates for 2015-16, 2016-17, 2017-18, 2018-19.

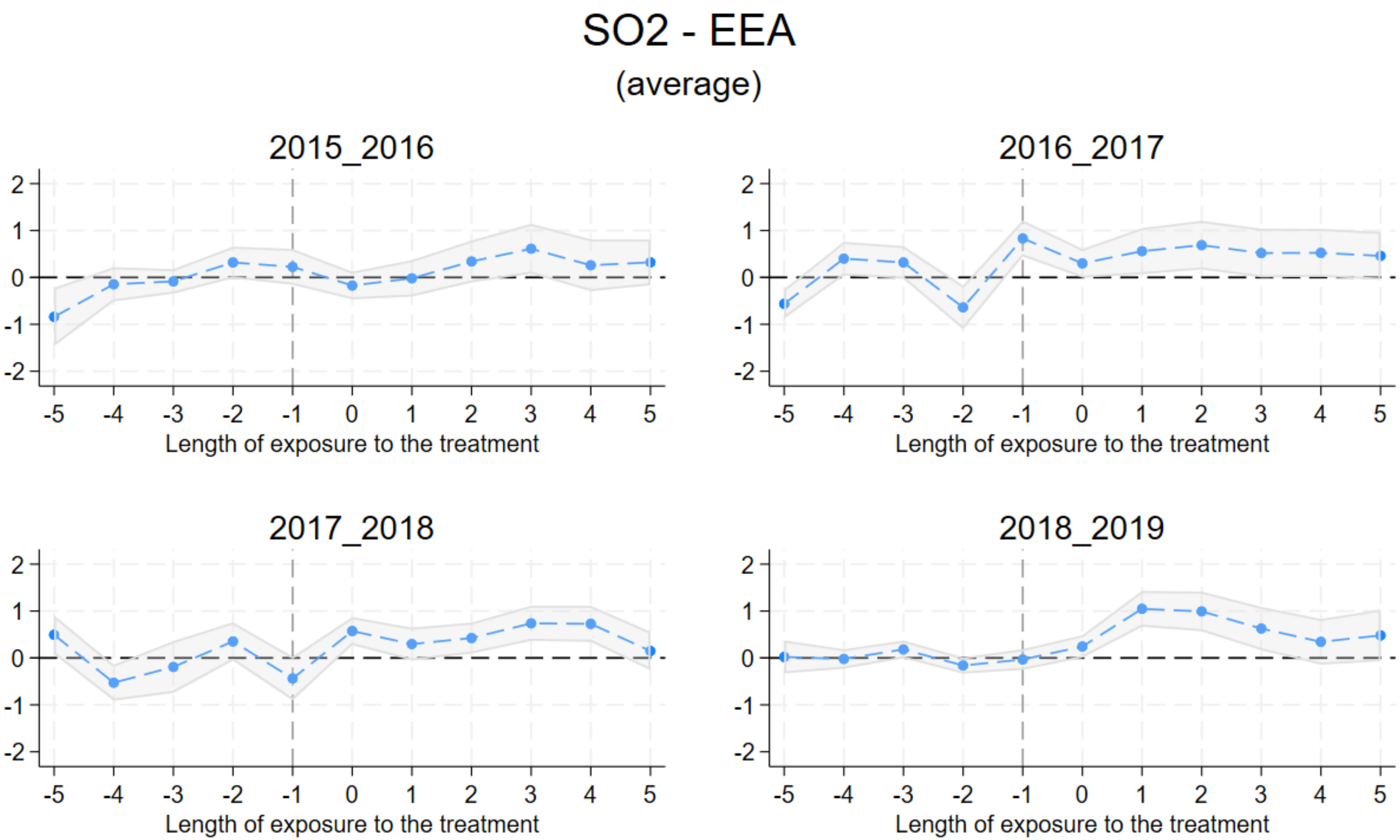

Figure A16: *CO* EEA main estimates for 2015-16, 2016-17, 2017-18, 2018-19.

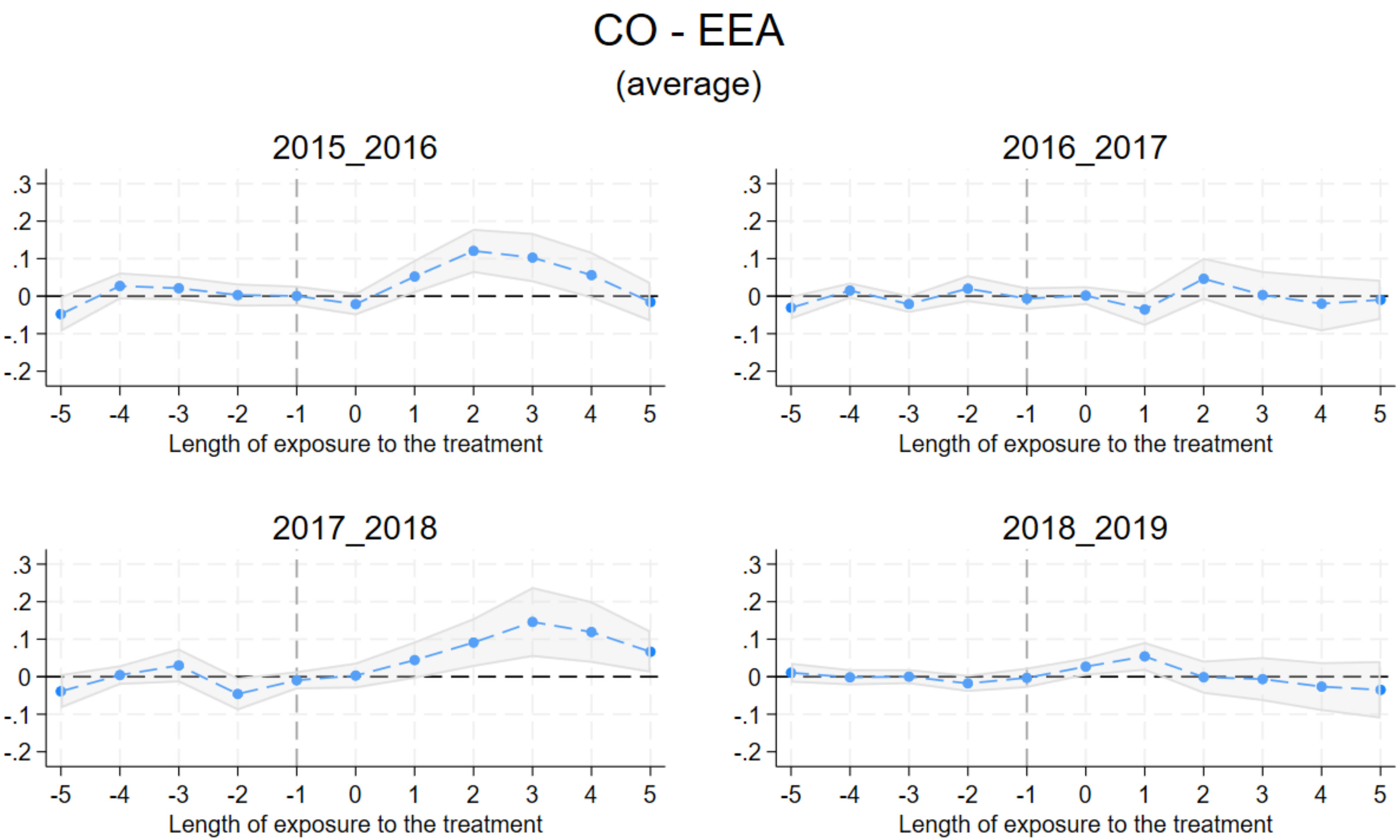

Figure A17: Average Treatment Effects on Placebo Outcomes: Hospitalization Rates (LHS) and In-Hospital Mortality Rates (RHS) per 10,000 Inhabitants, across 2015-2019

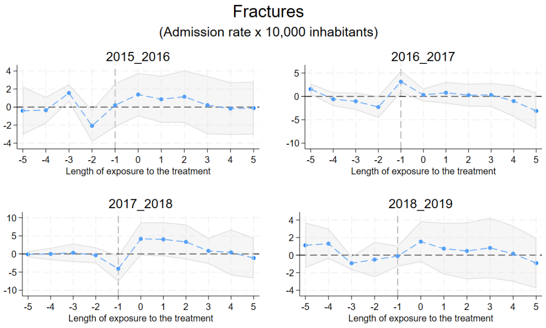

(a) Hospitalisations

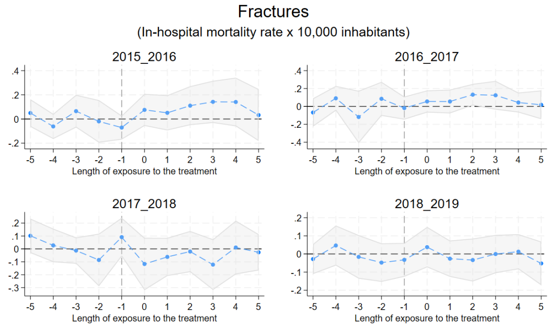

(b) In-hospital mortality

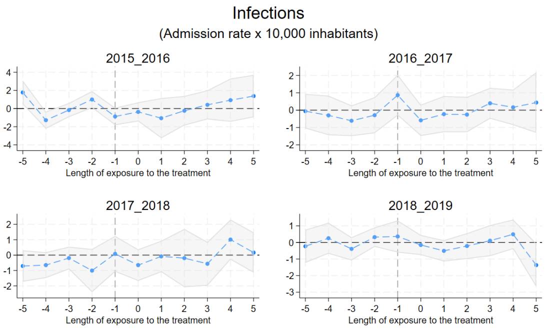

(c) Hospitalisations

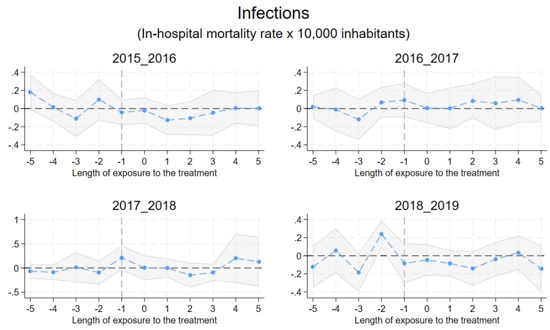

(d) In-hospital mortality

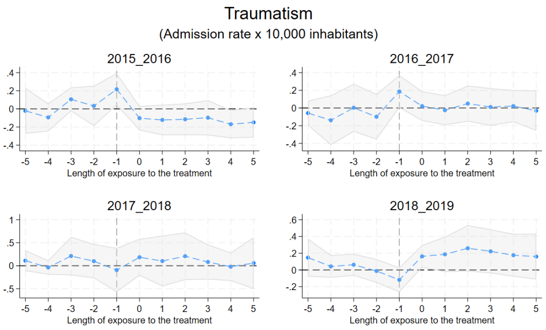

(e) Hospitalisations

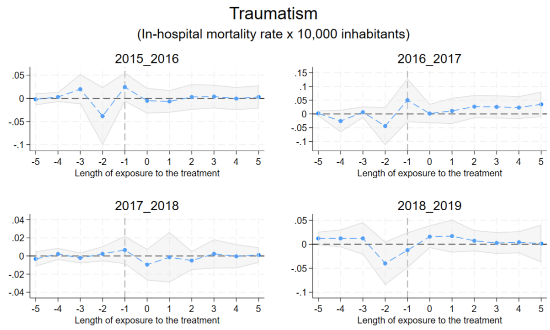

(f) In-hospital mortality

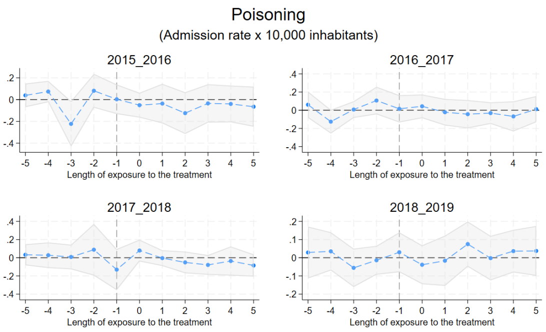

(g) Hospitalisations

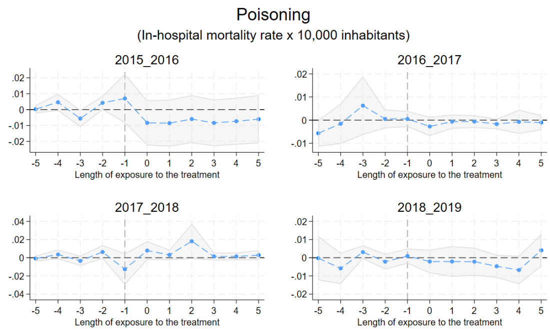

(h) In-hospital mortality

Notes: This Figure presents the Average Treatment Effect on the Treated (ATT) of residential heating activation on (a) hospitalization rates (left panels) and (b) in-hospital mortality rates (right panels) (both per 10,000 inhabitants) for placebo outcomes: (a,b) fractures (top row), (c,d) infections (second row), (e,f) trauma (third row), and (g, h) poisoning (bottom row). Estimates reflect biennial comparisons across the 2015-2019 period. The Figure continues on the following page.

Figure A17: Average Treatment Effects on Placebo Outcomes: Hospitalization Rates (LHS) and In-Hospital Mortality Rates (RHS) per 10,000 Inhabitants, across 2015-2019 (Continued)

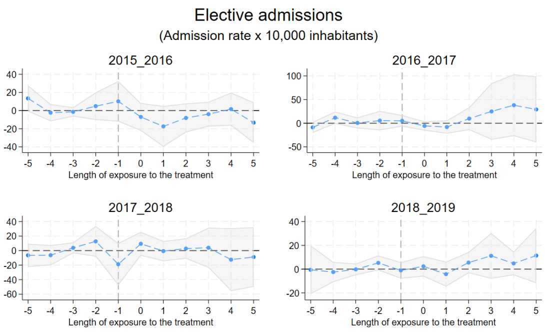

(i) Hospitalisations

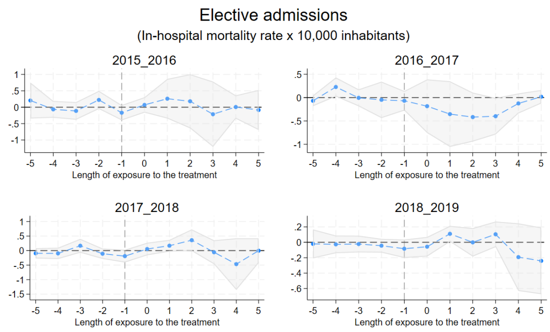

(j) In-hospital mortality

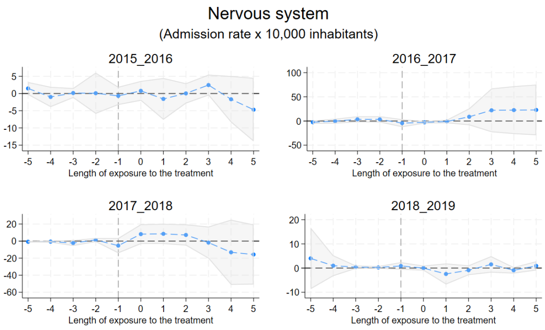

(k) Hospitalisations

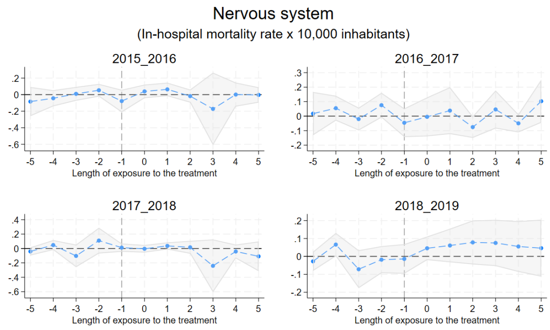

(l) In-hospital mortality

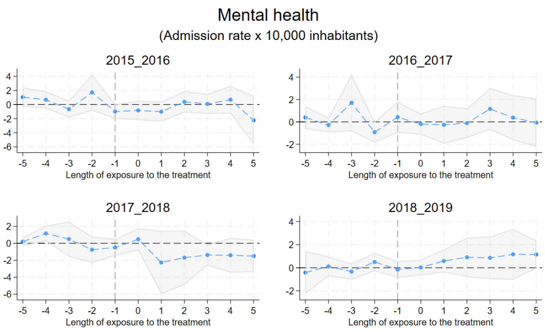

(m) Hospitalisations

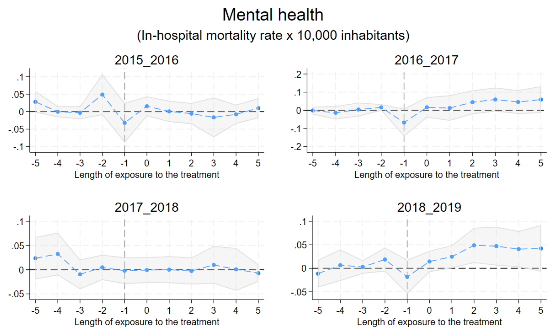

(n) In-hospital mortality

Notes (continued): This Figure presents the Average Treatment Effect on the Treated (ATT) of residential heating activation on (a) hospitalisation rates (left panels) and (b) in-hospital mortality rates (right panels) (both $\times$ 10,000 inhabitants) for additional placebo outcomes: (i,j) elective admissions (top row), (k,l) nervous system disorders (second row), and (m,n) mental health conditions (bottom row). Estimates reflect biennial comparisons across the 2015-2019 period.

Figure A18: Average Treatment Effects (ATT) of residential heating activation on $PM_{2.5}$ (CAMS and EEA), PM_{10} and NO_2 by climatic areas: B/C and D/E.

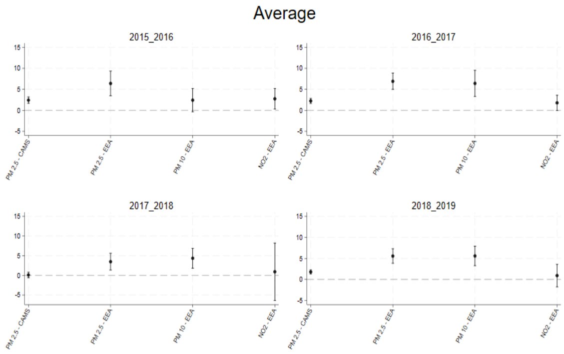

(a) ATT of residential heating activation on mean pollutants' concentrations in climatic zone B/C

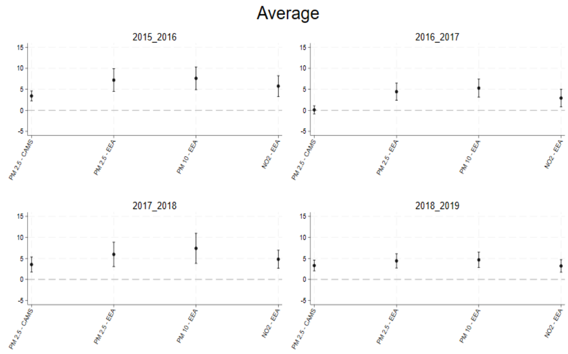

(b) ATT of residential heating activation on mean pollutants' concentrations in climatic zone D/E

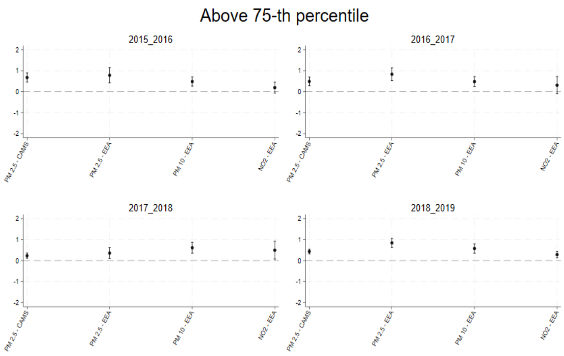

(c) ATT of residential heating activation on 75^{th} percentile pollutants' concentrations in climatic zone B/C

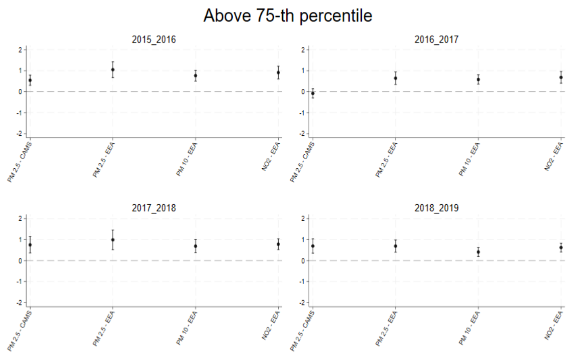

(d) ATT of residential heating activation on 75^{th} percentile pollutants' concentrations in climatic zone D/E

Notes: The Figure presents the Average Treatment Effects (ATT) of residential heating system activation on air pollution concentrations across different climatic zones. Panels (a) and (b) show impacts on mean pollution levels, with (a) focusing on climatic zone B/C and (b) on zone D/E, examining $PM_{2.5}$ (from both CAMS and EEA data), PM_{10}, and NO_2. The lower panels analyze effects at the 75^{th} percentile, with (c) for zone B/C and (d) for zone D/E, revealing how heating activation influences upper-tail pollution events.

Figure A19: Heterogeneous Average Treatment Effects (ATT) of residential heating activation on AMI

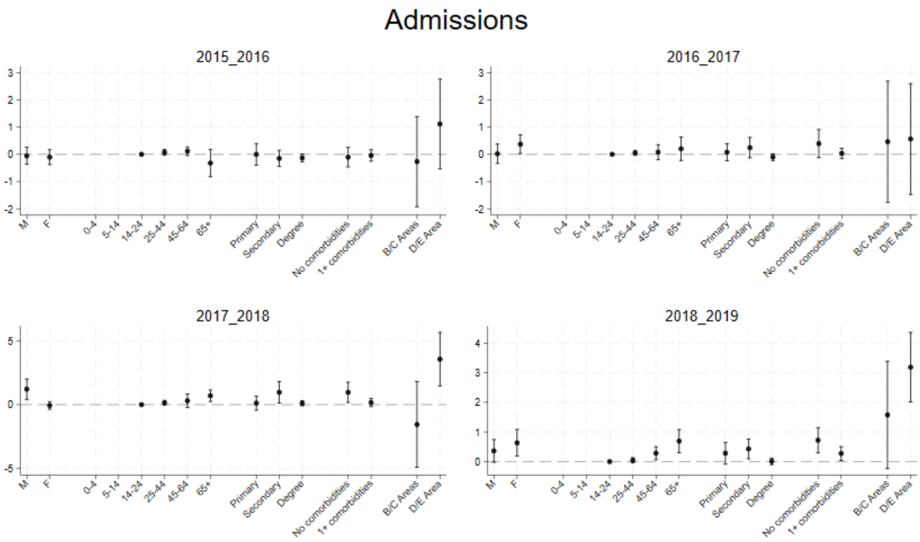

(a) Heterogeneous Average Treatment Effects (ATT) of residential heating activation on AMI - Hospitalisations

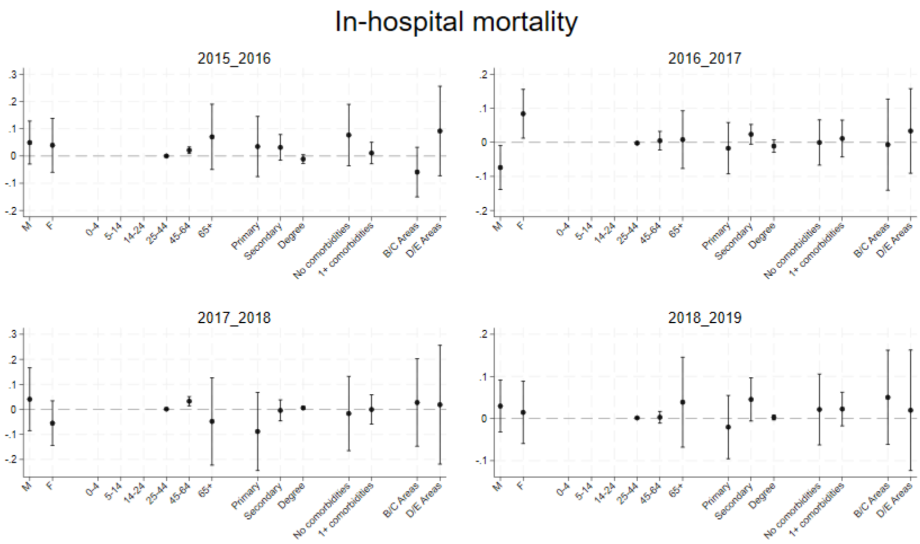

(b) Heterogeneous Average Treatment Effects (ATT) of residential heating activation on AMI - In hospital mortality

Notes: The Figure displays the Average Treatment Effect on the Treated (ATT) of residential heating activation on (a) AMI hospitalisations (upper panel) and (b) in-hospital mortality (lower panel). Results are stratified by gender, age group, educational attainment, comorbidity status (with/without), and climatic zone (B/C vs. D/E)

Figure A20: Heterogeneous Average Treatment Effects (ATT) of residential heating activation on STEMI

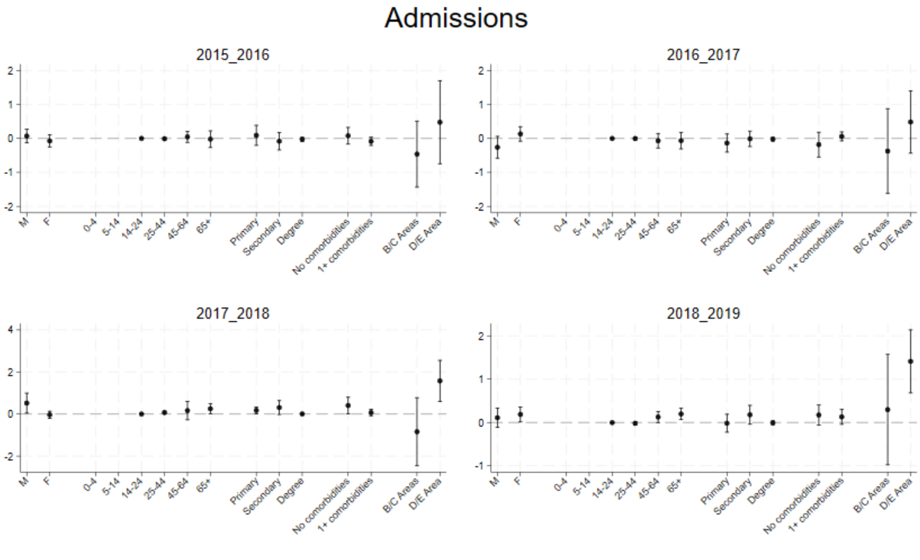

(a) Heterogeneous Average Treatment Effects (ATT) of residential heating activation on STEMI - Hospitalisations

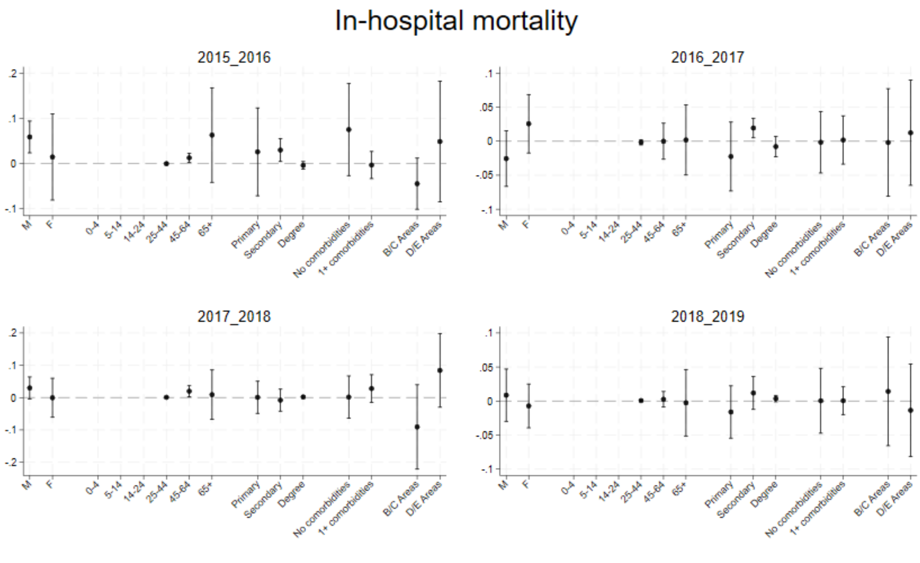

(b) Heterogeneous Average Treatment Effects (ATT) of residential heating activation on STEMI - In hospital mortality

Notes: The Figure displays the Average Treatment Effect on the Treated (ATT) of residential heating activation on (a) STEMI hospitalisations (upper panel) and (b) in-hospital mortality (lower panel). Results are stratified by gender, age group, educational attainment, comorbidity status (with/without), and climatic zone (B/C vs. D/E)

Figure A21: Heterogeneous Average Treatment Effects (ATT) of residential heating activation on NSTEMI

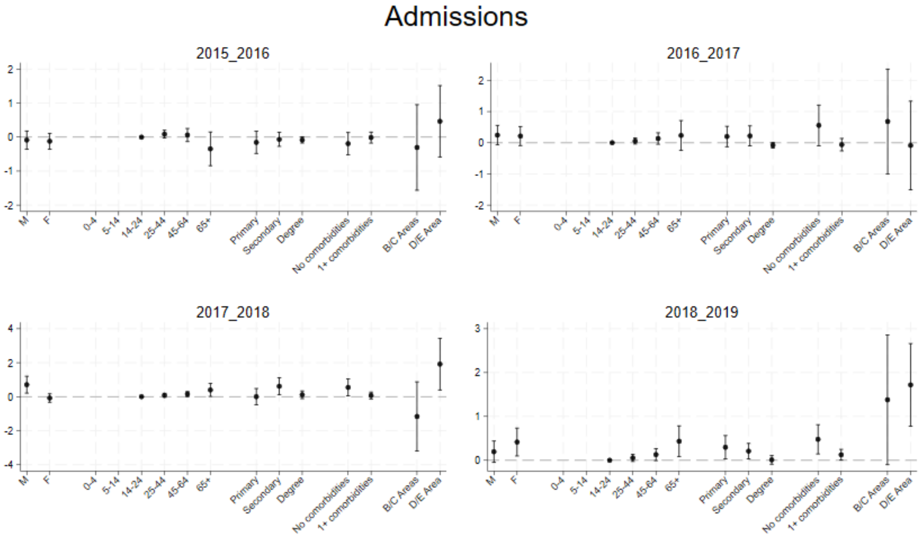

(a) Heterogeneous Average Treatment Effects (ATT) of residential heating activation on NSTEMI - Hospitalisations

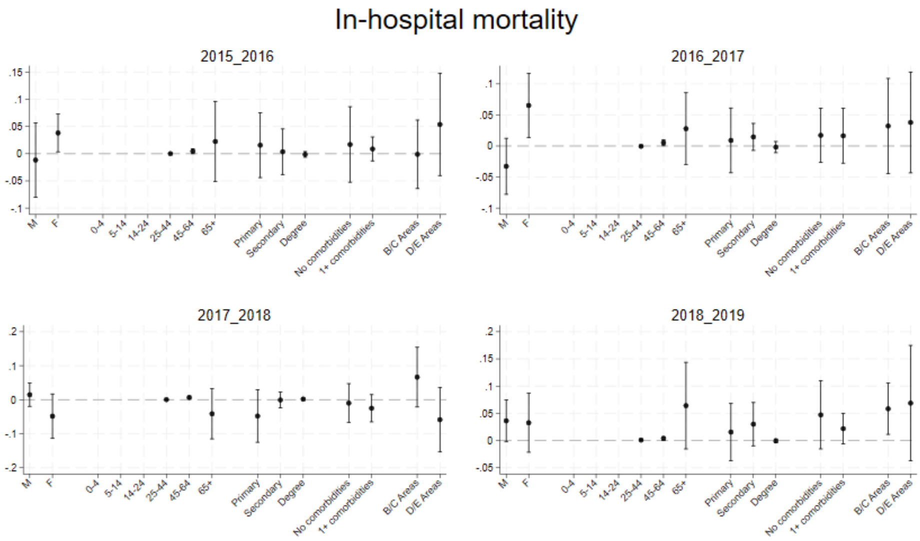

(b) Heterogeneous Average Treatment Effects (ATT) of residential heating activation on NSTEMI - In hospital mortality

Notes: The Figure displays the Average Treatment Effect on the Treated (ATT) of residential heating activation on (a) NSTEMI hospitalisations (upper panel) and (b) in-hospital mortality (lower panel). Results are stratified by gender, age group, educational attainment, comorbidity status (with/without), and climatic zone (B/C vs. D/E)

Figure A22: Heterogeneous Average Treatment Effects (ATT) of residential heating activation on Ischemic Stroke

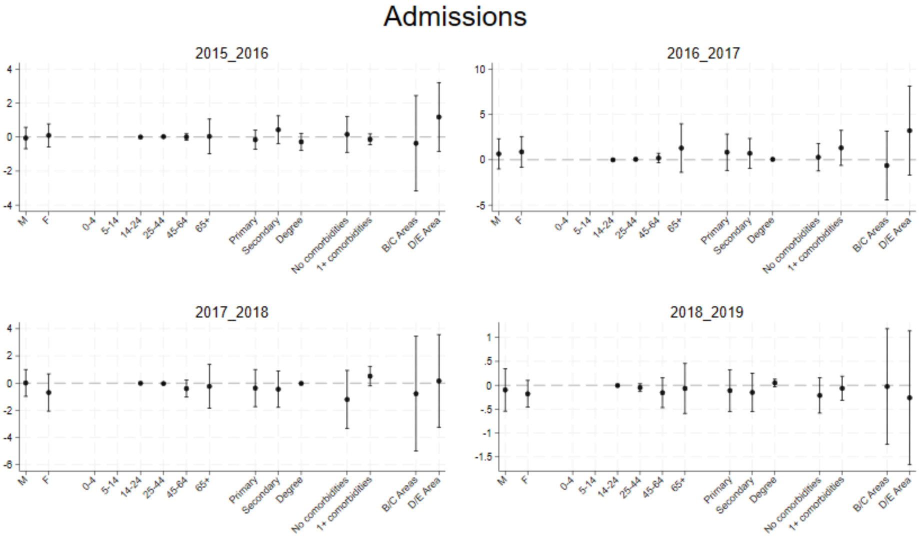

(a) Heterogeneous Average Treatment Effects (ATT) of residential heating activation on Ischemic Stroke - Hospitalisations

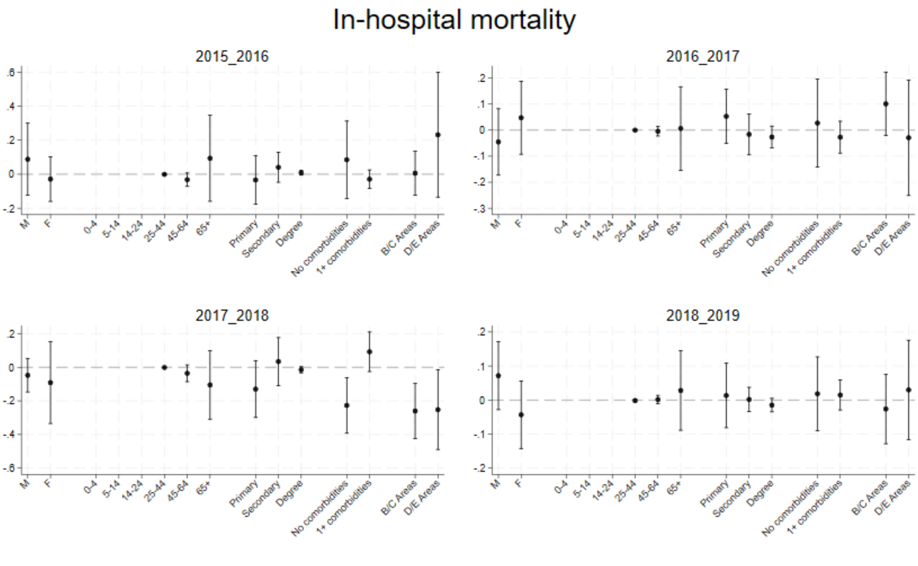

(b) Heterogeneous Average Treatment Effects (ATT) of residential heating activation on Ischemic Stroke - In hospital mortality

Notes: The Figure displays the Average Treatment Effect on the Treated (ATT) of residential heating activation on (a) Ischemic Stroke hospitalisations (upper panel) and (b) in-hospital mortality (lower panel). Results are stratified by gender, age group, educational attainment, comorbidity status (with/without), and climatic zone (B/C vs. D/E)

Figure A23: Heterogeneous Average Treatment Effects (ATT) of residential heating activation on Hemorrhagic Stroke

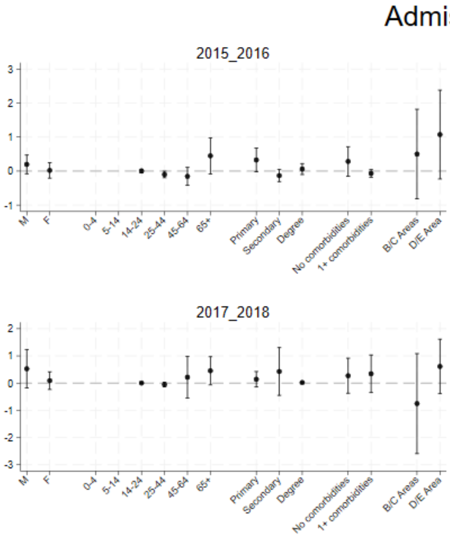

(a) Heterogeneous Average Treatment Effects (ATT) of residential heating activation on Hemorrhagic Stroke - Hospitalisations

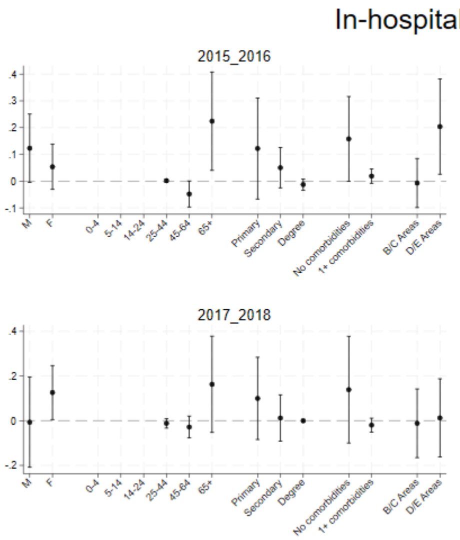

(b) Heterogeneous Average Treatment Effects (ATT) of residential heating activation on Hemorrhagic Stroke - In hospital mortality

Notes: The Figure displays the Average Treatment Effect on the Treated (ATT) of residential heating activation on (a) Hemorrhagic Stroke hospitalisations (upper panel) and (b) in-hospital mortality (lower panel). Results are stratified by gender, age group, educational attainment, comorbidity status (with/without), and climatic zone (B/C vs. D/E)

Figure A24: Heterogeneous Average Treatment Effects (ATT) of residential heating activation on COPD

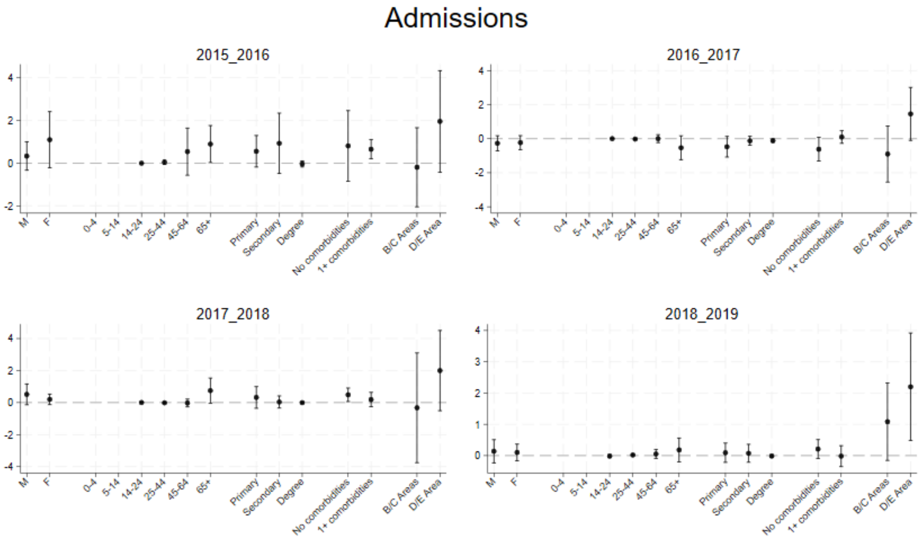

(a) Heterogeneous Average Treatment Effects (ATT) of residential heating activation on COPD - Hospitalisations

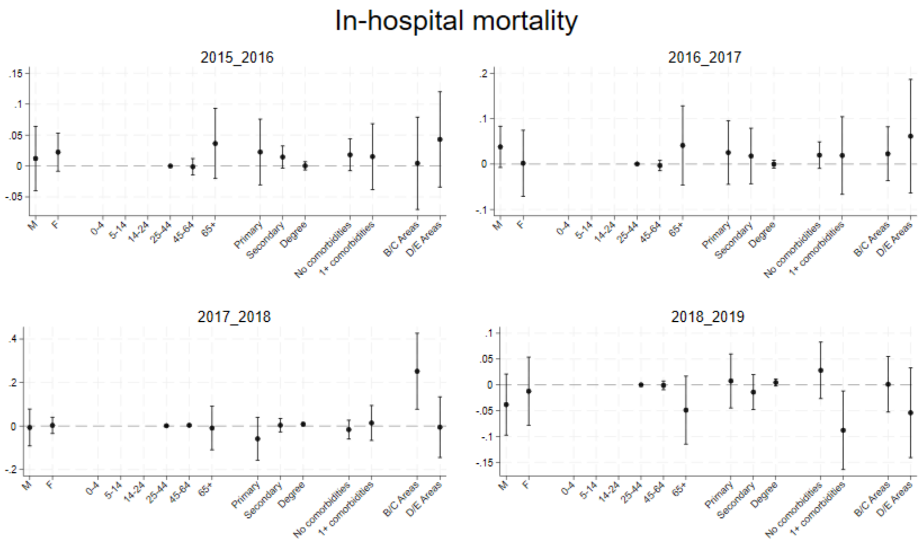

(b) Heterogeneous Average Treatment Effects (ATT) of residential heating activation on COPD - In hospital mortality

Notes: The Figure displays the Average Treatment Effect on the Treated (ATT) of residential heating activation on (a) COPD hospitalisations (upper panel) and (b) in-hospital mortality (lower panel). Results are stratified by gender, age group, educational attainment, comorbidity status (with/without), and climatic zone (B/C vs. D/E)

Table A5: Summary of Health Outcomes, Mortality, and Pollution Data (2015-2019)

	2015-2016			2016-2017			2017-2018			2018-2019		
	Obs	Mean	SD.	Obs	Mean	SD	Obs	Mean	SD	Obs	Mean	SD
I. Health outcomes - Hospitalisations												
AMI	5693	4.44	6.60	5694	4.41	6.48	5698	4.32	6.35	5687	4.40	7.91
STEMI	5693	1.86	3.65	5694	1.76	3.27	5698	1.65	2.84	5687	1.69	4.44
NSTEMI	5693	2.35	3.58	5694	2.44	3.77	5698	2.46	3.81	5687	2.49	3.96
Ischemic Stroke	5693	4.65	9.32	5694	4.49	9.20	5698	4.17	7.51	5687	3.83	6.09
Hemorrhagic Stroke	5693	1.33	2.84	5694	1.34	2.80	5698	1.34	2.69	5687	1.31	2.93
COPD	5693	3.07	6.15	5694	2.88	5.32	5698	2.66	4.74	5687	2.82	12.75
II. Health outcomes - Mortality												
AMI	5693	0.30	0.71	5694	0.30	0.73	5698	0.29	0.69	5687	0.28	0.92
STEMI	5693	0.15	0.49	5694	0.14	0.41	5698	0.14	0.43	5687	0.13	0.45
NSTEMI	5693	0.10	0.36	5694	0.11	0.46	5698	0.11	0.39	5687	0.11	0.63
Ischemic Stroke	5693	0.42	0.95	5694	0.40	0.94	5698	0.40	0.94	5687	0.35	0.80
Hemorrhagic Stroke	5693	0.32	0.86	5694	0.31	0.80	5698	0.32	0.85	5687	0.33	1.02
COPD	5693	0.13	0.44	5694	0.13	0.46	5698	0.13	0.46	5687	0.11	0.39
III. Pollution												
PM 2.5 (CAMS)	5693	16.40	7.06	5694	15.49	6.29	5698	12.83	6.23	5687	13.35	7.48
$> 15\ \mu g/m^3$	5693	3.20	1.77	5694	2.88	1.69	5698	1.90	1.79	5687	1.88	1.97
$> 25\ \mu g/m^3$	5693	1.04	1.50	5694	0.96	1.35	5698	0.60	1.17	5687	0.66	1.35
$> 75^{th}$ perc	5693	3.40	1.75	5694	3.09	1.67	5698	2.07	1.82	5687	2.05	1.99
$> 90^{th}$ perc	5693	1.56	1.70	5694	1.37	1.52	5698	0.85	1.39	5687	0.89	1.57
PM 2.5 (EEA)	4526	18.77	12.08	5061	17.74	11.35	5294	16.13	9.17	5539	15.63	8.57
$> 15\ \mu g/m^3$	4578	2.69	1.97	5077	2.38	1.89	5347	2.17	1.87	5642	2.13	1.82
$> 25\ \mu g/m^3$	4578	1.26	1.81	5077	1.10	1.60	5347	0.97	1.47	5642	0.84	1.43
$> 75^{th}$ perc	4578	2.49	1.99	5077	2.18	1.88	5347	1.98	1.86	5642	1.90	1.80
$> 90^{th}$ perc	4578	1.26	1.81	5077	1.10	1.60	5347	0.97	1.47	5642	0.84	1.43

Notes: The table provides summary statistics for the four biennia: 2015-16, 2016-17, 2017-18 and 2018-19. Panel (I) reports hospitalization rates, and Panel (II) presents in-hospital mortality for acute myocardial infarction (AMI), ST-elevation MI (STEMI), non-ST-elevation MI (NSTEMI), ischemic stroke, hemorrhagic stroke, and chronic obstructive pulmonary disease (COPD). Panel (III) provides summary statistics for air pollution exposure, including daily averages of $PM_{2.5}$ (CAMS and EEA), PM_{10} (EEA), NO_2 (EEA), SO_2 (EEA) and CO (EEA). For each pollutant, the Table also reports the number of days exceeding the WHO-defined hazardous thresholds. Air Quality Guidelines, updated 2021 by WHO, for various pollutants: $PM_{2.5}$ has a 1-day limit of $15\mu g/m^3$ (99th percentile: 5 $\mu g/m^3$, 3-4 exceedance days/year); PM_{10} has a 1-day limit of 45 $\mu g/m^3$ (99th percentile: 15 $\mu g/m^3$, 3-4 exceedance days/year); Nitrogen Dioxide ($NO2$) has a 1-hour limit of 200 $\mu g/m^3$, a 1-day limit of 25 $\mu g/m^3$, and a calendar year limit of 10 $\mu g/m^3$ (3-4 exceedance days/year); Sulfur dioxide (SO_2) has 24-hour limit of $40\mu g/m^3$ and a 10 minutes limit of 500; Carbon Monoxide (CO) has a 1-hour limit of 30 mg/m^3, a maximum daily 8-hour mean of 10 mg/m^3, and a 1-day limit of 4 mg/m^3 (3-4 exceedance days/year). Panel (IV) presents the average wind speed, temperature and precipitation. Panel (V) summarises the number of municipalities and hospital institutes for each biennium.

Table A5: Summary of Health Outcomes, Mortality, and Pollution Data (2015-2019)

	2015-2016			2016-2017			2017-2018			2018-2019		
	Obs	Mean	SD	Obs	Mean	SD	Obs	Mean	SD	Obs	Mean	SD
III. Pollution												
PM 10 (EEA)	5097	26.66	13.43	5427	26.12	12.91	5523	24.88	11.76	5533	25.13	10.91
$> 45\ \mu$g/m^3	5114	0.72	1.33	5475	0.69	1.16	5544	0.63	1.05	5603	0.59	1.06
$> 50\ \mu$g/m^3	5114	0.57	1.17	5475	0.54	1.00	5544	0.49	0.89	5603	0.44	0.90
$> 75^{th}$ perc	5114	1.67	1.77	5475	1.55	1.63	5544	1.46	1.60	5603	1.47	1.64
$> 90^{th}$ perc	5114	0.72	1.33	5475	0.69	1.16	5544	0.63	1.05	5603	0.59	1.06
NO2 (EEA)	5327	24.05	13.43	5542	23.01	13.09	5637	22.19	12.48	5662	20.78	11.90
$> 25\ \mu$g/m^3	5333	2.47	2.19	5557	2.30	2.10	5638	2.28	2.10	5663	2.07	2.06
$> 25\ \mu$g/m^3	5333	2.47	2.19	5557	2.30	2.10	5638	2.28	2.10	5663	2.07	2.06
$> 75^{th}$ perc	5333	1.75	1.98	5557	1.59	1.86	5638	1.57	1.83	5663	1.36	1.75
$> 90^{th}$ perc	5333	0.61	1.23	5557	0.56	1.13	5638	0.51	1.01	5663	0.39	0.88
SO2 (EEA)	5079	2.96	2.28	5443	2.79	2.21	5520	2.81	2.02	5543	2.75	2.20
$> 40\ \mu$g/m^3	5087	0.00	0.01	5458	0.00	0.01	5527	0.00	0.02	5562	0.00	0.01
$> 20\ \mu$g/m^3	5087	0.01	0.05	5458	0.01	0.09	5527	0.01	0.08	5562	0.01	0.05
$> 75^{th}$ perc	5087	0.92	1.54	5458	0.71	1.39	5527	0.72	1.34	5562	0.69	1.43
$> 90^{th}$ perc	5087	0.18	0.57	5458	0.17	0.60	5527	0.15	0.50	5562	0.19	0.77
CO (EEA)	5044	0.60	0.36	5374	0.55	0.32	5416	0.51	0.27	5471	0.48	0.26
> 4 mg/m^3	5049	0.00	0.00	5410	0.00	0.00	5431	0.00	0.01	5513	0.00	0.01
> 4 mg/m^3	5049	0.00	0.00	5410	0.00	0.00	5431	0.00	0.01	5513	0.00	0.01
$> 75^{th}$ perc	5049	2.57	2.41	5410	2.25	2.25	5431	2.05	2.17	5513	1.81	2.11
$> 90^{th}$ perc	5049	1.13	1.82	5410	0.87	1.54	5431	0.69	1.31	5513	0.61	1.23

Notes: The table provides summary statistics for the four biennia: 2015-16, 2016-17, 2017-18 and 2018-19. Panel (I) reports hospitalization rates, and Panel (II) presents in-hospital mortality for acute myocardial infarction (AMI), ST-elevation MI (STEMI), non-ST-elevation MI (NSTEMI), ischemic stroke, hemorrhagic stroke, and chronic obstructive pulmonary disease (COPD). Panel (III) provides summary statistics for air pollution exposure, including daily averages of $PM_{2.5}$ (CAMS and EEA), PM_{10} (EEA), NO_2 (EEA), SO_2 (EEA) and CO (EEA). For each pollutant, the Table also reports the number of days exceeding the WHO-defined hazardous thresholds. Air Quality Guidelines, updated 2021 by WHO, for various pollutants: $PM_{2.5}$ has a 1-day limit of 15μg/m^3 (99th percentile: 5 μg/m^3, 3-4 exceedance days/year); PM_{10} has a 1-day limit of 45 μg/m^3 (99th percentile: 15 μg/m^3, 3-4 exceedance days/year); Nitrogen Dioxide ($NO2$) has a 1-hour limit of 200 μg/m^3, a 1-day limit of 25 μg/m^3, and a calendar year limit of 10 μg/m^3 (3-4 exceedance days/year); Sulfur dioxide (SO_2) has 24-hour limit of 40μg/m^3 and a 10 minutes limit of 500; Carbon Monoxide (CO) has a 1-hour limit of 30 mg/m^3, a maximum daily 8-hour mean of 10 mg/m^3, and a 1-day limit of 4 mg/m^3 (3-4 exceedance days/year). Panel (IV) presents the average wind speed, temperature and precipitation. Panel (V) summarises the number of municipalities and hospital institutes for each biennium.

Table A5: Summary of Health Outcomes, Mortality, and Pollution Data (2015-2019)

	2015-2016			2016-2017			2017-2018			2018-2019		
	Obs	Mean	SD	Obs	Mean	SD.	Obs	Mean	SD.	Obs	Mean	SD
IV. Weather conditions												
Avg. wind speed	5693	2.46	0.84	5694	2.62	0.85	5698	2.73	0.90	5687	2.58	0.86
Avg. temperature	5693	15.75	6.85	5694	15.34	6.78	5698	15.16	7.18	5687	15.93	6.84
Precipitations	5693	1.82	1.41	5694	1.91	1.44	5698	1.90	1.53	5687	1.87	1.66
V. Data Coverage												
Municipalities		477			482			478			479	
Hospital Institutes		911			912			874			869	

Notes: The table provides summary statistics for the four biennia: 2015-16, 2016-17, 2017-18 and 2018-19. Panel (I) reports hospitalization rates, and Panel (II) presents in-hospital mortality for acute myocardial infarction (AMI), ST-elevation MI (STEMI), non-ST-elevation MI (NSTEMI), ischemic stroke, hemorrhagic stroke, and chronic obstructive pulmonary disease (COPD). Panel (III) provides summary statistics for air pollution exposure, including daily averages of $PM_{2.5}$ (CAMS and EEA), PM_{10} (EEA), NO_2 (EEA), SO_2 (EEA) and CO (EEA). For each pollutant, the Tablealso reports the number of days exceeding the WHO-defined hazardous thresholds. Air Quality Guidelines, updated 2021 by WHO, for various pollutants: $PM_{2.5}$ has a 1-day limit of 15μg/m^3 (99th percentile: 5 μg/m^3, 3-4 exceedance days/year); PM_{10} has a 1-day limit of 45 μg/m^3 (99th percentile: 15 μg/m^3, 3-4 exceedance days/year); Nitrogen Dioxide ($NO2$) has a 1-hour limit of 200 μg/m^3, a 1-day limit of 25 μg/m^3, and a calendar year limit of 10 μg/m^3 (3-4 exceedance days/year); Sulfur dioxide (SO_2) has 24-hour limit of 40μg/m^3 and a 10 minutes limit of 500; Carbon Monoxide (CO) has a 1-hour limit of 30 mg/m^3, a maximum daily 8-hour mean of 10 mg/m^3, and a 1-day limit of 4 mg/m^3 (3-4 exceedance days/year). Panel (IV) presents the average wind speed, temperature and precipitation. Panel (V) summarises the number of municipalities and hospital institutes for each biennium.

Table A6: 2021 World Health Organization (WHO) air quality guidelines (AQGs)

	$PM_{2.5}$	PM_{10}	NO_2	SO_2	CO
Annual	5	15	10	-	-
Daily	15	45	25	40	4

Notes: Air Quality Guidelines, updated 2021 by WHO, for various pollutants: $PM_{2.5}$ has a 1-day limit of 15μg/m^3 (99th percentile: 5 μg/m^3, 3-4 exceedance days/year); PM_{10} has a 1-day limit of 45 μg/m^3 (99th percentile: 15 μg/m^3, 3-4 exceedance days/year); Nitrogen Dioxide ($NO2$) has a 1-hour limit of 200 μg/m^3, a 1-day limit of 25 μg/m^3, and a calendar year limit of 10 μg/m^3 (3-4 exceedance days/year); Sulfur dioxide (SO_2) has 24-hour limit of 40μg/m^3 and a 10 minutes limit of 500; Carbon Monoxide (CO) has a 1-hour limit of 30 mg/m^3, a maximum daily 8-hour mean of 10 mg/m^3, and a 1-day limit of 4 mg/m^3 (3-4 exceedance days/year).

Table A7: Impact of Heating system activation on $PM_{2.5}$ EEA (2015-2019)

	2015-2016	2016-2017	2017-2018	2018-2019
	(1)	(2)	(3)	(4)
A. Average Effects				
ATT	7.127***	5.675***	6.967***	5.215***
	(1.171)	(1.043)	(1.256)	(0.763)
Mean of Y	19	18.17	16.31	15.67
SD of Y	12.29	11.93	9.622	8.922
Observations	3,792	4,434	4,819	5,169
B. Above 75th Percentile				
ATT	0.993***	0.811***	0.984***	0.865***
	(0.166)	(0.150)	(0.196)	(0.125)
Mean of Y	1.302	1.154	0.994	0.840
SD of Y	1.887	1.683	1.544	1.482
Observations	3,831	4,446	4,889	5,307

Notes: The table presents difference-in-differences estimates of the average treatment effect on the treated (ATT) of heating system activation on $PM_{2.5}$ EEA levels. Panel A shows effects on average $PM_{2.5}$ EEA levels, while Panel B focuses on the upper quartile of the outcome distribution. Standard errors at municipal level are in parentheses; *** p<0.01, ** p<0.05, * p<0.1.

Table A8: Impact of Heating system activation on PM_{10} EEA (2015-2019)

	2015-2016	2016-2017	2017-2018	2018-2019
	(1)	(2)	(3)	(4)
A. Average Effects				
ATT	6.776***	5.232***	7.331***	5.038***
	(1.153)	(0.972)	(1.480)	(0.810)
Mean of Y	27.01	26.56	25.29	25.45
SD of Y	13.57	13.66	12.12	11.54
Observations	4,320	4,763	4,965	5,088
B. Above 75th Percentile				
ATT	0.709***	0.530***	0.651***	0.500***
	(0.111)	(0.0986)	(0.134)	(0.0891)
Mean of Y	0.737	0.715	0.647	0.593
SD of Y	1.392	1.235	1.118	1.116
Observations	4,366	4,840	5,000	5,201

Notes: The table presents difference-in-differences estimates of the average treatment effect on the treated (ATT) of heating system activation on PM_{10} EEA levels. Panel A shows effects on average PM_{10} EEA levels, while Panel B focuses on the upper quartile of the outcome distribution. Standard errors at municipal level are in parentheses; *** p<0.01, ** p<0.05, * p<0.1.

Table A9: Impact of Heating system activation on SO_2 EEA (2015-2019)

	2015-2016	2016-2017	2017-2018	2018-2019
	(1)	(2)	(3)	(4)
A. Average Effects				
ATT	0.211	0.528***	0.447***	0.627***
	(0.200)	(0.197)	(0.141)	(0.188)
Mean of Y	2.994	2.864	2.815	2.753
SD of Y	2.400	2.437	2.211	2.424
Observations	4,265	4,728	4,973	5,204
B. Above 75th Percentile				
ATT	-0.0622	0.0733	0.0203	0.130**
	(0.0486)	(0.0490)	(0.0573)	(0.0599)
Mean of Y	0.159	0.171	0.130	0.183
SD of Y	0.588	0.679	0.533	0.867
Observations	4,273	4,839	5,009	5,282

Notes: The table presents difference-in-differences estimates of the average treatment effect on the treated (ATT) of heating system activation on SO_2 EEA levels. Panel A shows effects on average SO_2 EEA levels, while Panel B focuses on the upper quartile of the outcome distribution. Standard errors at municipal level are in parentheses; *** p<0.01, ** p<0.05, * p<0.1.

Table A10: Impact of Heating system activation on *CO* EEA (2015-2019)

	2015-2016	2016-2017	2017-2018	2018-2019
	(1)	(2)	(3)	(4)
A. Average Effects				
ATT	0.0470**	-0.00676	0.0725**	-0.00286
	(0.0216)	(0.0219)	(0.0290)	(0.0217)
Mean of Y	0.607	0.545	0.503	0.479
SD of Y	0.397	0.332	0.300	0.282
Observations	4,240	4,623	4,742	4,867
B. Above 75th Percentile				
ATT	0.179	0.0711	0.502***	0.0806
	(0.135)	(0.134)	(0.135)	(0.131)
Mean of Y	1.138	0.861	0.648	0.561
SD of Y	1.976	1.681	1.387	1.339
Observations	4,252	4,729	4,848	4,946

Notes: The table presents difference-in-differences estimates of the average treatment effect on the treated (ATT) of heating system activation on *CO* EEA levels. Panel A shows effects on average *CO* EEA levels, while Panel B focuses on the upper quartile of the outcome distribution. Standard errors at municipal level are in parentheses; *** p<0.01, ** p<0.05, * p<0.1.

Table A11: Average Treatment Effects of heating system activation under alternative treatment threshold definitions on: Pollutant Concentrations (Left Panel) vs. Regulatory Threshold Exceedances (Right Panel), across 2015-2019

	Pollutant Concentration				Days Over Threshold			
	2015-16	2016-17	2017-18	2018-19	2015-16	2016-17	2017-18	2018-19
PM 2.5 (CAMS)								
Above vs below median	3.070***	0.831*	3.423***	3.416***	0.610***	0.102	0.711***	0.759***
	(0.528)	(0.445)	(0.696)	(0.538)	(0.120)	(0.0979)	(0.147)	(0.131)
Above 66-33 percentile	3.970***	1.160	4.611***	4.611***	0.970***	0.148	0.969***	0.969***
	(0.784)	(0.728)	(0.781)	(0.781)	(0.228)	(0.154)	(0.187)	(0.187)
Above 75-25 percentile	5.971***	2.152**	5.606***	5.677***	1.604***	0.304	1.208***	1.256***
	(0.863)	(1.029)	(0.961)	(0.915)	(0.239)	(0.213)	(0.195)	(0.190)
PM 2.5 (EEA)								
Above vs below median	7.127***	5.675***	6.967***	5.215***	0.993***	0.811***	0.984***	0.865***
	(1.171)	(1.043)	(1.256)	(0.763)	(0.166)	(0.150)	(0.196)	(0.125)
Above 66-33 percentile	7.127***	5.675***	6.967***	5.215***	0.987***	0.591**	1.125***	1.125***
	(1.171)	(1.043)	(1.256)	(0.763)	(0.212)	(0.257)	(0.214)	(0.214)
Above 75-25 percentile	12.65***	8.576***	12.53***	9.582***	1.798***	1.070***	1.697***	1.412***
	(1.468)	(2.099)	(1.788)	(1.416)	(0.175)	(0.309)	(0.265)	(0.209)
PM 10 (EEA)								
Above vs below median	6.776***	5.232***	7.331***	5.038***	0.709***	0.530***	0.651***	0.500***
	(1.153)	(0.972)	(1.480)	(0.810)	(0.111)	(0.0986)	(0.134)	(0.0891)
Above 66-33 percentile	6.206***	4.865***	7.073***	7.073***	0.848***	0.559***	0.616***	0.616***
	(1.766)	(1.861)	(1.411)	(1.411)	(0.131)	(0.176)	(0.148)	(0.148)
Above 75-25 percentile	14.06***	11.23***	16.61***	10.36***	1.240***	0.940***	1.238***	0.881***
	(1.645)	(1.949)	(1.877)	(1.399)	(0.138)	(0.188)	(0.158)	(0.128)
NO2 (EEA)								
Above vs below median	4.896***	2.628***	4.457***	3.091***	0.769***	0.543***	0.600***	0.556***
	(0.998)	(0.804)	(0.873)	(0.619)	(0.124)	(0.116)	(0.113)	(0.0806)
Above 66-33 percentile	6.860***	2.391*	4.130***	4.130***	0.886***	0.617***	0.734***	0.734***
	(1.244)	(1.332)	(1.090)	(1.090)	(0.179)	(0.192)	(0.0831)	(0.0831)
Above 75-25 percentile	7.811***	4.767***	12.84***	6.126***	1.004***	0.906***	1.458***	0.899***
	(1.862)	(1.762)	(1.688)	(1.201)	(0.256)	(0.186)	(0.150)	(0.0870)

Notes: The table presents difference-in-differences estimates of the Average Treatment Effect on the Treated (ATT) of residential heating activation under alternative treatment thresholds. The left panel reports effects on air pollutant concentrations ($PM_{2.5}$, PM_{10}, and NO_2, measured in μg/m^3), while the right panel shows effects on annual exceedance days of regulatory thresholds. Treatment effects are estimated for three comparison groups: (i) above versus below median exposure, (ii) above the 66th versus below the 33rd percentile, and (iii) above the 75th versus below the 25th percentile of the treatment intensity distribution. Standard errors appear in parentheses with *** $p < 0.01$, ** $p < 0.05$, and * $p < 0.1$.

Table A12: Average Treatment Effects of heating system activation under Alternative Treatment Threshold Definitions on: Hospitalizations (Left Panel) vs. In-hospital mortality rates (Right Panel), across 2015-2019

	Hospitalizations				In-hospital mortality			
	2015-16	2016-17	2017-18	2018-19	2015-16	2016-17	2017-18	2018-19
AMI								
Above vs below median	1.215*	0.865	2.844***	2.675***	0.385***	-0.0224	-0.0475	0.113
	(0.648)	(0.755)	(0.768)	(0.489)	(0.147)	(0.149)	(0.249)	(0.110)
Above 66-33 percentile	1.639*	-0.266	2.520**	2.935***	0.711***	0.0283	-0.148	0.258*
	(0.964)	(1.138)	(1.252)	(0.710)	(0.200)	(0.185)	(0.192)	(0.136)
Above 75-25 percentile	2.603**	-0.652	2.984**	2.757***	1.111***	-0.0165	-0.235	0.390***
	(1.287)	(1.204)	(1.201)	(0.737)	(0.218)	(0.264)	(0.227)	(0.150)
STEMI								
Above vs below median	0.591	0.100	1.051***	1.180***	0.287**	-0.0130	0.0448	0.0492
	(0.441)	(0.402)	(0.359)	(0.290)	(0.116)	(0.106)	(0.106)	(0.0810)
Above 66-33 percentile	1.577***	-0.402	1.439**	1.590***	0.503***	0.0693	-0.150	0.0960
	(0.460)	(0.692)	(0.709)	(0.389)	(0.188)	(0.0964)	(0.148)	(0.0857)
Above 75-25 percentile	1.666**	-0.340	1.442**	1.290***	0.940***	0.0896	-0.134	0.131
	(0.676)	(0.940)	(0.676)	(0.439)	(0.183)	(0.133)	(0.140)	(0.0888)
NSTEMI								
Above vs below median	0.326	0.665	1.746***	1.355***	0.0835	0.0613	0.0105	0.161***
	(0.457)	(0.582)	(0.560)	(0.385)	(0.0909)	(0.0739)	(0.0889)	(0.0577)
Above 66-33 percentile	-0.436	0.311	1.673**	1.148**	0.0959	0.133	0.120	0.212***
	(0.659)	(1.035)	(0.710)	(0.550)	(0.0840)	(0.0968)	(0.0789)	(0.0775)
Above 75-25 percentile	0.245	0.0417	1.333*	1.047*	0.0387	0.125	0.0827	0.286***
	(0.663)	(0.775)	(0.787)	(0.556)	(0.103)	(0.125)	(0.101)	(0.0845)
Ischemic Stroke								
Above vs below median	0.532	2.850	0.961	-0.661	0.164	0.234	0.0515	0.182
	(0.857)	(2.101)	(1.475)	(0.521)	(0.262)	(0.201)	(0.233)	(0.144)
Above 66-33 percentile	-0.572	1.964	2.554*	-1.552	-0.0435	0.501	-0.295	-0.174
	(1.710)	(1.391)	(1.481)	(1.184)	(0.487)	(0.311)	(0.250)	(0.161)
Above 75-25 percentile	-0.193	3.620*	2.931*	-1.432	-0.517	0.999**	-0.465	-0.0734
	(2.829)	(1.956)	(1.716)	(1.091)	(0.776)	(0.397)	(0.366)	(0.184)
Hemorrhagic Stroke								
Above vs below median	0.511	1.310*	0.991	0.0552	0.446***	-0.0100	0.528*	0.124
	(0.555)	(0.783)	(0.646)	(0.427)	(0.173)	(0.164)	(0.280)	(0.128)
Above 66-33 percentile	-0.294	0.149	3.089	0.0972	0.336	-0.342	1.481**	0.142
	(0.679)	(0.706)	(2.031)	(0.641)	(0.248)	(0.272)	(0.619)	(0.186)
Above 75-25 percentile	-0.898	0.679	5.726**	0.782	0.479	-0.351	2.027***	0.307
	(1.108)	(0.882)	(2.252)	(0.621)	(0.332)	(0.368)	(0.750)	(0.200)
COPD								
Above vs below median	2.136**	1.279*	2.284**	1.828***	-0.00365	0.0559	0.0459	-0.0565
	(0.916)	(0.668)	(1.016)	(0.664)	(0.0822)	(0.113)	(0.137)	(0.0923)
Above 66-33 percentile	2.752***	1.523	2.889***	2.721***	0.0299	0.0389	0.0648	0.0257
	(0.999)	(1.345)	(0.904)	(0.850)	(0.131)	(0.149)	(0.130)	(0.113)
Above 75-25 percentile	2.997***	1.476	4.028***	3.122***	-0.162	-0.136	0.0319	0.0118
	(0.916)	(2.050)	(1.146)	(1.100)	(0.146)	(0.172)	(0.186)	(0.147)

Notes: The table presents difference-in-differences estimates of the Average Treatment Effect on the Treated (ATT) under alternative treatment thresholds. The left panel shows effects on the number of hospitalizations, while the right panel reports effects on in-hospital mortality rate for AMI, STEMI, NSTEMI, Ischemic Stroke, Hemorrhagic Stroke and COPD. Treatment effects are estimated for three comparison groups: (i) above versus below median, (ii) above the 66th vs. below the 33rd percentile, and (iii) above the 75th vs. below the 25th percentile based on the treatment intensity distribution. Standard errors are reported in parentheses. Significance levels: *** $p < 0.01$, ** $p < 0.05$, * $p < 0.1$.

Table A13: Robust Inference and Sensitivity Analysis on pollutants concentration using Honest DiD

	Average					Above 75-th Percentile				
	Lag 1	Lag 2	Lag 3	Lag 4	Lag 5	Lag 1	Lag 2	Lag 3	Lag 4	Lag 5
PM 2.5 (CAMS)										
2015-2016	0-25%	50-75%	75-100%	150-175%	100-125%	0-25%	50-75%	75-100%	150-175%	100-125%
2016-2017	50-75%	0-25%	100-125%	75-100%	75-100%	50-75%	0-25%	100-125%	75-100%	75-100%
2017-2018	50-75%	100-125%	50-75%	75-100%	100-125%	50-75%	100-125%	50-75%	75-100%	100-125%
2018-2019	25-50%	50-75%	75-100%	100-125%	125-150%	25-50%	50-75%	75-100%	100-125%	125-150%
PM 2.5 (EEA)										
2015-2016	0-25%	25-50%	100-125%	150-175%	100-125%	0-25%	25-50%	100-125%	150-175%	100-125%
2016-2017	-	50-75%	100-125%	75-100%	125-150%	-	50-75%	100-125%	75-100%	125-150%
2017-2018	25-50%	75-100%	75-100%	100-125%	100-125%	25-50%	75-100%	75-100%	100-125%	100-125%
2018-2019	25-50%	50-75%	75-100%	125-150%	100-125%	25-50%	50-75%	75-100%	125-150%	100-125%
PM 10 (EEA)										
2015-2016	-	25-50%	100-125%	150-175%	100-125%	-	25-50%	100-125%	150-175%	100-125%
2016-2017	-	25-50%	100-125%	75-100%	125-150%	-	25-50%	100-125%	75-100%	125-150%
2017-2018	25-50%	75-100%	75-100%	100-125%	75-100%	25-50%	75-100%	75-100%	100-125%	75-100%
2018-2019	25-50%	25-50%	50-75%	100-125%	75-100%	25-50%	25-50%	50-75%	100-125%	75-100%
NO_2 (EEA)										
2015-2016	-	25-50%	75-100%	75-100%	75-100%	-	25-50%	75-100%	75-100%	75-100%
2016-2017	-	25-50%	75-100%	75-100%	50-75%	-	25-50%	75-100%	75-100%	50-75%
2017-2018	25-50%	75-100%	75-100%	100-125%	75-100%	25-50%	75-100%	75-100%	100-125%	75-100%
2018-2019	-	25-50%	25-50%	75-100%	75-100%	-	25-50%	25-50%	75-100%	75-100%

Notes: The table reports the sensitivity analysis based on the Honest Difference-in-Differences framework developed by Rambachan & Roth (2023). The left panel presents results averaged across different lag specifications, while the right panel shows results for the top quartile of the treatment distribution (above the 75-th percentile). Lag columns correspond to treatment lags of 1 to 5 months before heating system activation. "-" indicates insufficient data for robust estimation in that cell.

Table A14: Robust Inference and Sensitivity Analysis on Hospitalisations Outcomes using Honest DiD

	Years	Lag 1	Lag 2	Lag 3	Lag 4	Lag 5
		(1)	(2)	(3)	(4)	(5)
Hospitalisations						
AMI	2015-2016	-	-	-	-	-
	2017-2018	-	50-75%	-	25-50%	25-50%
STEMI	2017-2018	-	25-50%	-	25-50%	-
NSTEMI	2017-2018	-	25-50%	-	-	25-50%
COPD	2015-2016	-	25-50%	25-50%	25-50%	25-50%
	2017-2018	-	25-50%	50-75%	50-75%	75-100%

Notes: The table shows sensitivity analyses for health-related hospitalisation outcomes using the Honest Difference-in-Differences methodology (Rambachan & Roth (2023)). Each column corresponds to a different lag (1-5 months before heating activation) between exposure and outcome. Dash "-" indicates insufficient data for robust estimation in that cell.

Table A15: Average Treatment Effects Estimates of heating system activation on Placebo Outcomes: Hospitalization Rates (left panel) and In-Hospital Mortality Rates (right panel) × 10,000 Inhabitants, across 2015-2019

	Hospitalizations				In-Hospital Mortality			
	2015-16	2016-17	2017-18	2018-19	2015-16	2016-17	2017-18	2018-19
	(1)	(2)	(3)	(4)	(1)	(2)	(3)	(4)
Fractures								
ATT	0.427	-0.595	1.707	0.449	0.0921	0.0625	-0.0428	-0.0111
	(1.186)	(0.995)	(2.249)	(1.325)	(0.0765)	(0.0538)	(0.0648)	(0.0386)
Infections								
ATT	0.207	-0.0814	0.00873	-0.446	-0.0369	0.0504	0.0247	-0.0751
	(0.886)	(0.476)	(0.550)	(0.386)	(0.0693)	(0.0832)	(0.148)	(0.0810)
Traumatism								
ATT	-0.128*	0.0243	0.127	0.193*	0.00320	0.0242	-0.00116	0.00542
	(0.0654)	(0.0879)	(0.238)	(0.116)	(0.0139)	(0.0224)	(0.00607)	(0.0140)
Poisoning								
ATT	-0.0387	-0.0228	-0.0307	0.0214	-0.00780	-0.00116	0.00218	0.00218
	(0.0714)	(0.0671)	(0.0321)	(0.0529)	(0.00780)	(0.00132)	(0.00209)	(0.00265)
Elective admissions								
ATT	-9.652	13.55	-2.683	5.595	-0.0290	-0.230	0.0206	-0.0549
	(9.142)	(18.68)	(10.92)	(6.251)	(0.243)	(0.143)	(0.166)	(0.0973)
Nervous system								
ATT	-1.299	11.43	-2.018	-0.138	-0.0485	0.00298	-0.0579	0.0582
	(2.523)	(13.60)	(9.408)	(0.378)	(0.0507)	(0.0487)	(0.0492)	(0.0549)
Mental health								
ATT	-0.532	0.0649	-1.364	0.931	0.000827	0.0384	-0.000147	0.0365**
	(0.380)	(0.642)	(0.950)	(0.755)	(0.0132)	(0.0311)	(0.0112)	(0.0147)

Notes: The left panel reports ATT estimates for hospitalization rates, while the right panel shows estimates for in-hospital mortality rates. All outcomes are measured × 10,000 inhabitants. Standard errors in parentheses. *** p<0.01, ** p<0.05, * p<0.1.

Table A16: ICD9-CM Classification of Placebo Outcomes

Variable	**ICD9-CM Classification**[27]	**Explanation**
Trauma	(dpr_3_n ≥ 800 and dpr_3_n ≤ 904) OR (dsec1_3_n ≥ 800 and dsec1_3_n ≤ 904)	Fractures, dislocations, and injuries
Nutrition	dpr_3_n = 783	Symptoms related to nutrition, metabolism, and development
Traumatism	dpr_3_n ≥ 950 and dpr_3_n ≤ 959	Traumatisms of nervous system and spinal cord, including traumatic complications
Poisoning	dpr_3_n ≥ 960 and dpr_3_n ≤ 979	Poisoning from drugs, medicines and biological substances
Elective	tiporic = 1	Planned/elective hospital admissions
Nervous System	dpr_3_n ≥ 320 and dpr_3_n ≤ 389	Diseases of nervous system and sensory organs
Mental Health	dpr_3_n ≥ 290 and dpr_3_n ≤ 319	Mental and behavioral disorders

Notes: The table presents the ICD-9-CM classification criteria used to identify placebo outcomes in the analysis. The diagnostic codes are drawn from primary diagnosis fields (dpr_3_n) and secondary diagnosis fields (dsec1_3_n) where specified.

Table A17: Robustness of Average Treatment Effects of heating system activation to alternative estimation strategies: population weighting, spillover adjustment, and augmented IPW estimation

	Pollutant Concentration				Days Over Threshold			
	2015-16	2016-17	2017-18	2018-19	2015-16	2016-17	2017-18	2018-19
PM 2.5 (CAMS)								
Weighted	3.956***	1.211**	3.676***	4.434***	0.861***	0.187	0.816***	0.948***
	(0.603)	(0.536)	(0.779)	(0.562)	(0.142)	(0.131)	(0.164)	(0.140)
Neighbors	2.408***	0.415	2.588***	1.813***	0.425***	0.031	0.527***	0.351**
	(0.576)	(0.456)	(0.765)	(0.620)	(0.132)	(0.102)	(0.166)	(0.159)
AIPW	3.424***	1.736**	6.171***	3.551***	0.567***	0.301*	1.239***	0.816***
	(0.524)	(0.764)	(1.791)	(0.470)	(0.114)	(0.164)	(0.323)	(0.126)
PM 2.5 (EEA)								
Weighted	8.979***	6.416***	7.522***	5.513***	1.223***	0.904***	1.017***	0.912***
	(1.302)	(1.178)	(1.248)	(0.667)	(0.158)	(0.170)	(0.206)	(0.118)
Neighbors	6.690***	4.889***	5.977***	3.186***	0.892***	0.631***	0.794***	0.468***
	(1.072)	(0.965)	(1.305)	(0.855)	(0.160)	(0.139)	(0.201)	(0.146)
AIPW	8.767***	6.265***	9.183***	5.236***	1.202***	0.879***	1.368***	0.900***
	(1.332)	(1.175)	(1.902)	(0.692)	(0.191)	(0.164)	(0.304)	(0.122)
PM_{10} (EEA)								
Weighted	7.663***	5.256***	6.895***	4.685***	0.874***	0.574***	0.687***	0.533***
	(1.403)	(1.064)	(1.507)	(0.919)	(0.133)	(0.122)	(0.144)	(0.112)
Neighbors	7.184***	4.865***	6.623***	3.750***	0.675***	0.472***	0.576***	0.341***
	(0.921)	(0.832)	(1.327)	(0.782)	(0.0932)	(0.0842)	(0.125)	(0.0909)
AIPW	7.004***	6.131***	12.68***	5.371***	0.776***	0.612***	1.143***	0.543***
	(1.121)	(1.104)	(3.750)	(0.773)	(0.119)	(0.120)	(0.303)	(0.0874)
NO_2 (EEA)								
Weighted	7.649***	3.466***	4.372***	4.547***	1.202***	0.725***	0.959***	0.866***
	(1.122)	(0.998)	(1.345)	(0.765)	(0.183)	(0.176)	(0.200)	(0.147)
Neighbors	5.026***	2.157***	3.612***	1.453***	0.744***	0.456***	0.474***	0.456***
	(0.742)	(0.706)	(0.735)	(0.551)	(0.086)	(0.088)	(0.098)	(0.065)
AIPW	3.956***	3.840***	5.324***	3.124***	0.776***	0.612***	1.143***	0.543***
	(1.087)	(0.840)	(1.471)	(0.550)	(0.119)	(0.120)	(0.303)	(0.087)

Notes: The table extends the main results by applying alternative estimation strategies. Specifically, we consider: (i) weighting estimates by the municipal population, (ii) adjusting for potential spillover effects from neighboring municipalities within a 30 km radius, and (iii) using the augmented Inverse Probability Weighting (AIPW) version of the Callaway & Sant'Anna (2021) estimator. The left panel reports effects on air pollutant concentrations ($PM_{2.5}$, PM_{10} and NO_2, measured in μg/m^3), while the right panel presents effects on the number of days exceeding regulatory pollution thresholds. Standard errors are reported in parentheses. Significance levels: *** $p < 0.01$, ** $p < 0.05$, * $p < 0.1$.

Table A18: Robustness of Average Treatment Effects of heating system activation on hospitalisations and in-hospital mortality to alternative estimation strategies: population weighting, spillover adjustment, and augmented IPW estimation

	Hospitalizations				In-hospital Mortality			
	2015-16	2016-17	2017-18	2018-19	2015-16	2016-17	2017-18	2018-19
AMI								
Weighted by population	0.832	0.713	1.740***	1.893***	0.292***	-0.0267	0.0507	0.112
	(0.506)	(0.570)	(0.567)	(0.358)	(0.0855)	(0.103)	(0.122)	(0.0730)
Nearest neighbours	1.475**	1.117	3.084***	2.669***	0.408***	-0.0293	-0.000410	0.0660
	(0.646)	(0.908)	(0.888)	(0.567)	(0.141)	(0.169)	(0.243)	(0.125)
AIPW	1.515*	0.0234	4.263***	2.951***	0.242*	-0.128	-0.221	0.0441
	(0.885)	(1.078)	(1.443)	(0.536)	(0.143)	(0.158)	(0.255)	(0.107)
STEMI								
Weighted by population	0.407*	0.151	0.804***	0.482**	0.163***	0.0131	0.0899	0.0211
	(0.246)	(0.258)	(0.263)	(0.233)	(0.0602)	(0.0655)	(0.0696)	(0.0547)
Nearest neighbours	0.715*	0.170	1.159***	1.170***	0.293**	-0.0419	0.0529	0.0195
	(0.406)	(0.445)	(0.367)	(0.304)	(0.114)	(0.126)	(0.101)	(0.0882)
AIPW	0.230	-0.0452	1.677***	1.159***	0.243**	-0.116	-0.0257	-0.0258
	(0.701)	(0.337)	(0.600)	(0.272)	(0.111)	(0.109)	(0.104)	(0.0748)
NSTEMI								
Weighted by population	0.299	0.530	0.959**	1.290***	0.113***	-0.00165	-0.00805	0.130***
	(0.375)	(0.441)	(0.379)	(0.257)	(0.0430)	(0.0521)	(0.0525)	(0.0447)
Nearest neighbours	0.486	0.826	1.865***	1.408***	0.117	0.0859	0.0204	0.138**
	(0.507)	(0.719)	(0.621)	(0.470)	(0.0947)	(0.0802)	(0.0864)	(0.0642)
AIPW	0.784	0.0162	2.393**	1.719***	-0.000670	0.0387	-0.0392	0.130**
	(0.579)	(0.985)	(1.033)	(0.465)	(0.0877)	(0.0788)	(0.0914)	(0.0578)
Ischemic Stroke								
Weighted by population	0.625	1.323***	1.075**	0.352	0.192**	0.241***	0.0859	0.0580
	(0.464)	(0.496)	(0.495)	(0.291)	(0.0961)	(0.0914)	(0.111)	(0.0875)
Nearest neighbours	0.554	2.358	0.983	-0.489	0.188	0.235	0.0480	0.208
	(0.900)	(2.116)	(1.386)	(0.613)	(0.268)	(0.218)	(0.270)	(0.142)
AIPW	0.232	4.404	2.457	-0.505	0.0683	0.143	-0.0564	0.0834
	(1.114)	(2.865)	(2.014)	(0.519)	(0.264)	(0.199)	(0.235)	(0.138)
Hemorrhagic Stroke								
Weighted by population	0.243	0.272	0.772**	0.478**	0.228**	-0.0258	0.398***	0.175**
	(0.252)	(0.264)	(0.300)	(0.206)	(0.0916)	(0.129)	(0.127)	(0.0839)
Nearest neighbours	0.612	1.334*	1.010*	0.243	0.521***	0.0601	0.552**	0.190
	(0.605)	(0.772)	(0.576)	(0.571)	(0.202)	(0.183)	(0.270)	(0.147)
AIPW	1.813	1.700	0.998	0.612	0.258	-0.0233	0.426	0.0177
	(1.277)	(1.221)	(0.836)	(0.583)	(0.161)	(0.163)	(0.278)	(0.112)
COPD								
Weighted by population	1.418**	1.051**	1.980***	1.425***	-0.0567	0.111**	0.0473	0.0129
	(0.567)	(0.498)	(0.490)	(0.379)	(0.0557)	(0.0539)	(0.0675)	(0.0516)
Nearest neighbours	2.527***	1.326*	2.426**	1.448*	0.0231	0.0313	0.0378	-0.0487
	(0.922)	(0.724)	(1.058)	(0.812)	(0.0906)	(0.129)	(0.136)	(0.109)
AIPW	2.026***	0.478	1.981**	1.553**	0.0154	-0.0121	-0.0278	-0.135
	(0.747)	(0.702)	(0.972)	(0.687)	(0.0750)	(0.117)	(0.140)	(0.0885)

Notes: The table extends the main results by applying alternative estimation strategies. Specifically, we consider: (i) weighting estimates by the municipal population, (ii) adjusting for potential spillover effects from neighboring municipalities within a 30 km radius, and (iii) using the augmented Inverse Probability Weighting (AIPW) version of the Callaway & Sant'Anna (2021) estimator. The left panel reports effects on hospitalisations, while the right panel presents effects on in-hospital mortality for AMI, STEMI, NSTEMI, Ischemic Stroke, Hemorrhagic Stroke and COPD. Standard errors are reported in parentheses. Significance levels: *** $p < 0.01$, ** $p < 0.05$, * $p < 0.1$.

Table A19: Correlations of environmental pollutants on immigration, emigration, and net inflow in municipalities.

	Immigration	Emigration	Net inflow	Immigration	Emigration	Net inflow	Immigration	Emigration	Net inflow	Immigration	Emigration	Net inflow	Immigration	Emigration	Net inflow
	(1)	(2)	(3)	(4)	(5)	(6)	(7)	(8)	(9)	(10)	(11)	(12)	(13)	(14)	(15)
PM 2.5 (CAMS), Lag 1	-1.3361	3.7390	-5.0743	-4.8826	2.0633	-6.9459	-4.8273	1.3445	-6.1719	-0.9815	0.4716	-1.4531	-1.3173	1.7942	-3.1114
	(3.023)	(2.627)	(3.862)	(3.912)	(3.498)	(4.904)	(4.308)	(3.812)	(5.372)	(4.666)	(4.006)	(5.709)	(4.944)	(4.216)	(6.031)
NO2 (EEA), Lag 1				2.7043	7.5399***	-4.8355	2.4101	6.4567**	-4.0465	2.6038	6.1740**	-3.5703	3.8393	5.8729**	-2.0337
				(2.740)	(2.479)	(3.502)	(2.967)	(2.646)	(3.816)	(3.058)	(2.644)	(3.979)	(3.201)	(2.742)	(4.138)
SO2 (EEA), Lag 1							-4.3876	-1.0269	-3.3607	-1.4938	-6.3786**	4.8847	-4.6919	-5.1081	0.4163
							(2.980)	(3.172)	(4.363)	(3.081)	(2.802)	(4.174)	(3.401)	(3.108)	(4.477)
CO (EEA), Lag 1										2.8905	-1.1187	4.0094	2.7564	-0.6581	3.4145
										(2.085)	(1.924)	(2.648)	(2.189)	(2.027)	(2.758)
Income, Lag 1	0.0004	-0.0009	0.0014	-0.0000	-0.0027	0.0027	0.0002	-0.0025	0.0027	-0.0002	-0.0029	0.0027	0.0002	-0.0035	0.0037
	(0.003)	(0.003)	(0.005)	(0.004)	(0.003)	(0.005)	(0.004)	(0.004)	(0.006)	(0.005)	(0.004)	(0.006)	(0.005)	(0.004)	(0.007)
Wind speed, Lag 1	-2.6279	-2.3748	-0.2523	-6.0093	-3.4196	-2.5898	-4.9947	-3.5573	-1.4376	-4.6514	-2.0895	-2.5620	-0.0179	-3.9357	3.9178
	(3.313)	(3.085)	(4.380)	(4.206)	(3.985)	(5.544)	(4.747)	(4.381)	(6.170)	(5.004)	(4.541)	(6.477)	(5.536)	(4.705)	(6.738)
Precipitations, Lag 1	-0.0106	-5.6074***	5.5980***	-1.1892	-5.1177***	3.9284	-0.6272	-5.5044***	4.8770*	0.6410	-2.4491	3.0900	0.4266	-0.6889	1.1154
	(1.561)	(1.399)	(2.079)	(1.842)	(1.788)	(2.455)	(2.112)	(2.115)	(2.863)	(2.248)	(2.017)	(2.855)	(2.403)	(2.134)	(3.008)
Constant	297.9368***	311.5024***	-13.5482	326.3402***	342.5775***	-16.2350	323.1113***	342.9060***	-19.7920	319.2874***	343.7409***	-24.4518	304.6163***	356.3817***	-51.7655
	(51.861)	(45.076)	(71.826)	(61.727)	(54.817)	(85.120)	(65.181)	(58.029)	(90.711)	(73.672)	(64.207)	(102.037)	(79.219)	(67.751)	(108.953)
Muncipal FE	Y	Y	Y	Y	Y	Y	Y	Y	Y	Y	Y	Y	Y	Y	Y
Year FE	Y	Y	Y	Y	Y	Y	Y	Y	Y	Y	Y	Y	Y	Y	Y
Municipal time trends	Y	Y	Y	Y	Y	Y	Y	Y	Y	Y	Y	Y	Y	Y	Y
Observations	38,126	38,126	38,126	31,182	31,182	31,182	28,762	28,762	28,762	25,853	25,853	25,853	23,629	23,629	23,629
R-squared															
Mean of Y	300.8	294.8	5.997	300.8	294.8	5.997	300.8	294.8	5.997	300.8	294.8	5.997	300.8	294.8	5.997
SD of Y	148.8	140.7	131.7	148.8	140.7	131.7	148.8	140.7	131.7	148.8	140.7	131.7	148.8	140.7	131.7

Notes: The table presents regression estimates examining the correlations of air pollution on migration patterns at the municipal level. The dependent variables are immigration, emigration, and net inflow (immigration minus emigration), with all independent variables lagged by one year. Key pollutants include $PM_{2.5}$, NO_2, SO_2 and CO concentrations, as well as income, wind speed, and precipitation. The models control for municipal fixed effects, year fixed effects, and municipal time trends. Coefficients for each pollutant are shown with standard errors in parentheses with statistical significance levels: *** $p < 0.01$, ** $p < 0.05$, * $p < 0.1$.

Acknowledgments

We thank the NCDC Climate Services Branch (CSB) for making available data on weather conditions. We acknowledge funding from the Catholic University of Milan D 3.2 strategic research grant “Fight against poverty: empirical research in support of public policies”. The usual disclaimers apply.

References

Bauernschuster, S., Hener, T. & Rainer, H. (2017), 'When labor disputes bring cities to a standstill: The impact of public transit strikes on traffic, accidents, air pollution, and health', *American Economic Journal: Economic Policy* **9**, 1–37.

Brook, R. D., Rajagopalan, S., Pope, C. A., Brook, J. R., Bhatnagar, A., Diez-Roux, A. V., Holguin, F., Hong, Y., Luepker, R. V., Mittleman, M. A., Peters, A., Siscovick, D., Smith, S. C., Whitsel, L. & Kaufman, J. D. (2010), 'Particulate matter air pollution and cardiovascular disease: An update to the scientific statement from the american heart association'.

Callaway, B. & Sant'Anna, P. H. (2021), 'Difference-in-Differences with multiple time periods', *Journal of Econometrics* **225**(2), 200–230.

Chay, K. Y. & Greenstone, M. (2003), 'The impact of air pollution on infant mortality: Evidence from geographic variation in pollution shocks induced by a recession', *The Quarterly Journal of Economics* **118**(3), 1121–1167.

Cheung, C. W., He, G. & Pan, Y. (2020), 'Mitigating the air pollution effect? the remarkable decline in the pollution-mortality relationship in hong kong', *Journal of Environmental Economics and Management* **101**, 102316.

de Chaisemartin, C. & D'Haultfœuille, X. (2020), 'Two-way fixed effects estimators with heterogeneous treatment effects', *American Economic Review* **110**(9), 2964–96.

DeCicca, P. & Malak, N. (2020), 'When good fences aren't enough: The impact of neighboring air pollution on infant health', *Journal of Environmental Economics and Management* **102**, 102324.

Deryugina, T., Heutel, G., Miller, N. H., Molitor, D. & Reif, J. (2019), 'The mortality and medical costs of air pollution: Evidence from changes in wind direction', *American Economic Review* **109**(12), 4178–4219.

European Environment Agency (2023), Air quality in europe 2023, Report, European Environment Agency.

Fan, M., He, G. & Zhou, M. (2020), 'The winter choke: Coal-fired heating, air pollution, and mortality in china', *Journal of Health Economics* **71**, 102316.

Fan, M., Jiang, H. & Zhou, M. (2023), 'Beyond particulate matter: New evidence on the causal effects of air pollution on mortality', *Journal of Health Economics* **91**, 102799.

Gazzetta Ufficiale della Repubblica Italiana - DPR 412/1993 (1993), 'Dpr 412/1993'. Regolamento recante norme per la progettazione, l'installazione, l'esercizio e la manutenzione degli impianti termici degli edifici ai fini del contenimento dei consumi di energia, in attuazione dell'art. 4, comma 4, della legge 9 gennaio 1991, n. 10.

Gazzetta Ufficiale della Repubblica Italiana - DPR 74/2013 (2013), 'Dpr 74/2013'. Regolamento recante definizione dei criteri generali in materia di esercizio, conduzione, controllo, manutenzione e ispezione degli impianti termici per la climatizzazione invernale ed estiva degli edifici e per la preparazione dell'acqua calda per usi igienici sanitari, a norma dell'articolo 4, comma 1, lettere a) e c), del decreto legislativo 19 agosto 2005, n. 192.

Giaccherini, M., Kopinska, J. & Palma, A. (2021), 'When particulate matter strikes cities: Social disparities and health costs of air pollution', *Journal of Health Economics* **78**, 102478.

He, G., Liu, T. & Zhou, M. (2020), ‘Straw burning, pm 2.5 and death: Evidence from china’, *Journal of Development Economics* .

ISPRA (2014), ‘Italian emission inventory 1990-2012’.

ISTAT (2011), 5° censimento generale della popolazione e delle abitazioni, Technical report, ISTAT.

ISTAT (2022), ‘Consumi energetici delle famiglie – anni 2020/2021’, Report statistico pubblicato online.

Margaryan, S. (2021), ‘Low emission zones and population health’, *Journal of Health Economics* **76**, 102402.

Mavromatis, T. & Voulanas, D. (2021), ‘Evaluating era-interim, agri4cast, and e-obs gridded products in reproducing spatiotemporal characteristics of precipitation and drought over a data poor region: The case of greece’, *International Journal of Climatology* **41**, 2118–2136.

Neidell, M. J. (2004), ‘Air pollution, health, and socio-economic status: the effect of outdoor air quality on childhood asthma’, *Journal of Health Economics* **23**, 1209–1236.

Palma, A., Petrunyk, I. & Vuri, D. (2022), ‘Prenatal air pollution exposure and neonatal health’, *Health Economics* **31**(5), 729–759.

Pope, I. C. A. & Dockery, D. W. (2012), ‘Journal of the air & waste management association health effects of fine particulate air pollution: Lines that connect health effects of fine particulate air pollution: Lines that connect’.

Rambachan, A. & Roth, J. (2023), ‘A more credible approach to parallel trends’, *Review of Economic Studies* **90**, 2555–2591.

Salva, J., Poništ, J., Rasulov, O., Schwarz, M., Vanek, M. & Sečkár, M. (2023), 'The impact of heating systems scenarios on air pollution at selected residential zone: a case study using aermod dispersion model', *Environmental Sciences Europe* **35**, 1–17.

Schlenker, W. & Walker, W. R. (2016), 'Airports, air pollution, and contemporaneous health', *Review of Economic Studies* **83**, 768–809.

WHO (2014), Household fuel combustion who guidelines for indoor air quality, Technical report, WHO.

Wooldridge, J. M. (2021), 'Two-Way Fixed Effects, the Two-Way Mundlak Regression, and Difference-in-Differences Estimators'. Issue: 3906345 Place: Rochester, NY.

Wu, C., Li, K. & Bai, K. (2020), 'Validation and calibration of cams pm2.5 forecasts using in situ pm2.5 measurements in china and united states', *Remote Sensing 2020, Vol. 12, Page 3813* **12**, 3813.

Zauli-Sajani, S., Thunis, P., Pisoni, E., Bessagnet, B., Monforti-Ferrario, F., Meij, A. D., Pekar, F. & Vignati, E. (2024), 'Reducing biomass burning is key to decrease pm2.5 exposure in european cities', *SCIENTIFIC REPORTS* **14**.

Zhang, J. & Smith, K. R. (2007), 'Household air pollution from coal and biomass fuels in china: Measurements, health impacts, and interventions', *Environmental Health Perspectives* **115**, 848–855.